EXPERIMENTAL INVESTIGATIONS ON DOUBLE TOOL TURNING PROCESS

A Thesis Submitted in Partial Fulfilment of the

Requirements for the Degree of

DOCTOR OF PHILOSOPHY

by

Kalidasan R.

(Roll No. 10610326)

Department of Mechanical Engineering

Indian Institute of Technology Guwahati

Guwahati−781039

INDIA

May 2017

Department of Mechanical Engineering,
Indian Institute of Technology Guwahati,
Guwahati−781039
INDIA

Date:

CERTIFICATE

It is certified that the work contained in the Thesis entitled **"Experimental Investigations on Double Tool Turning Process"** submitted by **Mr. Kalidasan R.** to the Indian Institute of Technology Guwahati for the award of the degree of Doctor of Philosophy has been carried out under our supervision in the Department of Mechanical Engineering, Indian Institute of Technology Guwahati. This work has not been submitted elsewhere for the award of any other degree or diploma.

Dr. S. Senthilvelan
Professor
Department of Mechanical Engineering,
Indian Institute of Technology Guwahati,
Guwahati−781039, Assam,
INDIA

Dr. U.S. Dixit
Professor
Department of Mechanical Engineering,
Indian Institute of Technology Guwahati,
Guwahati−781039, Assam,
INDIA

Dedicated to God

Acknowledgement

I would like to express my immense gratitude and profound thanks to all those who have helped me in different ways during the tenure of my PhD work at IIT Guwahati. My sincere apologies, if I have inadvertently missed out a few names.

I am highly indebted to my supervisors Prof. S. Senthilvelan and Prof. U.S. Dixit for their guidance, support and encouragement during the research work. I am very grateful to them as their advices and motivation kept me at high spirits and lead to the successful completion of my research work. I take this opportunity to express my heartfelt thanks to the doctoral committee members, Prof. D. Chakraborty, Dr. S.N. Joshi and Prof. A. Perumal for their valuable suggestions and encouragement during the period of my research work. I am very grateful to the past and present heads of the mechanical engineering department, Prof. D. Chakraborty, Prof. P. Mahanta and Prof. A.K. Dass for extending the various facilities during my doctoral programme.

I am obliged to all the workshop staff for their cheerful readiness to help me in conducting the experiments. In this regard, I wholeheartedly thank Mr. N.K. Das, Mr. C. Banika, Mr. B.K. Choudhury, Mr. D. Khaklary, Mr. U. Gohain, Mr. M.C. Medhi, Mr. D.K. Deka, Mr. N. Saikia, Mr. P. Saikia, Mr. K.C. Deka and Mr. D. Chetri. I wish to express my sincere thanks to Mr. Yatin Manocha, Mr. Ramanuj Viswakarma, Mr. Vaibhav Jaiswal, Mr. Sandeep Kumar, Mr. Shufen Rajkumar, Mr. Vikas Kumar, Mr. Amit Raj and Mr. Arvind for their fruitful association during the various phases of my research work.

I wish to convey my thanks to Dr. V. Sateesh Kumar, Dr. Biswajith Parida, Dr. A. Muthuraja, Dr. A. Johnney Martens, Dr. Vinod Yadav, Dr. D.K. Yaduwanshi, Dr. G.N. Shelke, Mr. M. Kodeeswaran, Mr. Polash Pratim Dutta, Mr. Srikant Prasad, Mr. N. Sivaramakrishnan, Mr. M. Borad Barkachary, Mr. C. Ravi Chandra Rao, Mr. Shahidul Islam, Mr. Karthik Pandian, Ms. Saritha Bharati, Mr. Aayan Islam and Mr. Aditya for making my stay at IIT Guwahati as a home away from home.

I would like to commemorate my parents Late S. Rathinam Pillai and Late R. Saroja. Their divine inspiration helped me to navigate during the tough times of my research period. Last but not the least; I am very thankful to all my family members. From the bottom of my heart, I express my deep gratitude to my father-in-law Mr. R. Kolappa Pillai, mother-in-law K. Vijayammal, wife Bindu Kalidasan and my two daughters K. Harshita and K. Pritika for their affection, support, patience and motivation towards my research work. Ultimately I bow my head to the God in deepest gratitude and seek blessings.

Date: Kalidasan R.
IIT Guwahati.

Abstract

Machining is a widely used manufacturing process. This work explores the simultaneous machining by two single point cutting tools to enhance the productivity of the turning process. In order to perform a double tool turning process a conventional lathe was modified. A tool holding fixture was developed and mounted at the rear side of the lathe carriage. In double tool turning process the various process parameters are cutting speed, feed, depth of cut and distance between the two cutting tools. Experimental investigation was carried out to determine the influence of cutting parameters on cutting forces, cutting temperature, cutting tool vibration, diametral error, tool wear and surface roughness. The chip morphology was also studied.

In the present work, it was observed experimentally that the rear cutting tool experienced lesser cutting force than front cutting tool at certain cutting condition, while turning grey cast iron. This is attributed to the reduction in coefficient of friction of the rear cutting tool, caused by the cleansing effect of the front cutting tool. At other cutting conditions, there is no significant difference in cutting forces between the front and rear cutting tool. It was found that the temperature rise in the workpiece caused due to the front and rear cutting tool remained uninfluenced by the distances between the cutting tools. An analytical model was developed for single tool turning process based on ductile fracture mechanics approach and experiments were also performed on mild steel work material. The analytically predicted cutting force and cutting temperature was correlated with the experimental results. For the selected cutting conditions it was observed that with the increase in cutting speed the cutting tool vibration of both the tools reduced. The rear cutting tool vibration was lesser than the front cutting tool. One obvious reason is that the rear cutting tool is mounted over the fixture made of cast iron while the front cutting tool fixture is made of steel.

In double tool turning process the deflection of the workpiece due to front cutting tool is resisted by the rear cutting tool, as the cutting forces of the tools acts opposite to each other. Moreover the rear cutting tool acts as a follower rest apart from removing material from the workpiece. It was realized that the diametral error got reduced by 80% while turning grey cast iron at a cutting speed of 116 m/min, 0.24 mm/rev feed, 1 mm depth of cut and 10 mm distance between the cutting tools. The diametral error was found to be higher at the tailstock end due its lesser rigidity and lesser at the headstock end due to its higher rigidity. In comparison with single tool

turning for depths of cut of 1.5 mm and 2 mm, a significant reduction in diametral error was observed for double tool turning process. At higher depths of cut, the resistance offered by the rear cutting tool against the workpiece deflection was more than at lower depth of cut. The radial deflection of the workpiece was calculated theoretically based on simple strength of materials approach. The experimental results were in agreement with the theoretical results. The front cutting tool machined the material as well as heated the workpiece slightly. The effective coefficient of friction of the rear tool was lesser than the front cutting tool. However, the average surface temperature of the workpiece near the rear cutting tool was higher than that near the front cutting tool and this may be due to strain hardening. The rear cutting tool experienced lesser wear compared to front cutting tool. The chips generated during double tool turning process were examined using a scanning electron microscope. Morphology of the chip produced by the front cutting tool exhibited cracks and streaks with fracture as the dominant failure. The rear cutting tool generated chip with cracks, streaks and micro pores along with fracture.

In this thesis, experimental investigation was also conducted to determine the influence of machining parameters on the average surface roughness of AISI 1050 steel and grey cast iron work surfaces. It was observed that the average surface roughness decreases with the increase in cutting speed. On increasing the feed for AISI 1050 steel, initially the average surface roughness decreased up to 0.12 mm/rev feed and thereafter it increased. For grey cast iron the average surface roughness increased with feed for all cutting conditions. A similar behaviour was observed for depth of cut except for low feeds. The average surface roughness was not affected by tool separation distance. An approximate cost analysis was carried out for single tool and double tool turning process. Double tool turning process produced a good surface finish and less diametral error. It was cost effective compared to conventional turning process.

Keywords: Cutting forces, cutting temperature, cutting speed, diametral error, tool wear, tool vibration and surface roughness, turning, multi-tool machining

Contents

List of Figures.....xii

List of Tables.....xvii

Nomenclature.....xviii

1 Introduction..... 1

1.1 Parallel Turning Process..... 2

1.2 Cutting Forces..... 4

1.3 Cutting Temperature..... 5

1.4 Cutting Tool Vibration..... 6

1.5 Tool Wear..... 6

1.6 Surface Roughness and Dimensional Deviation..... 7

1.7 Objectives and Organisation of the Thesis..... 7

2 Review of Literature..... 9

2.1 Introduction..... 9

2.2 Multi-tool Machining..... 10

2.3 Cutting Force, Temperature and Tool Wear in Machining..... 12

2.3.1 Cutting Force..... 12

2.3.2 Cutting Temperature and Heat Generation..... 13

2.2.3 Tool Wear and Tool Life..... 15

2.4 Surface Roughness..... 17

2.5 Dimensional Deviation..... 18

2.6 Chip Morphology..... 20

2.7 Cutting Tool Vibration..... 21

2.8 Research Gaps..... 22

2.9 Scope and Objectives of the Present Work..... 23

3 Details of Experiment……..…….... 26

3.1 Introduction……... 26

3.2 Development of Cutting Tool Fixture…….…… 26

3.3 Experimental Setup…….…... 27

3.4 Measurement of Cutting Forces and Cutting Temperature…….…… 29

3.5 Measurement of Cutting Tool Vibration…….…… 31

3.6 Measurement of Diametral Error of Workpiece and Cutting Tool Wear…… 32

3.7 Surface Roughness Measurement…… 34

3.8 Conclusion…… 35

4 Cutting Forces, Cutting Temperature and Cutting Tool Vibration in Double Tool Turning Process…….. 36

4.1 Introduction…….. 36

4.2 Experimental Procedure……... 37

4.2.1 Experimental Setup……..... 37

4.2.2 Workpiece and Cutting Tool Material…… 40

4.2.3 Cutting Conditions……...40

4.3 Results and Discussion……..40

4.3.1 Effect of Distance Between Cutting Tools on Cutting and Feed Forces……... 40

4.3.2 Effect of Depth of Cut and Cutting Speed on the Forces for 2 mm Distance Between the Cutting Tools…… 43

4.3.3 Effect of Distance Between the Front and Rear Cutting Tools on the Cutting Temperature…….. 44

4.4 Estimation of Cutting Forces and Cutting Temperature in Single Tool Turning with a Simplified Model…… 47

4.5 The Influence of Machining Parameters on Cutting Tool Vibration in Double Tool Turning Process…….. 56

4.6 Conclusion……... 59

5 Diametral Error, Cutting Tool Wear and Chip Morphology in Double Tool Turning Process……... 61

5.1 Introduction……... 61

5.2 Experimental Procedure…… 62

5.3 Results and Discussion……..64

5.3.1 The Effect of Depth of Cut…… 66

5.3.2 Physical Explanation for the Improvement of the Accuracy through the Double Tool Turning…….. 68

5.3.3 Temperature during Double Tool Turning…… 70

5.3.4 Cutting Tool Wear…….. 71

5.3.5 Chip Morphology……73

5.4 Conclusion..……... 76

6 The Influence of Machining Parameters on Surface Roughness in Double Tool Turning Process……... 77

6.1 Introduction……... 77

6.2 Experimental Procedure……77

6.3 Results and Discussion……..78

6.3.1 Effect of Cutting Speed on Surface Roughness…… 78

6.3.2 Effect of Feed on Surface Roughness……..... 83

6.3.3 Effect of Depth of Cut and Tool Separation Distance on Surface Roughness……88

6.3.4 Comparison of Surface Roughness Between Double Tool Turning Process and Conventional Turning Process……... 91

6.4 Cost Comparison of Single and Double Tool Turning Process …….. 93

6.5 Conclusion..……..... 95

7 Conclusions and Scope for Future Work…… 96

7.1 Conclusions..…….. 96

7.1.1 Effect of Cutting Parameters on Cutting Forces, Cutting Temperature and Cutting Tool Vibration.....96

7.1.2 Influence of Cutting Parameters on Diametral error, Tool Wear and Chip Morphology……..97

7.1.3 Effect of Cutting Parameters on Surface Roughness in Double Tool Turning Process……..98

7.2 Scope for Future Work……..99

References……...100

Publications from the Present Thesis……...111

List of Figures

Figure 1.1	A schematic of double tool parallel turning process	1
Figure 1.2	Different configurations of multi-tool machining process (a**)** Simultaneous cylindrical turning and drilling (b) Parallel turning of two features with tools on the same side (c) Parallel turning of two features with two tools on opposite side (d) Synchronous turning with tools on opposite sides	3
Figure 2.1	Flow chart of research plan	25
Figure 3.1	Front and rear tool holding assembly	26
Figure 3.2	Experimental setup of double tool turning process	28
Figure 3.3	Schematic diagram of measurement of cutting forces and temperature	29
Figure 3.4	Force measurement system (a) Four component dynamometer (b) Single channel charge amplifier (c) Four channel charge amplifier	30
Figure 3.5	Infrared camera for temperature measurement	30
Figure 3.6	Arrangement of accelerometers	32
Figure 3.7	Diametral error measurement by dial gauge	33
Figure 3.8	Tool maker's microscope	33
Figure 3.9	Scanning electron microscope	33
Figure 3.10	Surface roughness measurement by Pocket Surf	34
Figure 3.11	Surface roughness measurement by 3D profilometer	35
Figure 4.1	Experimental setup showing front and rear cutting tool	37
Figure 4.2	Measured cutting forces in the double tool turning of grey cast iron (75 m/min cutting speed, 0.08 mm/rev feed, 1 mm depth of cut, 2 mm distance between cutting tools and 58 mm workpiece diameter)	38
Figure 4.3	Time domain vibration signal of front cutting tool while turning grey cast iron (75 m/min cutting speed, 0.08 mm/rev feed, 1 mm depth of cut, 2 mm tool separation distance and 58 mm workpiece diameter)	39

Figure 4.4	Frequency domain vibration signal of front cutting tool while turning grey cast iron (75 m/min cutting speed, 0.08 mm/rev feed, 1 mm depth of cut, 2 mm tool separation distance and 58 mm workpiece diameter)	39
Figure 4.5	Effect of cutting speeds over cutting forces on the front cutting tool while turning grey cast iron (0.08 mm/rev feed and 1 mm depth of cut)	41
Figure 4.6	Effect of cutting speeds over cutting forces on the rear cutting tool while turning grey cast iron (0.08 mm/rev feed and 1 mm depth of cut)	41
Figure 4.7	Variation of feed force in double tool turning of grey cast iron (0.08 mm/rev feed, 1 mm depth of cut and 2 mm distance between the two cutting tools)	44
Figure 4.8	Effect of cutting speed and distance between the front and rear cutting tool on work material surface temperature	45
Figure 4.9	Thermographic image while machining grey cast iron with coated carbide front and rear cutting tool (75 m/min cutting speed, 0.08 mm/rev feed, 1 mm depth of cut and 2 mm distance between cutting tools)	46
Figure 4.10	Surface temperature of work material at various periods of machining	47
Figure 4.11	The flow chart of the main program for obtaining the cutting force by minimizing shear angle using interval-halving method	51
Figure 4.12	The flow chart of the subroutine for estimating the cutting force	52
Figure 4.13	Thermogram of mild steel workpiece during cutting (75 m/min cutting speed, 0.08 mm/rev feed, 0.5 mm depth of cut and 10 mm distance between cutting tools)	55
Figure 4.14	Thermogram of mild steel workpiece during cutting (75 m/min cutting speed, 0.08 mm/rev feed, 1 mm depth of cut and 10 mm distance between cutting tools)	55
Figure 4.15	Thermogram of mild steel workpiece during cutting (120 m/min cutting speed, 0.24 mm/rev feed, 1 mm depth of cut and 10 mm distance between cutting tools)	56
Figure 4.16	Front cutting tool vibration amplitude in cutting direction (0.08 mm/rev feed and 1 mm depth of cut)	58
Figure 4.17	Rear cutting tool vibration amplitude in cutting direction (0.08 mm/rev feed and 1 mm depth of cut)	58
Figure 5.1	A schematic of diametral deviation of a slender workpiece	61

Figure 5.2	Measured cutting forces of the front and rear cutting tools in double tool turning of grey cast iron (116 m/min cutting speed, 0.24 mm/rev feed, 1 mm depth of cut and 10 mm separation distance between the cutting tools)	63
Figure 5.3	Measurement of the diametral error	63
Figure 5.4	Diametral error of the machined surface of grey cast iron at 1 mm depth of cut (116 m/min cutting speed and 0.24 mm/rev feed)	64
Figure 5.5	Variation of cutting force while turning from tailstock to chuck with single cutting tool for grey cast iron work material (116 m/min cutting speed, 0.24 mm/rev feed and 1 mm depth of cut)	65
Figure 5.6	Variation of cutting force while turning from tailstock to chuck with two cutting tools for grey cast iron work material (116 m/min cutting speed, 0.24 mm/rev feed and 1 mm depth of cut)	66
Figure 5.7	Diametral error at 1.5 mm depth of cut for grey cast iron work material (116 m/min cutting speed and 0.24 mm/rev feed)	66
Figure 5.8	Diametral error at 2 mm depth of cut for grey cast iron work material (116 m/min cutting speed and 0.24 mm/rev feed)	67
Figure 5.9	Theoretical and experimental workpiece deflection for single tool turning process (116 m/min cutting speed, 0.24 mm/rev feed and 1 mm depth of cut)	69
Figure 5.10	Theoretical and experimental workpiece deflection for double tool turning process (116 m/min cutting speed, 0.24 mm/rev feed 1 mm depth of cut and 10 mm separation distance between the cutting tools)	69
Figure 5.11	Tool-work interface temperatures while turning with two tools (116 m/min cutting speed, 0.24 mm/rev feed and 1 mm depth of cut)	71
Figure 5.12	Measured flank wear of front and rear cutting tools (0.24 mm/rev feed, 1 mm depth of cut and cutting speed 150–200 m/min)	72
Figure 5.13	Flank wear (a) Of front cutting tool at 150X magnification (0.24 mm/rev feed and 1 mm depth of cut) (b) Of front cutting tool at 500X magnification (0.24 mm/rev feed and 1 mm depth of cut) (c) Of rear cutting tool at 150X magnification (0.24 mm/rev feed and 1 mm depth of cut) and (d) Of rear cutting tool at 500X magnification (0.24 mm/rev feed and 1 mm depth of cut)	73

Figure 5.14	Back surface of the generated chip (a) From the front cutting tool (0.24 mm/rev feed and 1 mm depth of cut) and (b) From the rear cutting tool (0.24 mm/rev feed and 1 mm depth of cut)	74
Figure 5.15	Free surface of the generated chip (a) From the front cutting tool (0.24 mm/rev feed and 1 mm depth of cut) and (b) From the rear cutting tool (0.24 mm/rev feed and 1 mm depth of cut)	74
Figure 5.16	Chip segmentation formation generated (a) From the front cutting tool (0.24 mm/rev feed and 1 mm depth of cut) and (b) From the rear cutting tool (0.24 mm/rev feed and 1 mm depth of cut)	74
Figure 6.1	Variation of surface roughness with cutting speed for AISI 1050 steel for 1 mm depth of cut and 2 mm tool separation distance (a) For feeds of 0.04, 0.12 and 0.20 mm/rev (b) For feeds of 0.08, 0.16 and 0.24 mm/rev	79
Figure 6.2	Variation of surface roughness with cutting speed for grey cast iron for 1 mm depth of cut and 2 mm tool separation distance (a) For feeds of 0.04, 0.12 and 0.20 mm/rev (b) For feeds of 0.08, 0.16 and 0.24 mm/rev	80
Figure 6.3	Thermogram of AISI 1050 steel (75 m/min cutting speed, 0.04 mm/rev feed, 1 mm depth of cut and 2 mm tool separation distance)	82
Figure 6.4	Thermogram of grey cast iron (75 m/min cutting speed, 0.04 mm/rev feed, 1 mm depth of cut and 2 mm tool separation distance)	82
Figure 6.5	Variation of surface roughness with feed for AISI 1050 steel for 1 mm depth of cut and 2 mm tool separation distance (a) For the cutting speeds ranging from 75 to 225 m/min (b) For the cutting speeds ranging from 100 to 250 m/min	84
Figure 6.6	Three dimensional topography of AISI 1050 steel at 0.04 mm/rev feed (75 m/min cutting speed, 1 mm depth of cut 2 mm tool separation distance)	85
Figure 6.7	Three dimensional topography of AISI 1050 steel at 0.12 mm/rev feed (75 m/min cutting speed, 1 mm depth of cut 2 mm tool separation distance)	86
Figure 6.8	Three dimensional topography of AISI 1050 steel at 0.24 mm/rev feed (75 m/min cutting speed, 1 mm depth of cut 2 mm tool separation distance)	87
Figure 6.9	Variation of surface roughness with feed for grey cast iron for 1 mm depth of cut and 2 mm tool separation distance (a) For cutting speed ranging from 75 m/min to 225 m/min (b) For cutting speed ranging from 100 to 250 m/min	87
Figure 6.10	Variation of surface roughness with depth of cut for AISI 1050 steel (125 m/min cutting speed and 2 mm tool separation distance)	89

Figure 6.11 Variation of surface roughness with depth of cut for grey cast iron (125 m/min cutting speed and 2 mm tool separation distance) 90

Figure 6.12 Variation of surface roughness with tool separation distance for AISI 1050 steel and grey cast iron (200 m/min cutting speed, 0.12 mm/rev feed and 1 mm depth of cut) 91

List of Tables

Table 3.1	Composition of the work material	28
Table 3.2	Cutting tool signature	29
Table 4.1	Effect of depth of cut on cutting and feed force in double tool turning of grey cast iron (75 m/min cutting speed, 0.08 mm/rev feed and 2 mm distance between cutting tools)	43
Table 4.2	Cutting forces and workpiece surface temperature while double tool turning of typical mild steel with TiN coated tungsten carbide tools (75 m/min cutting speed, 0.08 mm/rev feed and 1 mm depth of cut)	53
Table 5.1	Variation of cutting forces for various depths of cut	68
Table 6.1	Values of cutting parameters	78
Table 6.2	Variation of peak to valley height and average surface roughness with feed for AISI 1050 steel	86
Table 6.3	Average surface roughness of double tool turning and conventional turning process for AISI 1050 steel	92
Table 6.4	Average surface roughness of double tool turning and conventional turning process for grey cast iron	93

Nomenclature

A	Initial yield stress
a	Proportionality constant
B	Hardening modulus (constant of J-C model)
b	Exponential constant
C	Strain rate dependency coefficient
C_o	Operating cost per unit time
C_p	Production cost per piece
C_t	Tool cost
c	Heat capacity
d	Depth of cut
F	Force
f	Feed
F_x	Feed force
F_y	Radial force
F_z , F_c	Main cutting force
F_f	Frictional force

F_t	Fraction of tool consumed while machining a workpiece
i	Inclination angle
k	Thermal conductivity
n	Work hardening exponent
m	Thermal softening coefficient
P_p	Power due to plastic deformation process
p_{wp}	Proportion of heat conducted into workpiece
r	Cutting ratio
r_n	Tool nose radius
R	Specific work of surface formation (fracture toughness)
R_a	Average surface roughness
R_{max}	Peak to valley height
t_c	Chip thickness
t_0	Uncut chip thickness
T	Process temperature
T_a	Ambient temperature
T_m	Melting temperature
T_N	Thermal number
T_p	Production time per workpiece

V	Cutting speed
w	Width of cut
x	Machining time per workpiece
Y_s	Shear yield stress
α	Rake angle
α_e	Effective rake angle
α_b	Back rake angle
α_s	Side rake angle
α_n	Normal clearance angle
$\alpha_{n'}$	Auxiliary normal clearance
β	Friction angle
κ_a	Auxiliary cutting edge angle
κ_p	Principal cutting edge angle
γ_n	Normal rake angle
γ	Maximum shear strain
ϕ	Shear angle
ψ	Side cutting edge angle
μ	Coefficient of friction
ε	Equivalent strain
$\dot{\varepsilon}$	Equivalent strain-rate
$\dot{\varepsilon}_0$	Reference strain-rate

ε_{max}	Maximum equivalent strain
ρ	Density
θ_p	Temperature rise in the cutting zone

Chapter 1

Introduction

Machining, metal forming, metal casting and metal joining are some of the important manufacturing processes. Turning, milling, drilling and grinding are some of the widely used conventional machining processes. Among these machining processes, turning is the most popular and versatile machining process. A brief history of machining process has been provided by Dixit *et al.* (2017). Turning process was developed by Egyptians around 1500 BC. As per some records, the lathe was in use around third century BC in Greek and Roman civilization. It was used to turn wood and bone (Trent and Wright 2000). One Eleusinian inscription dated circa 360 BC provides evidence for the use of lathe for turning of bronze. Turning is a material removal process used to produce axisymmetric parts by feeding the cutting tool against the rotating workpiece. Here the cutting tool material is harder than the workpiece material. One way of increasing the productivity in a turning process is to use more than one cutting tool.

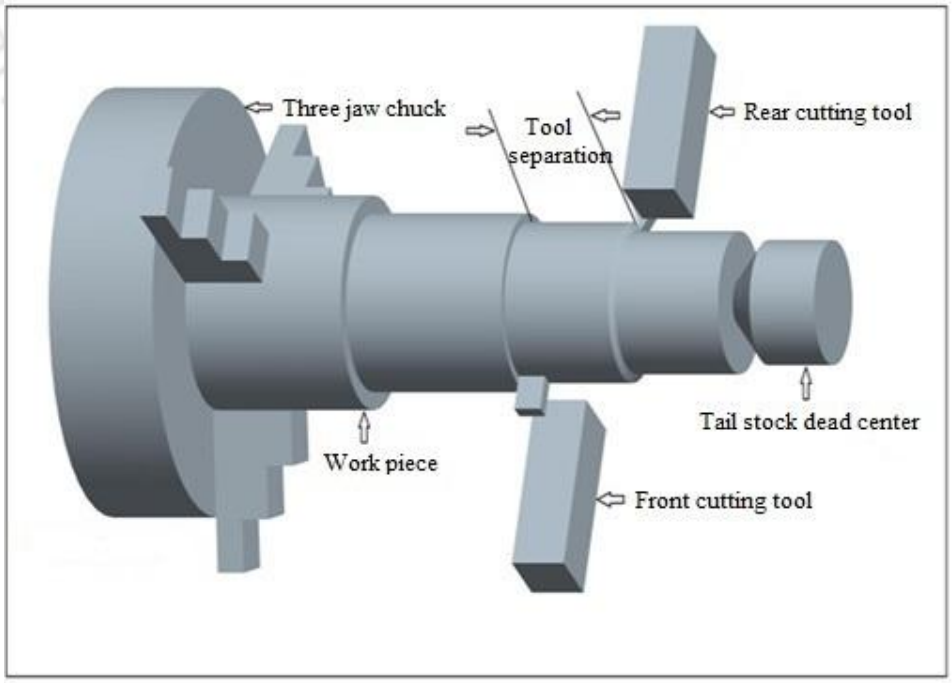

Figure 1.1. A schematic of double tool parallel turning process

This thesis investigates experimentally the parallel turning process from the view point of increasing the productivity. The parallel turning process is considered as a form of multi-tool turning process. A three dimensional model of two-tool parallel turning process is shown in Figure 1.1. The keywords of this thesis are parallel turning process, cutting forces, cutting temperature, cutting tool vibration, tool wear, surface roughness and dimensional deviation. These are briefly introduced from Sections 1.1–1.6. The objective and organisation of the thesis is presented in the last section of this chapter.

1.1 Parallel Turning Process

Parallel turning or multi-tool turning is normally attempted for heavy removal of material, minimising the cost and maximizing the rate of material removal. Since turning is a fundamental and an important machining operation, the present study focuses on multi-tool turning operation, particularly on double tool parallel turning process. Before the advent of computer numerical control (CNC) machines, multiple tool lathes were employed in high volume material removal processes. Multiple tool lathes are basically a single purpose high production machines intended for producing stepped shafts, in batch and mass production shops. Multiple tool lathes are provided with two or more carriages each carrying several single-point cutting tools operating simultaneously. This enables the reduction of machining time because the carriages operate simultaneously. The front carriage mounts the tools for turning the steps of the shafts and travels with longitudinal feed along the lathe axis. The rear carriage has only the cross feed and is used to cut grooves, face shoulders, turn chamfers and produce contoured surfaces with form tools. Multiple tool lathes operate on a semi-automatic cycle. The operator loads the workpiece on a work holding device such as chuck, the required operation is performed by automatic mechanism operated by cams or hydraulic means, and finally the finished component is unloaded. This feature allows one operator to handle several machine tools at the same time. The construction of multiple tool lathes is distinguished from the exceptionally high rigidity of the components such as bed, carriages, headstock and tailstock. This is necessitated by the large total chip cross section when the stock is removed concurrently by several cutting tools. Multiple tool lathes are often equipped with hydraulic tracer controlled slides for turning cylindrical and contoured surfaces of

revolution. The arrangement of the units and the construction of such lathes are based on reproducing the shape of a template or master. It is not very clear since when the industries started using multi-tool simultaneous turning. In the milling arena, straddle milling has been used since long time. In straddle milling, two identical cutters are mounted in a horizontal milling machine arbor separated by a distance. These two cutters simultaneously machine two parallel vertical surfaces and balance the thrust forces of each other. Sometimes more than two cutters may be used. Similar types of applications are found in grinding area, where two or more surfaces are ground simultaneously.

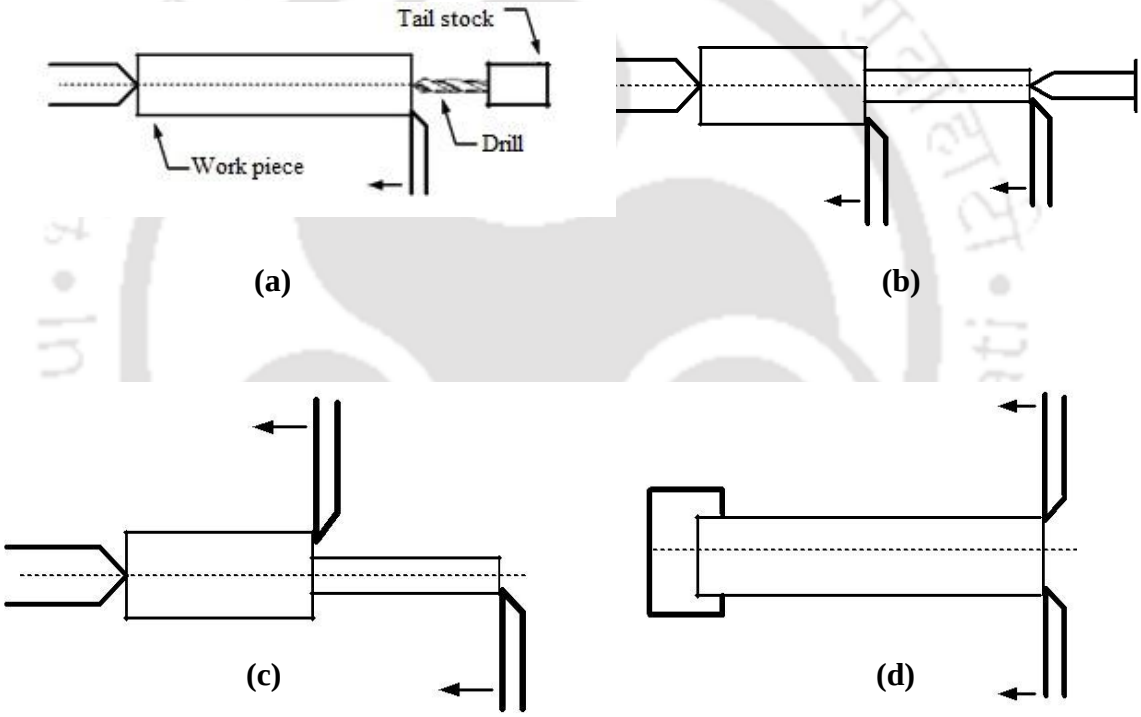

Figure 1.2. Different configurations of multi-tool machining process **(a)** Simultaneous cylindrical turning and drilling, **(b)** Parallel turning of two features with tools on the same side **(c)** Parallel turning of two features with two tools on opposite side **(d)** Synchronous turning with tools on opposite sides

While using multiple cutting tools, simultaneous machining can be carried out in a number of ways. Various possibilities are shown in Fig.1.2. The schematic of cylindrical turning and drilling simultaneously is given in Fig. 1.2(a). The turning tool is mounted on the carriage and drilling bit in the tailstock. Figure 1.2(b) shows a cylindrical turning operation, where two features are being machined simultaneously

with two tools kept on the same side. It is usual to have two tools moving with the same feed, but it may be possible to have independent movement of these tools. Figure 1.2(c) is showing a similar arrangement with the difference that the tools are mounted on the opposite side of the cylindrical workpiece. This arrangement balances the forces and provides more accuracy. In essence, one cutting tool acts as a follower rest for the other cutting tool. However, the tool paths are asynchronous. A synchronous machining with two tools is shown in Fig. 1.2(d). Here, both the tools are just opposite to each other.

The research work on multiple-tool simultaneous turning started in 1960s. It can be divided into two broad categories: (1) Science of metal cutting and (2) Optimization of the process. The work in the first category is very sparse and as the case in general machining area, the literature lacks a concrete model of metal cutting. In the area of optimization significant work has been done. The major performance parameters are cutting forces, cutting temperature, tool vibration, tool wear, tool life, surface finish and dimensional accuracy. Apart from these, cutting tool geometry, tool and work material and cutting fluid also influence the performance of the turning process. Among these, the important parameters such as cutting forces, cutting temperature, cutting tool vibration, tool wear, surface roughness and dimensional deviation are discussed as follows.

1.2 Cutting Forces

In conventional turning, three force components are involved. The vertical force is the main cutting force (F_z) which acts along the cutting direction. The feed force (F_x) acts in the direction of feed and the radial force component (F_y) acts in the radial direction of the workpiece. The radial force component is also known as passive force. Cutting forces are measured either by strain gauge type dynamometer or piezoelectric type dynamometer. The piezoelectric type dynamometer is superior to strain gauge type dynamometer because of higher sensitivity and stiffness. It also posses high frequency bandwidth and is capable of measuring the dynamic forces accurately. Higher frequency bandwidth dynamometers are preferred as it can capture larger variation in force signals during the machining process. The cutting forces directly depends on the machining process parameters such as cutting speed, feed and depth of

cut apart from cutting tool geometry, work and tool material. They also influence the cutting temperature, surface finish and dimensional deviation of the workpiece. In the case of two tool parallel turning process both the front and rear tool experiences cutting forces whose direction are opposite and the magnitude are different for the same cutting condition. Unlike the conventional turning process, in multi-tool turning process the distance between the cutting tools (tool separation) is an additional cutting parameter apart from cutting speed, feed and depth of cut.

1.3 Cutting Temperature

In metal cutting operation the heat is generated in the cutting region. There are three main zones in the cutting region. They are primary, secondary and tertiary shear deformation zones. The heat generated in the primary shear deformation zone is due to the plastic deformation of the work material. The friction between the rake face of the tool and chip causes heat generation in the secondary shear deformation zone whereas the friction between tool flank and the machined surface causes heat generation in the tertiary shear deformation zone. The cutting temperature rises because of the heat generation in the cutting zone. Higher cutting temperature adversely affects the tool life. It decreases the wear resistance and hardness of the cutting tool. It also increases the tool wear thereby reducing the tool life. Higher cutting temperatures also cause poor surface finish and dimensional inaccuracy of the machined surface. Therefore it becomes important to maintain lower cutting temperature during the machining process. The cutting temperatures are measured by thermocouples, radiation pyrometers, and thermal paints. Additionally metallographic techniques and physical vapour deposition coatings are also employed. Tool-work thermocouple measures the average temperature of the contact area between the cutting tool and work material. On the other hand, the embedded thermocouple measures the temperature of a particular point in the cutting zone. The non-contact infrared thermographic technique uses radiation to measure the cutting zone temperature. Infrared cameras are used for this purpose. The emissivity of the work material should be known *a priori*. The advantages of infrared camera over thermocouple are faster response time and no physical contact with the heat source. One main disadvantage of this method is that it is limited to accessible surfaces only.

1.4 Cutting Tool Vibration

Apart from the main cutting forces, the cutting tool vibration plays a major role in achieving the required surface finish and dimensional tolerance in any machining process. Excessive tool vibration leads to chatter and premature tool failure. The tool life is also influenced by its vibration level. The state of the cutting tool can be identified from the amplitude of the vibration signal. Accelerometers are used to measure the vibration signals of cutting tool. The obtained time domain vibration signals are converted into frequency domain signals by Fast Fourier Transform (FFT). Tool condition monitoring systems employs high frequency (4000 to 8000 Hz) vibration signals to evaluate the tool wear. The low frequency (0 to 4000 Hz) vibrational signals are insensitive to tool wear and the natural frequency of the tool holder falls in this range.

1.5 Tool Wear

Tool wear is defined as the loss of material from the cutting tool surface. The cutting efficiency essentially depends on it. Crater wear and flank wear are the two main classes of tool wear. The former occurs on the rake face while the latter occurs on the flank face of the cutting tool. Tool wear is also caused due to micro-chipping, oxidation and diffusion. At low cutting speed and feed abrasion wear is predominant while at higher cutting temperatures oxidation and diffusion wear becomes predominant. Direct and indirect methods are utilized to measure the tool wear. Scanning electron microscope, optical microscope, confocal laser scanning microscope and stylus profilers are used in direct methods. While cutting forces, cutting temperature, tool vibration, acoustic emission and surface roughness are measured to evaluate the tool wear in indirect methods. The tool life crucially relies on tool wear. Tool life is the time period of machining during which the cutting tool delivers a desired and satisfactory performance. Higher tool life leads to higher productivity and decreased machining cost. The apparent manifestations of cutting tool wear are higher surface roughness of the machined work surface, increased magnitude of cutting forces due to loss of sharpness of the cutting edge and dimensional inaccuracy of the machined workpiece.

1.6 Surface Roughness and Dimensional Deviation

The surface roughness and dimensional deviation are important attributes of the machined product quality. The most widely used measures of surface roughness are the centreline average and root mean square values. The measure of evenness of a surface is indicated by its surface roughness value which is usually mentioned in micrometres. Lower surface roughness gives higher surface finish and vice versa. The degree of variation between the actual measured dimension of the machined workpiece and desired dimension is referred as dimensional deviation. It is a machining error mainly affected by the cutting force. Unfortunately, the reliable physical models to estimate surface roughness and dimensional deviation are not available. Many researchers have used soft computing approaches comprising neural network, fuzzy logic and genetic algorithms either individually or in combination to predict surface roughness.

1.7 Objectives and Organisation of the Thesis

The primary objectives of the present thesis are to study the effect of process parameters on the cutting performance in double tool parallel turning process. The influence of the process parameters like cutting speed, feed, depth of cut and tool separation distance over the cutting forces, temperature, cutting tool vibration, surface roughness and dimensional deviation are studied experimentally. The thesis consists of seven chapters that are organized as follows.

- The first chapter provides the introduction, objectives and organization of the thesis.

- The second chapter presents the literature survey of multi-tool machining. The review is based on the cutting forces involved in turning along with the temperature generation, cutting tool vibration, tool wear, tool life, surface roughness and dimensional deviation. Finally the challenging issues, scope and detailed objectives of the present thesis are described.

- The third chapter elaborates the experimental details including the design and fabrication issues pertaining to the rear tool fixture. Methodology of

measurement of cutting force, temperature, tool vibration, surface roughness and dimensional deviation are also explained.

- The fourth chapter deals with the influence of the process parameters on cutting forces and temperature generated in double tool parallel turning. Theoretical analysis is used to justify the experimental findings.

- Chapter 5 discusses the effect of turning parameters on machining accuracy and dimensional deviation in double tool turning process. Apart from this, chip morphology and cutting tool wear is also studied.

- The sixth chapter discusses the effect of double tool turning process variables on surface roughness. A comparison is drawn between conventional turning and double tool turning process in terms of achieved surface roughness.

- The seventh chapter presents the conclusions and scope for future work.

Chapter 2

Review of Literature

2.1 Introduction

In present era of economic development there is a great need for producing high quality machined components at reduced cost. This can be achieved by using sophisticated machine tools and decreasing the machining time. Some of the methods adopted to reduce the machining times are using higher operating conditions, performing many operations simultaneously, employing jigs and fixtures and employing computer numerical control machine tools. Higher cutting conditions in turning imply higher cutting speed, feed and depth of cut. Among the three parameters, increasing the cutting speed has got many advantages compared to the other two. This had led to the concept of high speed machining. Superior surface finish, higher accuracy, increased productivity, reduced tool wear and higher tool life are some of the advantages of high speed machining. Even though there are a lot of advantages, still certain inherent drawbacks persists when machining at high speed. Higher investment and maintenance cost, reduced tool life and higher tool wear rates are some of its demerits. Ultimately this has led the researchers to explore some other methods of improving the productivity. An alternate method of increasing the productivity is by engaging more tools at the same time to machine a component. It gives rise to multi-tool machining. Section 2.2 presents a review of available literature on multi-tool machining.

In any machining operation measurement of cutting forces are of paramount importance in order to estimate the power consumption and process efficiency. It is equally important to monitor the cutting temperature as it plays a major role in determining the tools wear and tool life. Section 2.3 presents literatures on cutting forces, cutting temperatures and tool wear in machining. The usage of more than one cutting tool leads to improved surface finish of the machined component. Therefore surface roughness aspect is reviewed in Section 2.4. The cutting tools apart from removing the work material also provide support to the workpiece in multi-tool

turning. The cutting tool also performs the function of follower rest in case of multi-tool turning process. Hence the diametral error is minimised while turning slender jobs in lathe. From this point of view the review of literatures related to dimensional deviation is presented in Section 2.5. The chips that are generated in machining reveal the mechanism of metal cutting and in this aspect literature related to chip morphology are reviewed in Section 2.6. Cutting tool vibration plays an important role in determining the surface roughness and tool life. Excessive vibration leads to chatter. Thus it is very important to maintain the vibration levels to minimum. The research works on cutting tool vibration is given in Section 2.7. The research gaps are given is Section 2.8. The detailed scope and objectives of the present work is presented in Section 2.9.

2.2 Multi-tool Machining

The research papers on the multi-tool machining are very less in comparison to conventional turning process, even though it offers ample scope of increasing the productivity. Researchers in the past had focussed mainly on the optimization of process parameters in multi-tool machining. McCullough (1963) calculated the tool life for the maximum production rate and tool life for the minimum cost for multi-tool operations in which the total cycle time was controlled by the speed of the spindle. Zompi *et al.* (1979) and Ravignani *et al.* (1979) presented the tool failure patterns in multi-tool machining. Probability theories were used to assess the tool life. In the second part of their work, the tool life distribution was considered by taking into account the progressive wear and sudden tool fracture. Sheikh *et al.* (1980) proposed various tool replacement strategies for multi-tool and single tool production machines. They showed how the optimal cutting conditions are affected by the tool change policies. The three approaches followed by them are preventive planned tool change policy, scheduled tool change policy and failure replacement policy. The optimum spindle speed was found using probabilistic models of tool life. Levin and Dutta (1996) proposed a computer aided process planning system for parallel machining process. Turning and milling operations were performed simultaneously. It improved the accuracy with reduction in part cycle time. The authors also developed architecture for parallel machines that can accommodate any number of machining

unit. Sudhakara and Landers (2003) designed an output feedback controller for parallel turning process taking the non-linearity of cutting forces into consideration. The stability boundary was evaluated numerically by reversed trajectory method. Tang *et al.* (2008) suggested a novel heuristic algorithm based on Particle Swarm Optimization (PSO) to optimise the process parameters for two-tool parallel turning operation. PSO provided the optimum solution in less computational time. El-Hossainy (2010) developed a turning tool having two cutting edges. It was proclaimed that new tool reduced the surface roughness, straightness and roundness errors by 58, 65 and 50 percentage respectively, for a particular machining condition. Budak (2011) studied the dynamics and stability of parallel turning process in time domain and frequency domain. An improvement in process stability was obtained due to the interaction between two cutting tools. An analytical model was constructed and the experimental results were matched with the results of the analytical model. Ozturk *et al*. (2016) predicted the stability limits in parallel turning process for two different cases. It was concluded that most stable conditions are obtained when the natural frequency of the two cutting tools are slightly different from each other. On the other hand, poor stability occurs when the two cutting tools have exactly the same natural frequency. Recently Yadav (2017) developed a mathematical model and optimised the cutting parameters in duplex turning process using a combined Taguchi-Response Surface Methodology hybrid approach. It was reported that the surface finish improved significantly in hybrid approach compared to Taguchi method.

From the available literature, it is seen that very little work has been done on the aspect of cutting forces, cutting tool vibration, surface roughness, dimensional error and cutting temperatures generated in the individual tools during simultaneous engagement during multi-tool machining/turning process. In multi-tool turning the depth of cut is shared among the number of tools. This reduces the cutting forces acting on individual tool. Hence it improves the machining accuracy and reduces the surface roughness. The next section deals with the cutting force, cutting temperature and tool wear aspects in machining, for single tool turning process. The literature survey on single tool turning process helps in setting the research direction for multi-tool turning process.

2.3 Cutting Force, Temperature and Tool Wear in Machining

With the development of new machine tools capable of higher material removal rate (MRR), the significance of machining at high cutting speed has increased tremendously at present. Nowadays machining is carried out in the range of 3 to 5 times higher than the conventional machining speeds. It leads to reduced processing times, improved workpiece accuracy and surface integrity. Certainly there are some limitations too. The main performance parameters in a machining process are cutting forces, cutting temperature and tool wear. These factors determine the production costs, process efficiency and tool life.

2.3.1 Cutting Force

Cost effective application of machining technology requires a basic understanding of the relationship between process variables and cutting conditions. The studies on cutting forces generated during the machining process are of great significance, especially with respect to change in cutting speed, feed and depth of cut. Excessive amount of cutting forces can cause high frequency vibration of large magnitudes which in turn affects the tool life and workpiece surface finish. It also results in tool breakage and premature tool failure. Several research works on cutting forces generated during machining especially at higher cutting speeds were performed by various researchers in the past.

Recht (1985) analysed the machining of 4340 steel using a tungsten carbide tool coated with titanium carbide. It was shown that the Merchant's classical equation based on minimum work approach as applied to machining at low speed is also applicable to machining at high speed. It was observed that with increase in speed from 242 m/min to 2121 m/min the friction coefficient (μ) decreases from 0.6 to 0.26. This is because of high heat generation which causes the asperities in the chip to melt. Apart from this, high temperatures are generated, which leads to rapid tool wear creating a crater which modifies the flank wear directly. Sutter *et al*. (1998) conducted metal cutting experiments to determine the cutting forces. It was observed that the cutting forces decreased with the increase in cutting speed. The reduction in friction coefficient is the main cause for reduced cutting forces. The experiments were

conducted at both low and high cutting speeds. Ren and Altintas (2000) determined the cutting forces and cutting temperature in the deformation zone. A mold steel and carbide tool was used as work material and cutting tool respectively. It was found that the optimal chamfer angle was −15° when dry cutting P20 mold steel with carbide tool at a cutting speed of 240 m/min. Kang *et al*. (2001) studied the use of multi-sensors in machinability evaluation and condition monitoring while machining hardened material. Dynamometer, accelerometer and gap sensors were used. It was concluded that all these sensors are sensitive to tool load, cutting conditions, spindle vibration and tool deflections. Sutter and Molinari (2005) measured thrust force component along with longitudinal force component. The work and tool materials were 42CrMo4 medium carbon steel and carbide tool. The real coefficient of friction was determined by considering the forces near the cutting edges. It was noted that a minimum tool-chip friction coefficient has been found for the lowest depth of cut. Existence of a critical speed (15−25 m/s) for which the cutting forces for medium carbon steels are minimum was also confirmed. Yigit *et al*. (2008) investigated experimentally the machining of nodular cast iron with a coated carbide tool at various cutting speeds. The cutting forces decreased on increasing the cutting speed. The cause for a drop in cutting force was attributed to the reduction in the yield strength of the work material.

In majority of the cases, it can be seen from that the cutting forces are increased proportionately while increasing the cutting speeds in machining. Higher cutting forces in turn lead to higher cutting temperatures and more amount of heat generation. It also leads to premature tool failure and higher tool wear rate. In some extreme cases it prompts tool breakage. Hence it is necessary to maintain low cutting temperature during machining. The next section deals with cutting temperature and heat generation in machining.

2.3.2. Cutting Temperature and Heat Generation

Large quantity of material removed in short time causes higher heat generation in the cutting zone followed by a sharp rise in temperature. This heat which is concentrated near the cutting edge of the tool affects the cutting tool performance while machining. Dewes *et al*. (1999) mentioned two main theories regarding cutting temperatures while machining at high speeds. The first one proposed by Salomon is that there was a

peak cutting temperature at an intermediate cutting speed and the cutting temperature reduces when the cutting speed is increased beyond that point. The second one proposed by McGee suggested that the temperature increased with cutting speed up to the melting point of the workpiece. While cutting iron and steel the heat generation and cutting temperature are the controlling factors. Based on this, a review of literature is presented which is as follows.

Dewes *et al*. (1999) measured the temperature during machining of hardened mold/die steel by using both tool work thermocouple and Infrared camera. Interface temperature measured using the thermocouple when machining with the workpiece at 0 °C was between 200−300 °C. Cutting temperature increased with cutting speed and it did not reduce at higher speeds. Infrared technique indicated lower temperature than the thermocouple method with value ranges of 68−390 °C. A relatively low measured cutting temperature makes tungsten carbide to be used successfully for the high speed machining of hardened steels. Sutter *et al.* (2003) conducted experiments to measure the temperature fields while machining at high cutting speed. The tool and work material pair is coated carbide and alloy steel. Pyrometric technique (Infrared camera) for temperature measurement was used. It was concluded from the experiment that there exists a hot spot in the chip temperature distribution. This hot spot is located near the tool-chip interface at a distance of 300−350 μm from tool tip and the temperature is 825 °C. The chip temperature increases with increase in cutting speed and it is very dominant in the range of 20−30 m/s. The temperature stabilises for cutting speeds greater than 40 m/s. With the increase in depth of cut the chip temperature increases following the same trends like cutting speed.

In high speed external turning process, Muller *et al*. (2004) used a two colour pyrometer to measure the temperature over the workpiece and chip. The work and tool materials are AISI 1045, AA 7075, Ti-6Al-4V and SiC whisker reinforced mixed ceramic oxide, uncoated cemented carbide inserts. Producing holes in the tool inserts was a big hurdle in the experimental work. It was found that the cutting forces and temperature increased asymptotically with the rise in cutting speed. The highest temperature rise with cutting speed is found at conventional speeds for all materials. Karpat and Ozel (2008) presented analytical and experimental validation of a thermal model when machining at higher cutting speed with chamfered tools. The effect of

cutting conditions, heat generation and resultant temperature distribution at the tool and in workpiece was investigated. The tool and work material pair is CBN and AISI 4340 steel. It has been observed that the temperatures increased with increasing uncut chip thickness. This also resulted in the decrease in friction factor.

There are many detrimental effects of high cutting temperatures produced during machining. This further gets aggravated on increasing the cutting parameters such as cutting speed, feed and depth of cut. One of the major factors influencing productivity is tool wear and tool life. It is dealt in the following section.

2.2.3 Tool Wear and Tool Life

In machining the tool wear and tool life depends mainly on the following factors:

- The material of the machined component
- Cutting tool material and its shape
- Cutting conditions
- The machining process

Two main types of wear are abrasion wear and adhesive wear. When cutting at conventional speeds abrasion wear dominates. When the cutting speed is increased, tool wear happens mainly by diffusion process and hence adhesive wear dominates. Krammer (1987) developed specific strategies for developing new tooling systems for machining at high cutting speed. At these speeds crater wear predominates with the crater deepening until edge failure occurs. It was reported that the wear rate decreases with increasing cutting speed. Gatto and Luliano (1994) analysed the tool wear while machining of nickel alloy with silicon carbide whisker reinforced alumina cutting tool. It was seen that chipping of tool became dominant which destroyed the cutting edge. Higher plastic deformation increases the temperature that favours work material adhesion over the tool and whisker pull out. Chip hardening and transverse material flow inside the chip produces segmentation increasing the abrasive characteristics of the chip there by enhancing the notch formation. Abukhshim *et al*. (2004) conducted an experimental investigation of the tool-chip contact length and wear in high speed turning of EN 19 steel with uncoated carbide tool. The cutting speeds ranging from 200 to 1200 m/min with feeds of 0.14 mm/rev and 0.2 mm/rev and a depth of cut of

0.1 mm was employed. The tool-chip contact length is found to increase for cutting speeds from 400 m/min to 1200 m/min. Sliding friction is common in conventional machining; at high speed machining seizure takes place and sticking friction occurs. Characteristic chip curl could account for a significant increase in the chip contact width observed in the case of high cutting speed. All these are applicable for high speed machining using uncoated carbide tools. For advanced PVD coated tools, contact conditions, temperature fields and tool wear are left for future investigation.

Nouari and Molinari (2005) experimentally verified a diffusion wear model of 42CrMo4 steel with an uncoated cemented tungsten carbide with mean temperature at interface and distributed temperature at interface. Crater wear was considered to be dominant at high cutting speed and high feed. It was observed that the contact length decreases and maximum temperature increases with increase in cutting speed. Increasing the feed resulted in increase in the maximum cutting temperature and an increase in contact length. There was a significant reduction in tool life at high cutting speeds and high temperature is the main cause of reduction in tool life. Lin *et al*. (2008) used a coated cutting tool to enhance the tool life while machining AISI 4340 steel. It was noted that at 260 m/min Alcrona performed 95 % better in tool wear than TiAlN coated carbide tool under the same machining condition. It is also observed that the use of coolant emulsion increases the tool life proportionally with respect to the cutting speed and reduces the wear progression significantly. The wear behaviour modelling of newly coated tool was left unexplored. Iqbal *et al.* (2009) presented a contact model of tool-chip interface while orthogonal turning of AISI 1045. A decreasing trend was observed for contact length with increasing cutting speed for all undeformed chip thickness values for AISI 1045 steel. List *et al*. (2009) made an experimental investigation of tool wear in high speed machining by using a ballistic setup. The tool and work material employed was uncoated carbide insert and low carbon steel. The research findings show that the crater wear size increases with the increase in cutting time duration.

From the literature survey it is observed that the cutting forces increases on increasing the cutting speed. It is due to the inertia effects caused by the momentum change of the workpiece when it passes through the primary shear deformation zone. Moreover on increasing the cutting speed the frictional forces on the rake face of the

tool varies thus causing shear localised chips. The fluctuating frictional force reduces the tool life. Apart from this the tool-chip contact length increases. The sticking friction conditions prevail at these interfaces increasing the tool wear rate. Higher chip sliding velocity increases the heat generation and temperature. Most of the machining operations are carried out with carbide tools which can withstand temperatures up to 1100 °C beyond which the cutting tool loses its strength. These temperatures are common while machining at higher cutting speed, thereby imposing a restriction on the machining process. Diffusion wear predominates at high temperatures there by causing crater wear in addition to flank wear. Multi-tool turning process has a potential to overcome these limitations and it would be interesting to explore it.

2.4 Surface Roughness

Surface roughness is an important factor that determines the quality of a machined surface. It depends on many parameters such as cutting condition, machine tool vibration, cutting tool and work holding devices. The cutting speed, feed and depth of cut have a major influence on the surface roughness of the finished component. A lot of research work has been directed towards improving the surface quality of the machined component. Some relevant literatures are reported in the following paragraph.

Sarma and Dixit (2009) conducted metal cutting experiments and compared the surface roughness produced by dry and air cooled turning of grey cast iron. It was noted that the air cooled turning process reduced the surface roughness and increased the tool life. Nalbant *et al*. (2009) investigated experimentally the effects of different types of inserts and cutting parameters on the surface roughness of steel. It was found that coated carbide inserts provided surface finish superior to uncoated carbide inserts. Correia and Davim (2011) performed experimental studies on AISI 1050 steel with conventional and wiper cemented carbide inserts. It was manifested that the wiper inserts surpassed the conventional inserts and produced superior surface finish even at higher feed. Ramesh *et al*. (2012) determined experimentally the effect of cutting parameters on surface roughness while turning titanium alloy. It was declared that the feed was the most influential factor affecting the surface roughness. Gunay and Yucel

(2013) estimated the average surface roughness of white cast iron while turning with ceramic and cubic boron nitride tools. It was established that cutting speed and feed significantly affected the surface finish of the machined surface. Apart from these experimental studies, many researchers (Choudhury and El-Baradie, 1997; Risbood *et al*., 2003; Jiao *et al*., 2004; Sahin and Motorcu, 2005; Reddy and Rao, 2006; Jesuthanam *et al*., 2007; Lu, 2008) had predicted the surface roughness in turning. Many soft computing techniques such as neural network, fuzzy logic, genetic algorithms and hybrid network and response surface methodology were used for predicting the surface roughness. Cakir *et al*. (2009) developed a regression model to estimate the surface roughness by considering both the cutting parameter and coating material of the cutting tool insert.

It can be perceived that significant amount of research work has been done on modelling and predicting the surface roughness for various machining processes. One of the methods of improving the surface quality of the turned component is to use multiple tools. This can be realized by making use of more than one tool to machine the workpiece simultaneously. The advantages gained in multi-tool machining process are reduced surface roughness resulting in superior surface finish, shortened machining time, higher productivity and minimal diametral error. In addition the tool life increases due to decreased tool wear. The fatigue life of the component is also increased due to superior surface finish. The overall quality of the machined component is increased. Apart from this, the machining accuracy is also increased in multi-tool machining. It is achieved by reduced dimensional error or dimensional deviation. This aspect is dealt in the subsequent section.

2.5 Dimensional Deviation

In turning dimensional deviation refers to the deviation between the actual dimension and the desired dimension of the workpiece. It is one of the important attributes of the machined product. The cutting forces generated during turning causes the workpiece to deflect which results in machining error. The machining error also depends on the rigidity of the machine tool and its vibration level. Reduction of dimensional error leads to improved machining accuracy. Kops *et al*. (1993) formulated an improved analysis of estimating the workpiece accuracy based on the emerging diameter. It was

stated that the effect of depth of cut is more dominant for slenderness ratio greater than 6. Investigations revealed that for lower slenderness ratio the maximum deflection occurs at tailstock and for higher slenderness ratio it is at 60% of workpiece length from the headstock. Phan *et al*. (2002) developed a new model using FEM to compute the workpiece deflection. All the three force components and three usual methods of mounting the workpiece on a lathe are taken into account. Closed form finite element solutions are derived, which is a function of the cutting tool position.

Mayer *et al.* (2000) proposed a geometric analysis of the elastic deflections of the machine-workpiece-tool system due to the cutting force for predicting the diameter error. It was mentioned that both radial and axial cutting force component are significant. The tangential component of cutting force and the coupling between this force and the actual depth of cut is insignificant. Carrino *et al.* (2002a) proposed a new model to evaluate the machining accuracy and dimensional errors in bar turning. The deflections due to tool, workpiece and work holder was taken into account. The cutting forces were calculated based on unified generalized mechanics of cutting approach. In the second part the same authors, Carrino *et al.* (2002b) validated the proposed model through experimental tests. The workpiece clamped in a chuck, supported between two centres and clamped in a chuck and supported by a centre in the tailstock are the three conditions of workpiece fixturing that was considered in the experiments. A good agreement between the numerical model and experimental results was reported.

Polini and Prisco (2003) compared the bar diameter error calculated by specific cutting resistance model, Kronenberg cutting force model and unified-generalised mechanics of cutting force model. It was mentioned that the experimental results matched with unified-generalised mechanics of cutting force model developed by Armarego. Jianliang and Rondi (2006) developed a model to predict the diametral error of slender bar. The model consists of geometric analysis of diametral error, finite element model of workpiece deflection and statistical model of cutting forces. It was concluded that the diametral error mainly depends on the location of the follower rest, depth of cut and feed. Segonds *et al.* (2006) characterised the slender workpiece flexure during numerical control (NC) turning of an aluminium alloy. It was

mentioned that corrected path compensation program for workpiece flexure could eliminate the need of tailstock centre.

2.6 Chip Morphology

In metal cutting chips are formed due to the deformation of the metal ahead of the cutting tool. Chip formation is caused by the shearing process. Chip formation depends upon the work material, *viz.*, ductile or brittle material. It also depends on cutting speed, feed, depth of cut, cutting tool geometry and lubricant used. The chips are broadly classified into continuous chip, discontinuous chip, continuous with built up edge and serrated chips. Continuous chips are produced while machining ductile metals at high cutting speed and low feed. Discontinuous chips are produced while machining hard and brittle materials like grey cast iron, brass and bronze. Here the feed is higher and the machining is carried out in the absence of coolant with negative rake cutting tool. When a ductile material is machined at low cutting speed and high feed without coolant, continuous chips with built up edge are produced. Serrated chips are formed due to fluctuating high and low shear strain produced while machining titanium alloys, austenitic stainless steel and nickel based super alloys. The type of chip generated during machining can give details about machining process efficiency, tool wear and surface roughness of the machined workpiece.

Huang *et al*. (1996) applied the gradient theory of thermo-viscoplastic instability in simple shear to analyse the chip formation during orthogonal machining. Parameters related to strain hardening and thermal softening were investigated to find the effect of cutting condition on shear localization and shear band formation. It was observed that on increasing feed and decreasing the cutting speed the shear band spacing increased. Katuku *et al*. (2009) studied the chip characteristics while dry turning ASTM Grade 2 austempered ductile iron (ADI) with polycrystalline cubic boron nitride (PCBN) cutting tools under finishing conditions were carried out. The tool wear was related to the chip characteristics. It was noted that at cutting speeds greater than 150 m/min abrasion wear and thermally activated wear were the main wear mechanisms which was caused due to shear localization within the primary and secondary shear zones of chip. It was also reported that cutting speeds between 150 and 500 m/min were optimum for the production of workpieces with acceptable

cutting tool life, flank wear rate and lower dynamic cutting forces. Mian *et al*. (2011) studied the chip formation and associated mechanism in micro cutting of different materials. The wavelet transformation technique was used to decompose acoustic emission (AE) signals generated from orthogonal micro milling. Acoustic emission emanates from rapid release of elastic strain energy within a material under stress which radiates from the source to the surface of the work material. Chip morphology was correlated to the computed energies of the decomposed frequency bands. The utility and importance of AE signals in characterising chip formation in micromachining was revealed. Shashikant *et al.* (2013) investigated the chip segmentation, while machining titanium alloys at elevated temperature (100–350 °C). An optical and scanning electron microscope was employed to study the chips and chip roots. It was found that shear band formation appears to be the dominating mechanism of chip segmentation up to a preheating temperature of 260 °C. The fracture along the shear plane increases at 350 °C. Preheating affects the shear band thickness to a considerable amount and it reduces with the increase in temperature. It also increases the spacing between the shear band thicknesses and reduces the cutting force fluctuation.

It can be observed from these research works that chip features can reveal a lot of information about the machining process. It is also noted that even though a lot of investigation has been done in conventional turning, no work has been reported in double tool turning from the view point of chip morphology. This creates an interest for the author to explore this area.

2.7 Cutting Tool Vibration

Cutting tool vibration plays a major role in determining the surface roughness and tool life. Many attempts have been made by the researchers to correlate tool wear with vibration signal. Mehta *et al*. (1983) investigated experimentally the interaction between the tool wear and the vibrations that occurred during the face milling process. It was shown that an increase in vibration frequency leads to higher tool wear rate, provided the vibration amplitudes are in excess of a certain critical values. Zeng and Forssberg (1994) monitored the grinding parameters by measuring the vibration signals. The time domain wave form was transformed to frequency domain power

spectra. The variations in grinding parameters were related to the changes in the source of vibration signals by principal component analysis. Salgado and Alonso (2006) applied singular spectrum analysis (SSA) to analyse the vibration signals acquired in a turning process to extract information that correlated with the state of the tool. Neural network was used to predict the tool flank wear. In further extension of work by Alonso and Salgado (2008) cluster analysis was used to group the independent frequencies obtain by the decomposition of singular spectrum analysis. Here feed forward back propagation neural network algorithm was used to predict the flank wear. Similarly Risbood *et al*. (2003) predicted the surface finish and dimensional deviation in a turning process by taking into account the acceleration of radial vibration of tool holder. Abu-Mahfouz (2003) analysed the vibration signatures for predicting the wear rate in drilling process. Fast Fourier Transform, power spectral density and wavelet coefficient were estimated and fed as input to a soft computing technique to estimate the flank wear of the drill. For the same process El-Wardnay *et al*. (1996) predicted the drill failure along with the drill wear by recording and analysing the vibration signals. Cepstrum analysis was employed in predicting the drill breakage because of higher accuracy compared with spectral analysis method. On similar lines for an end milling process, Orhan *et al*. (2007) presented the relationship between the cutting tool displacement amplitude, velocity and acceleration with tool wear. It was concluded that the wear rate of the tool can be effectively monitored by the vibration signals. It can be observed from the above literatures that for various conventional machining processes such as turning, grinding, milling and drilling the vibration signals was effectively used to monitor and predict the tool wear as well as tool failure. However, in case of multi-tool turning no work has been reported.

2.8 Research Gaps

Researchers have been fascinated by metal cutting due to its economic and technical importance. Among all the machining process turning is a very widely used process. Many efforts have been directed towards improving the productivity of the process. A small increase in productivity can lead to large amount of cost savings. Multi-tool

turning process has got many advantages apart from increasing the productivity. Researchers need to pay attention to the following aspects of multi-tool turning:

- The machining performance dependents on several parameters. Among them the cutting forces and temperatures generated during process are of prime importance. In this aspect a lot of research work has been done on single tool turning process. Double tool turning remains a less explored area.
- Use of two tools simultaneously improves the product quality in double tool turning process. The diametral error and the tool wear in double tool turning is another domain where there is hardly any documented research work. It offers an ample scope to explore it.
- Surface roughness in double tool turning is an area that has received inadequate attention inspite of its ability to produce good surface finish.

2.9 Scope and Objectives of the Present Work

Based on the literature survey and identified major challenges, it is decided to investigate the following aspects of double tool turning process in this research work:

1. **Experimental investigation on cutting forces and temperature during double tool turning process:**

   The first objective of the present thesis is to study experimentally the effect of cutting speed, feed, depth of cut and tool separation distance on the cutting forces and cutting temperatures generated during the double tool turning process. A theoretical model is developed for conventional turning, to determine the cutting forces and cutting temperature. A comparison is drawn between the experimental results and the theoretical results. The theoretical model can be used to augment the experimental results. This reduces time and avoids the wastage of work material.

2. **Investigations on diametral error, tool wear and chip morphology during double tool turning process:**

   Another major objective of the present thesis is to carry out experimental investigation on diametral error, tool wear and chip morphology. When two tools

are simultaneously engaged for turning, apart from material removal the tools may provide support to each other. Thus the diametral error may reduce and lead to increased machining accuracy. Since the depth of cut is distributed over two cutting tools, the cutting force can reduce. This can decrease the tool wear and increase the tool life. Apart from this, the chip morphologies of the chips generated by front and rear cutting tool are also studied.

3. **Experimental investigation on the effect of machining parameters on surface roughness generated during double tool turning process:**

   The last objective of the research work deals with surface finish aspect. Usage of multiple tools is expected to improve the surface finish. In the present research work the effect of cutting speed, feed, depth of cut and tool separation distance on surface roughness of grey cast iron and AISI 1050 steel is studied.

The flow chart showing the research plan is presented in Figure 2.1.

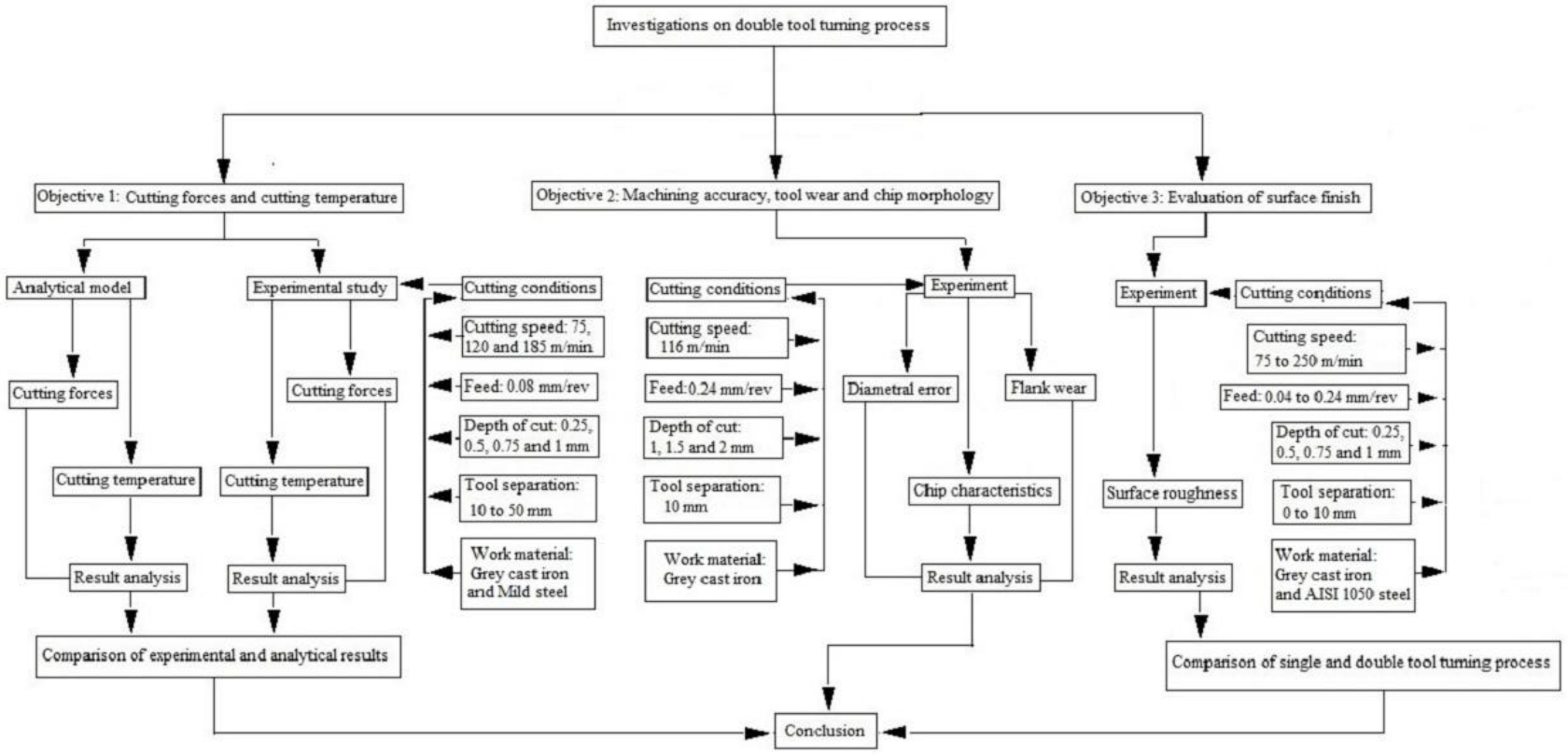

Figure 2.1 Flow chart of research plan

Chapter 3

Details of Experiments

3.1 Introduction

In the present research work, double tool turning process is evaluated through experiments. In order to perform double tool turning process, a conventional lathe was modified (Yatin, 2013; Ramanuj, 2013). A tool holding fixture was fabricated and attached to the rear side of the lathe carriage in addition to the front side cutting tool. The main process parameters in double tool parallel turning are cutting speed, feed, depth of cut and separation distance between the two cutting tools. Cutting forces, cutting temperature, cutting tool vibration, diametral error, cutting tool wear and surface roughness are measured during the experiments. In this chapter the development of cutting tool fixture along with the experimental setup is described. The procedure for the measurement of cutting forces, cutting temperature, cutting tool vibration, diametral error of the workpiece, tool wear and surface roughness of the workpiece are also explained.

3.2 Development of Cutting Tool Fixture

In order to hold the rear cutting tool a fixture is developed. The front and rear tool holding assembly is shown in Figure 3.1.

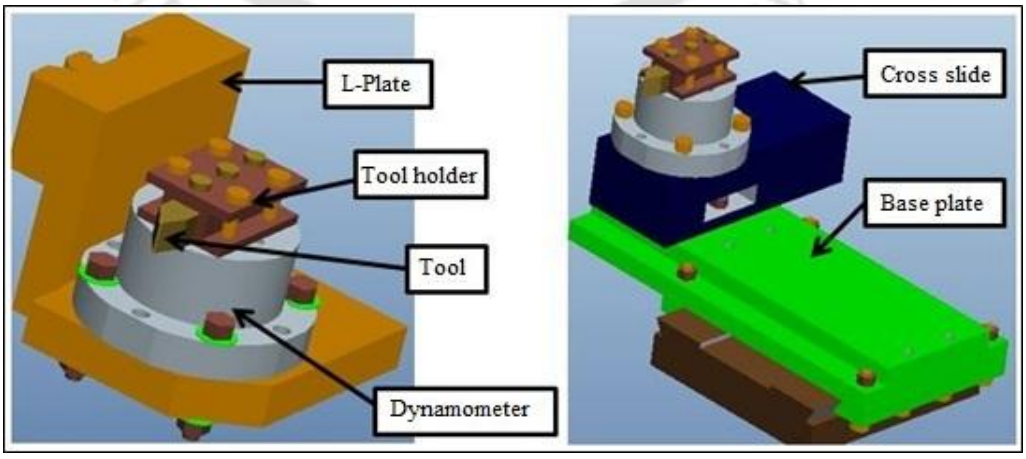

Figure 3.1. Front and rear tool holding assembly

Apart from the present Ph.D. work, 4 M.Tech. students have worked on this setup (Yatin, 2013; Ramanuj, 2013; Vaibhav, 2014; Sandeep, 2015). The front cutting tool is fixed to a tool holder. The tool holder is attached to a dynamometer. The dynamometer is mounted over a mild steel fixture which was already available. Considering the economy of resources and time, it was decided to use it. The rear tool holding assembly consists of a base plate over which a cross-slide is attached. A dynamometer is mounted over the cross-slide. A tool holder holding the rear cutting tool is attached to the dynamometer. The rear cutting tool fixture is attached to the conventional lathe carriage at the rear side. The front cutting tool has independent feed and depth of cut. The rear cutting tool has the same feed as that of the front cutting tool as they are mounted on the same carriage. The depth of cut of the rear cutting tool can be varied by means of independent cross-slide. Hence the depth of cut of the front and rear cutting tool can be individually controlled, enabling equal or unequal depths of cut for front and rear cutting tools. The distance between the front and rear cutting tool is known as tool separation distance and this can be varied by moving the cross-slide of the front cutting tool. In this arrangement the front cutting tool always precedes the rear cutting tool. The tool separation distance can also be kept zero so that synchronous turning can be achieved. Thus by means of these tool fixtures, double tool parallel turning operation was performed in a conventional lathe.

3.3 Experimental Setup

The photograph of the experimental setup is shown in Figure 3.2. The turning experiments were carried out on a high speed precision lathe (Make: HMT, Model: NH-26). It is a high precision, high rigidity and high speed lathe consisting of wide bed and short spindle. A 3-phase 11 kW induction motor is used to drive the spindle of the lathe. The lathe has 23 different speeds ranging between 40−2040 rpm and 27 different feeds ranging from 0.04−2.24 mm/rev. The workpiece is mounted between a chuck and a revolving centre of the tailstock. The experimental setup is developed to measure cutting forces, cutting temperature, cutting tool vibration and the diametral error of the workpiece. In the present study, cylindrical bars of grey cast iron and AISI 1050 steel are used as work materials. The workpieces are of round bar of various diameters ranging from 50 to 75 mm with a length of 250 mm. The

composition of work materials was determined by energy-dispersive X-ray spectroscopy (EDS) using a scanning electron microscope (Make: LEO, Model: 1430vp) and is reported in Table 3.1. AISI 1050 is a standard grade carbon steel and has numerous applications. It is used for axles, bolts, forged connecting rods, crankshafts, gears and torsion bar. It is relatively easier to machine and produces continuous chips under steady state machining condition. Grey cast iron is a widely used cast material. It is used as a cylinder block in internal combustion engines, pump housing, machine tool bed and casing of rotors. It has got good machinability and produces discontinuous chips under steady state machining condition.

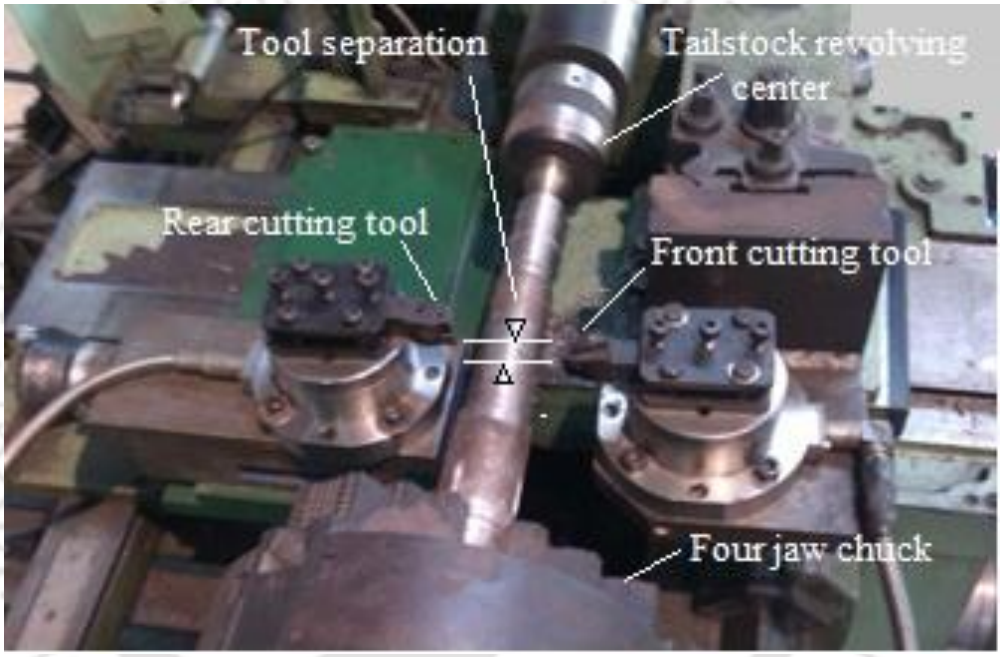

Figure 3.2. Experimental setup of double tool turning process

Table 3.1. Composition of the work material

Work material	Weight percentage of elements					
	C	Si	P	S	Mn	Fe
Grey cast iron	3.65	1.4	0.12	0.35	0.56	Balance
AISI 1050	0.55	-	0.04	0.05	0.06	Balance

Selection of correct cutting tool for machining is of great importance. Recently multi-layer coatings are used for machining steel and cast iron. They are mainly used in high speed machining process. The cutting conditions are chosen based on the rear

tool fixture rigidity. The upper limit of cutting speed was fixed as 250 m/min. The depth of cut was limited to the maximum of 2 mm for each tool by considering the cutting tool vibration and workpiece surface roughness. All the experiments were carried out under dry conditions. For machining the work materials at these cutting conditions TiN coated tungsten carbide was found suitable and hence it was used. The cutting tool insert specification was WNMG 080408 KM 4235 and the corresponding tool holder is DWLNR 2020 K08 (Make: Sandvik). The triangular shaped inserts are rigidly mounted on the tool holder by mechanical clamping. The rigidity of the front tool holder was higher than the rear tool holder. The cutting tool geometry as per ISO 3002/1-1982 is as per Table 3.2.

Table 3.2. Cutting tool signature

Inclination angle i	7°
Normal rake angle γ_n	4°
Normal clearance angle α_n	6°
Auxiliary normal clearance $\alpha_{n'}$	2°
Auxiliary cutting edge angle κ_a	5°
Principal cutting edge angle κ_p	95°
Tool nose radius r_n	0.8 mm

3.4 Measurement of Cutting Forces and Cutting Temperature

The cutting performance was mainly evaluated by measuring the cutting forces and cutting temperatures. The Figure 3.3 shows the schematic diagram for simultaneous measurement of cutting forces and cutting temperature.

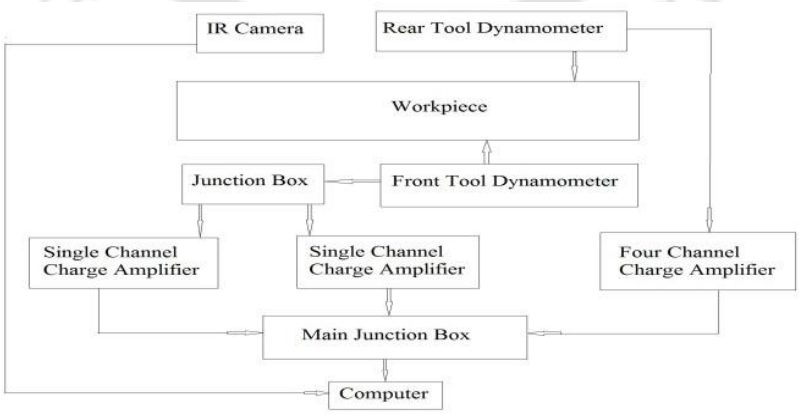

Figure 3.3. Schematic diagram of measurement of cutting forces and temperature

(a)

(b) **(c)**

Figure 3.4. Force measurement system **(a)** Four component dynamometer **(b)** Single channel charge amplifier **(c)** Four channel charge amplifier

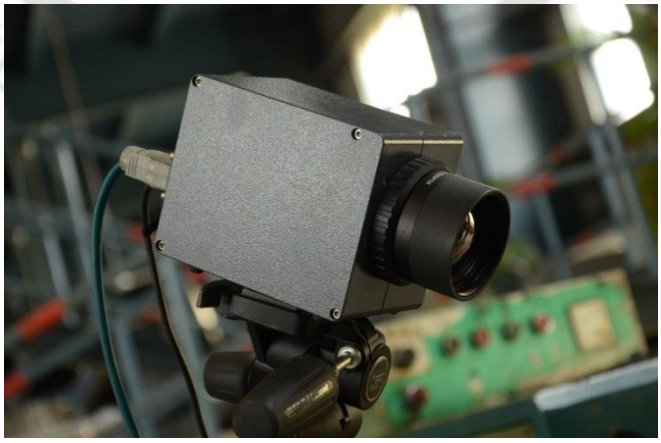

Figure 3.5. Infrared camera for temperature measurement

A four component piezoelectric type dynamometer (Make: Kistler, Model: 9272) was used to measure the main cutting force (F_z) and the feed force (F_x). It is shown in Figure 3.4 (a). Two dynamometers were used to measure the cutting forces of front and rear cutting tool simultaneously. The dynamometer has a threshold of 0.01 N along the feed force direction and 0.02 N along the main cutting force direction. It has a linearity of ±1% of the full scale output. The front cutting tool dynamometer is connected to two single channel charge amplifiers (Make: Kistler, Model: 5015) as shown in Figure 3.4 (b). The rear cutting tool dynamometer is connected to integrated four channel charge amplifier (Make: Kistler, Model: 5070) as shown in Figure 3.4 (c). The charge amplifier was calibrated and set to measure force ranging from 0 to 1000 N along the feed direction and 0 to 2000 N along the cutting direction. The sensitivity values are set as −3.626 pC/N for F_x and −7.627 pC/N for F_z component. For all the experimental measurements (force, surface temperature and surface roughness) at least three trials were conducted and the average value was used for further analysis. In most of the cases, the repeatability error was less than 10%. The main junction box receives the force signals from these charge amplifiers and sends to the computer. DynoWare software was used for acquisition of force signals and storing it. The cutting temperature plays a major role in machining. Tool work thermocouple and Infrared cameras are widely used for measuring the cutting zone temperature. The latter has more advantages than the former in terms of accuracy and sensitivity. In the present work, an Infrared camera is used to determine the average temperature of the cutting zone. Figure 3.5 shows the photograph of InfraTec varioCAM hr head 400 IR uncooled camera with measuring range from –40 °C to 2000 °C and a sensitivity of 30 mK at 30 °C. With regard to calibration, the IR camera was calibrated for ice point of 0 °C and steam point of 100 °C.

3.5 Measurement of Cutting Tool Vibration

The cutting tool vibration along the direction of main cutting force was measured. For measuring vibration signals, accelerometers (Make: Bruel & Kjaer, Model: 4395) were mounted on both the cutting tools. Figure 3.6 shows the arrangement of the accelerometers used for measuring the vibration signals of front and rear cutting tools.

The sensitivity of the accelerometer is 0.991 mV/g. It has a measuring range of ±7500 m/s^2. The measurement frequency ranges of the accelerometers are from 0.3 Hz to 18 kHz. The sampling rate was fixed as 16 kHz. A four channel charge amplifier (Make: Bruel & Kjaer, Model: 2692-A-0I4), data acquisition system (Make: National Instruments, Model: USB-6212) and NI LabVIEW 2009 software was used for processing the acquired vibration signals. The data acquisition system has 16 channels.

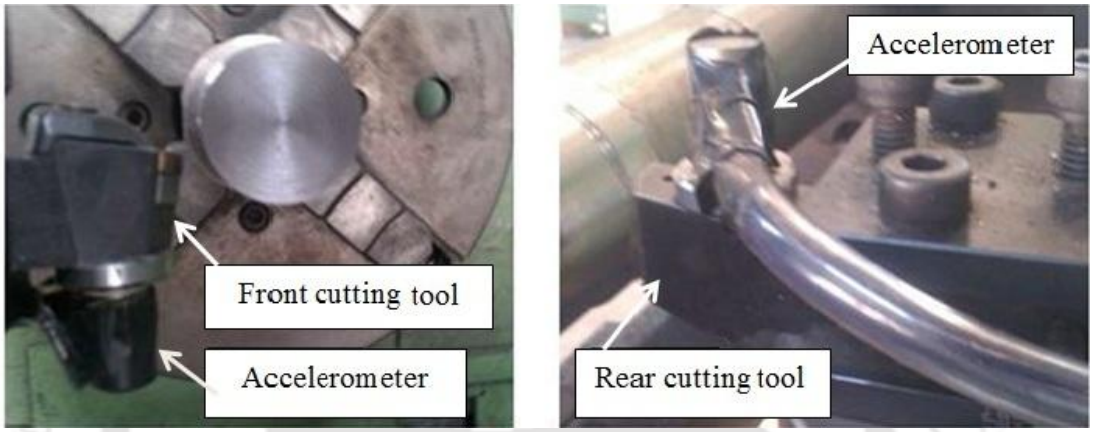

Figure 3.6. Arrangement of accelerometers

The acceleration along the tangential direction to cutting was measured for both the front and rear tool as it is a dominant signal compared to the feed and radial direction. Output of the accelerometers was acquired in a PC through charge amplifier and data acquisition system. The front and rear cutting tools that are mounted on the tool holder had an overhang of 30 mm which in turn is attached with accelerometers. The accelerometers were attached to the tool shank near the cutting edge. The time domain and frequency domain plots of front cutting tool and rear cutting tool vibration were obtained for various cutting conditions.

3.6 Measurement of Diametral Error of Workpiece and Cutting Tool Wear

In turning process, the cutting forces acting on the workpiece cause deviation from the desired diameter. This deviation is called diametral error; it is mainly influenced by the radial component of the cutting force. The diametral error is measured by a dial gauge (Make: Mitutoyo) having an accuracy of 1 µm. The dial gauge is moved from tailstock to chuck without removing the workpiece from the chuck. The workpiece is

divided into 11 equal divisions for a length of 220 mm. For every division, the work piece was rotated by 60° and the diametral deviation was measured on six equidistant points on the circumference and average value was recorded. The machining experiments were repeated three times and a good repeatability was observed.

Figure 3.7. Diametral error measurement by dial gauge

Figure 3.8. Tool maker's microscope

Figure 3.9. Scanning electron microscope

Figure 3.7 shows the diametral error measurement by a dial gauge when the workpiece is held between the chuck and the revolving centre of the tailstock. The tool life and tool wear are the most vital machining performance indicators. The conventional tool wear parameters are flank wear land and crater wear depth. In this research, the crater wear was negligible as coated tool was used. Hence the tool wear was evaluated in terms of flank wear. The cutting tool insert's flank was periodically measured with the aid of tool maker's microscope (Make: Mitutoyo, Model: TM-505) to determine the flank wear. At the end of machining experiments, cutting tool inserts and collected chips were observed under the scanning electron microscope (Make: LEO, Model: 1430vp). Figure 3.8 and Figure 3.9 shows the photograph of tool maker's microscope and scanning electron microscope.

3.7 Surface Roughness Measurement

Surface roughness is an important factor that determines the quality of a machined surface. It depends on many parameters such as cutting condition, machine tool vibration, cutting tool and work holding devices. The cutting speed, feed and depth of cut has a major influence on the surface roughness of the finished component. A lot of research work has been directed towards improving the surface quality of the machined component. The surface roughness was measured by Pocket Surf (Make: Mahr GMBH) and it is shown in Figure 3.10. The stylus moves along the length of the workpiece in the direction of feed.

Figure 3.10. Surface roughness measurement by Pocket Surf

The evaluation length was taken as 2.4 mm with cut off length as 0.8 mm. The surface roughness was measured at three different locations on the machined surface and the average was taken. Additionally a 3D profilometer (Make: Taylor Hobson) was also used for surface roughness measurement. It is shown in Figure 3.11. The scanned area for 3D surface roughness measurement was 0.8 mm X 0.8 mm.

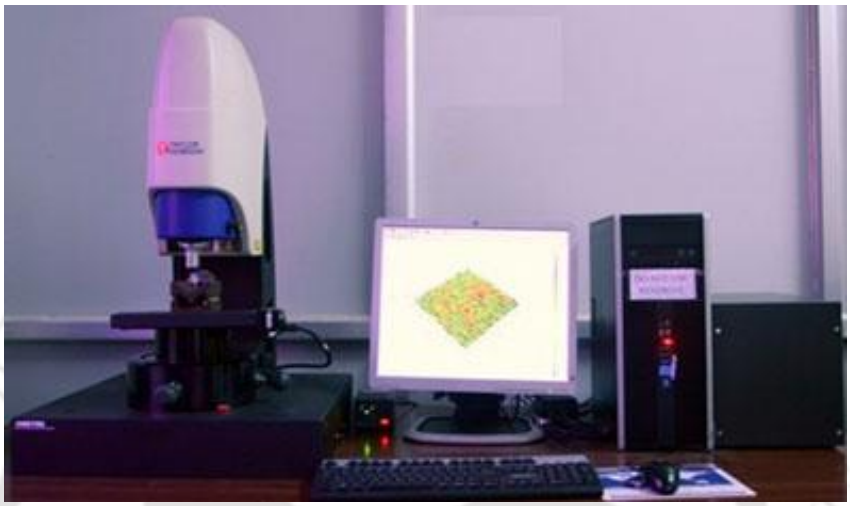

Figure 3.11. Surface roughness measurement by 3D profilometer

3.8 Conclusion

In this chapter details of experiments are explained. The fixtures holding the cutting tools were fabricated. An experimental setup for performing double tool turning process was developed by modifying a conventional centre lathe. The methodology for the simultaneous measurement of cutting forces and cutting temperatures were presented. The procedure for the measurement of cutting tool vibration, tool wear, diametral error and surface roughness is also presented. The photographs of the instruments used for the measurement of the above mentioned parameters are shown. Metal cutting experiments are performed for various cutting conditions. The effect of the cutting conditions on cutting forces, cutting temperatures and cutting tool vibration are discussed in Chapter 4.

Chapter 4

Cutting Forces, Cutting Temperature and Cutting Tool Vibration in Double Tool Turning Process

4.1 Introduction

Significant amount of research work has been carried out to understand the importance of the cutting forces and cutting temperature in the conventional turning process. The present study focuses on multi-tool turning operation, as turning is a fundamental machining process. Multi-tool lathes were used widely in the industries to improve the productivity, before the advent of computer numerically controlled machines. The research works on multi-tool machining were mainly directed towards optimisation of process parameters. However, no attempts were made to understand the cutting forces and temperature due to the usage of multiple cutting tools. From the Chapter 2 on literature survey, it was observed that no work has been carried out to understand the influence of cutting parameters such as cutting speed, feed, depth of cut and tool separation distances on cutting forces and temperature in the double tool turning process, although a lot of work has been carried out on single tool machining.

In this research work, an attempt is made to understand the effect of front cutting tool forces and temperature on the rear cutting tool. In this work, two single point cutting tools were utilised for turning grey cast iron at various cutting speeds, depths of cut and distances between the cutting tools. Further for single tool turning process, an analytical model based on ductile fracture mechanics was developed and experiments were also performed with mild steel. It was used to estimate the cutting forces and cutting temperature for mild steel. The analytical model helps in providing theoretical explanation for the experimental results. In addition to cutting forces, cutting tool vibration is of vital importance as it plays a major role in determining the surface roughness of the machined component. Hence it becomes essential to study the effect of cutting conditions on cutting tool vibration. The present research work

also attempts to understand the effect of cutting speed and tool separation distances over the vibration behaviour of the front cutting tool and rear cutting tool during the double tool turning process.

4.2 Experimental Procedure

The experimental methodology is described in this section. The cutting conditions employed and the work and cutting tool materials used in metal cutting experiments are also mentioned.

4.2.1 Experimental Setup

Multi-tool turning experiments were conducted on a modified centre lathe (Make: HMT, Model: NH-26). The details have been mentioned in Section 3.3 of Chapter 3. Figure 4.1 shows the photograph of the experimental setup along with two cutting tools. A tool fixture developed by Yatin *et al*. (2013) was mounted on the rear side of the lathe carriage to hold the second cutting tool.

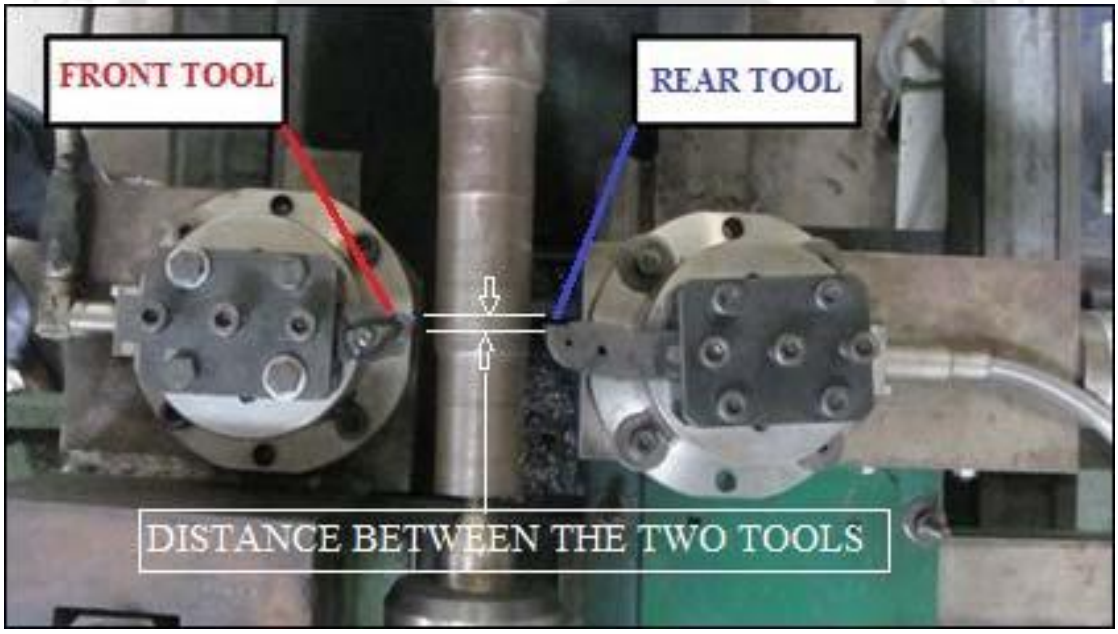

Figure 4.1. Experimental setup showing front and rear cutting tools

Figure 4.2 shows the cutting force signals of the front and rear cutting tools during turning for the specified cutting conditions. The cutting force (F_z) and feed force (F_x) of the front cutting tool and rear cutting tool was measured by two individual four component piezoelectric dynamometer (Make: Kistler, Model: 9272).

Since the rear cutting tool is kept in an inverted position, the direction of cutting force of rear cutting tool is opposite to the front cutting tool. This can be noted from Figure 4.2. The cutting force fluctuations is more for the front cutting tool as it is mounted over the fixture made of steel, whereas the rear cutting tool is mounted over the fixture made of cast iron leading to lesser vibrations and lesser force fluctuations.

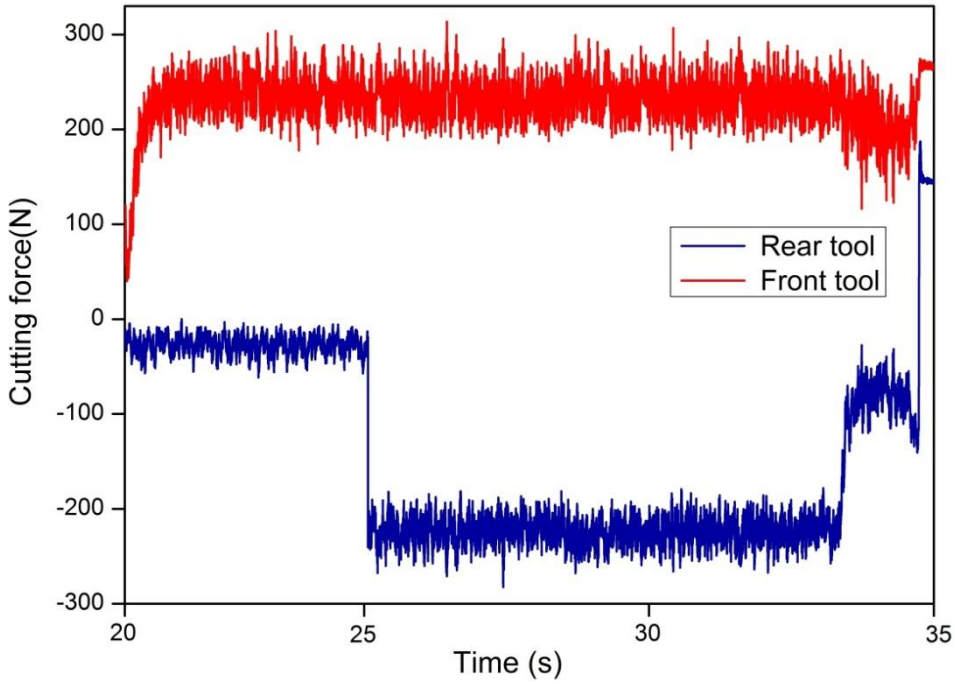

Figure 4.2. Measured cutting forces in the double tool turning of grey cast iron (75 m/min cutting speed, 0.08 mm/rev feed, 1 mm depth of cut, 2 mm distance between cutting tools and 58 mm workpiece diameter)

Accelerometer was used to measure the acceleration along the cutting direction for both the front cutting tool and rear cutting tool. The vibration signal along this direction is found to be most influential compared to the feed and radial direction. The time domain and frequency domain plots of front tool for a cutting speed of 75 m/min, 0.08 mm/rev feed and 1 mm depth of cut are shown in Figure 4.3 and Figure 4.4. The time domain vibration signals are converted to frequency domain signals by Fast Fourier Transform to reveal its power spectral density. It is observed that vibrations are predominant at 4000 Hz frequency. The cutting tool overhang distance also plays a major role in determining the magnitude of tool vibration. In the present work an overhang distance of 30 mm is kept for both front and rear cutting tool. The fundamental frequency of the front and rear cutting tool are obtained by excitation test and its value was found to be 337 Hz and 417 Hz respectively.

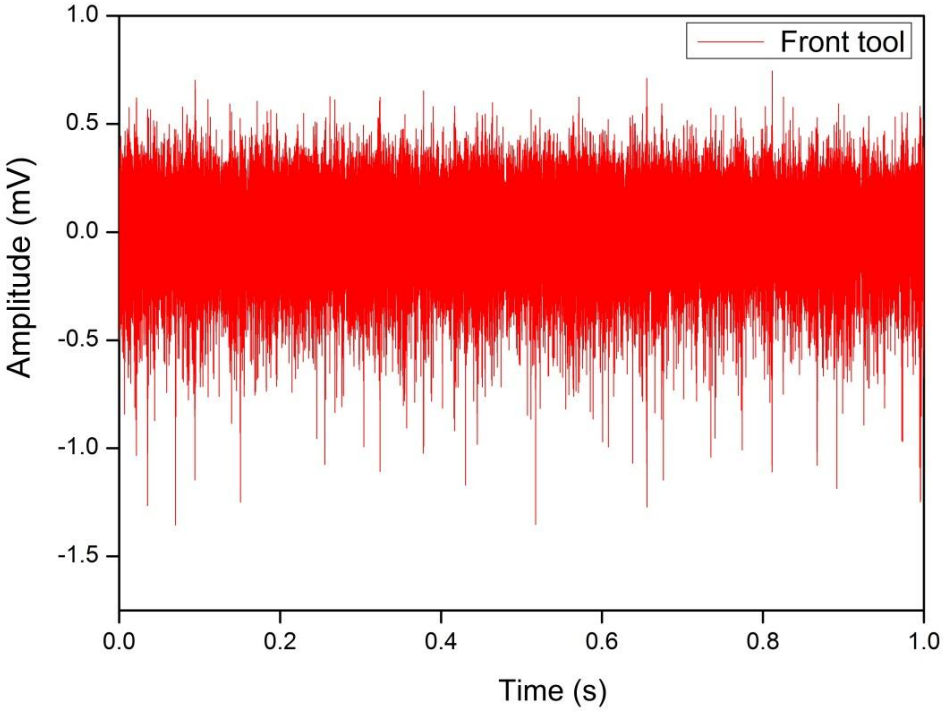

Figure 4.3. Time domain vibration signal of front cutting tool while turning grey cast iron (75 m/min cutting speed, 0.08 mm/rev feed, 1 mm depth of cut, 2 mm tool separation distance and 58 mm workpiece diameter)

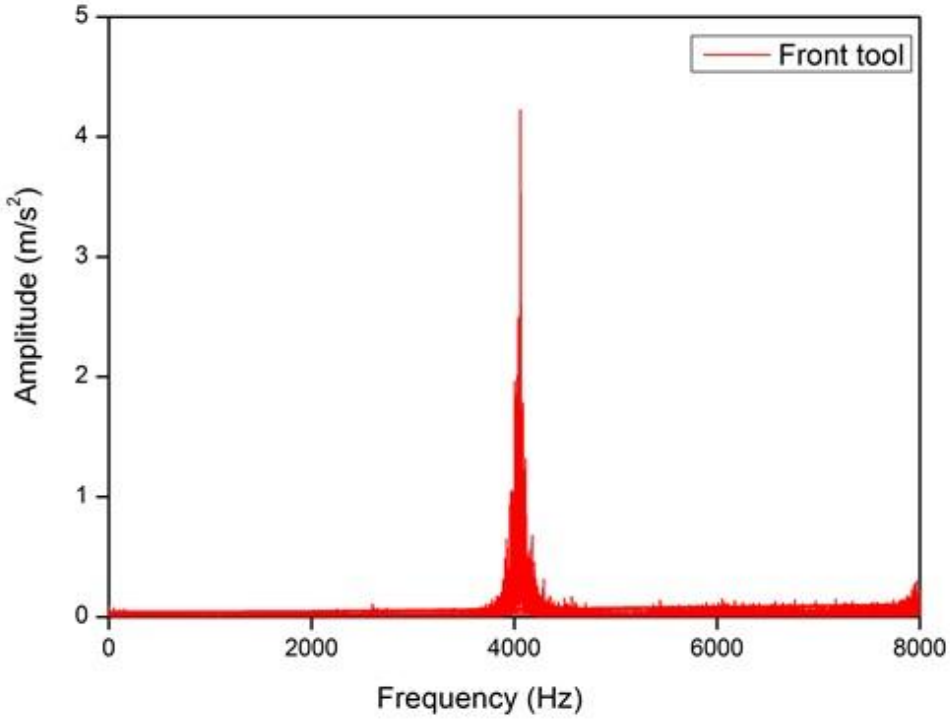

Figure 4.4. Frequency domain vibration signal of front cutting tool while turning grey cast iron (75 m/min cutting speed, 0.08 mm/rev feed, 1 mm depth of cut, 2 mm tool separation distance and 58 mm workpiece diameter)

4.2.2 Workpiece and Cutting Tool Material

Grey cast iron and mild steel rods of 58 mm diameter and 250 mm length were taken as work material for turning operation. The machining length was kept as 150 mm, due to the constraint imposed by the front tool dynamometer. The workpiece was held between the chuck and tailstock. For the front and rear cutting tools WNMG 080408 KM 4235 TiN coated carbide inserts (Make: Sandvik) were used. The corresponding tool holder is DWLNR 2020 K08 (Make: Sandvik). The cutting tool signature is mentioned in Table 3.2 of Chapter 3. The TiN coated tungsten carbide inserts were selected as the cutting speeds during machining were below 200 m/min.

4.2.3 Cutting Conditions

Machining was performed at cutting speeds of 75, 120, and 185 m/min and at a feed of 0.08 mm/rev. The depth of cut was taken as 0.25, 0.5, 0.75 and 1 mm individually and kept equal for the front and rear cutting tools. The distance between the two cutting tools was varied to the maximum of 50 mm and machining was carried out under dry conditions as the graphite present in grey cast iron acts as a lubricant.

4.3 Results and Discussion

In machining, measurement of cutting force helps in estimating the power consumption. In the present study, when both the front and rear cutting tools are engaged simultaneously in turning operation and are separated by certain distance between them, it is logical to investigate the effect of the distance between cutting tools over the force components.

4.3.1 Effect of Distance Between Cutting Tools on Cutting and Feed Forces

To understand the effect of distance between the cutting tools on the cutting forces, the distance between the cutting tools was varied from 10 mm to 50 mm in the interval of 10 mm, while turning grey cast iron. A depth of cut of 1 mm was given individually to both the front and rear cutting tools and a constant feed of 0.08 mm/rev was maintained for all the experiments. The variation of cutting force (F_z) and feed force (F_x) components with the distance between the front and rear cutting

tools is illustrated in Figure 4.5 and Figure 4.6. The experimental data were best fitted with polynomial curves of third order with high value of coefficient of determination (R^2).

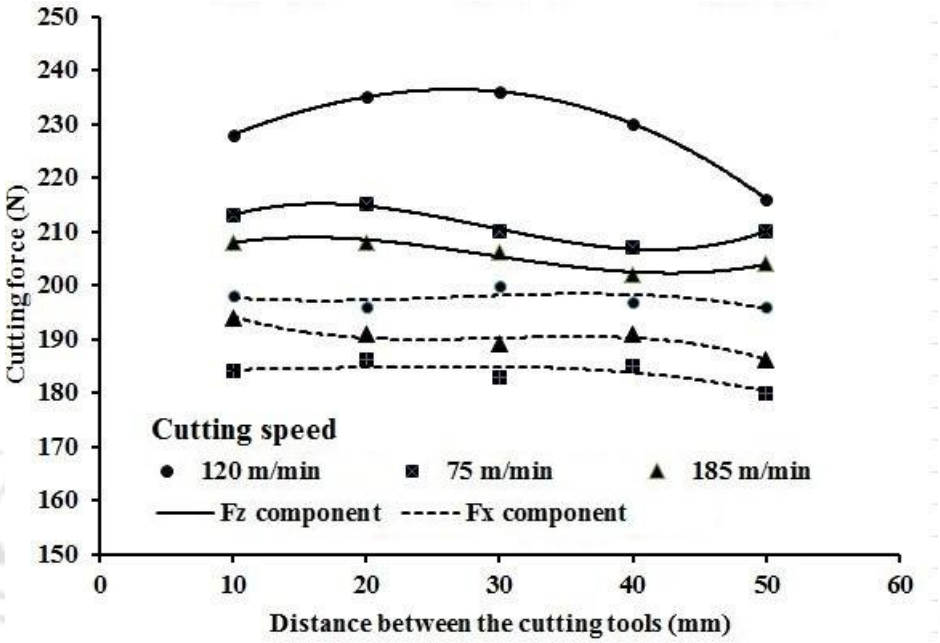

Figure 4.5. Effect of cutting speeds over cutting forces on the front cutting tool while turning grey cast iron (0.08 mm/rev feed and 1 mm depth of cut)

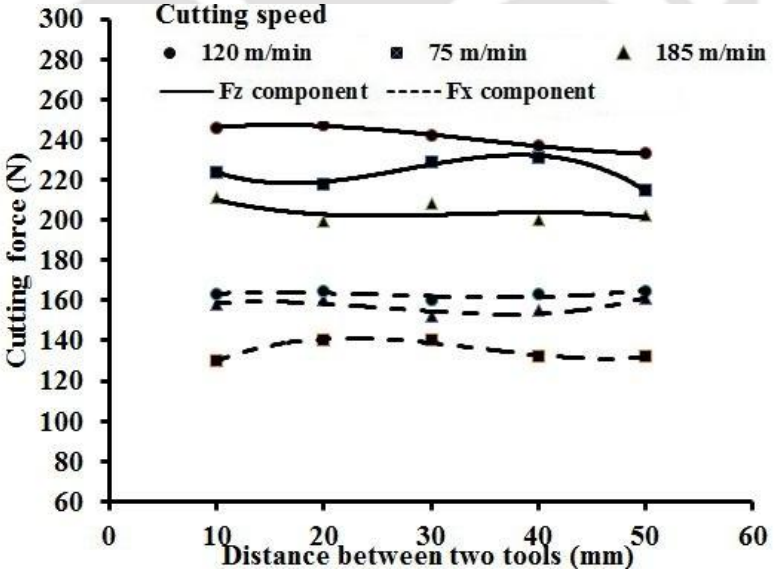

Figure 4.6. Effect of cutting speeds over cutting forces on the rear cutting tool while turning grey cast iron (0.08 mm/rev feed and 1 mm depth of cut)

For both the front and rear cutting tools, there is a slight variation (around 10%) in the main cutting force component (F_z) for the distances ranging from 10 mm

to 50 mm. This variation may be due to non-uniform material properties. On the other hand, there is significant variation of cutting forces with the cutting speed. The cutting force values were the highest at the cutting speed of 120 m/min. This type of behaviour, i.e., the lesser cutting force values at low and high speed is common in metal cutting (Dearnley, 1985; Yigit *et al*., 2008; Camusu 2008). It may be due to built up edge formation at the intermediate cutting speed (Trent and Wright, 2000). At high cutting speed, the cutting temperature increases and this reduces the shear yield strength of the material at the primary deformation zone. Hence, the cutting forces are the lowest at 185 m/min. At a low cutting speed of 75 m/min, friction and vibration are lesser. Hence, in this condition also the cutting forces are lower, although more than 185 m/min cutting speed.

The feed force component (F_x) of the front and rear cutting tools was almost independent of distance between the tools. For the front cutting tool, the cutting force was the lowest at 185 m/min, whilst the feed force was the lowest at 75 m/min. On the other hand, for the rear cutting tool both the forces are the lowest at 185 m/min. The maximum and minimum feed forces obtained are 200 N and 180 N for front tool (Figure 4.5). The corresponding values for rear tool are 165 N and 130 N (Figure 4.6). It is interesting to note that ratio of feed force to cutting force varies from 0.84 to 0.93 for front cutting tool and 0.63 to 0.74 for rear cutting tool. The ratio of feed force to cutting force gives an indication of friction during machining. The greater is the friction due to flank wear, the more is the ratio of feed force to cutting force (Yellowley and Lai, 1993). A simple Merchant's analysis considering obliquity provides the average equivalent coefficient of friction for front tool as 0.8 and for rear tool as 0.6. Incidentally, it was reported long back that in orthogonal cutting the coefficient of friction varies between 0.5 and 1.0 (Chisholm, 1951). It is expected that the rear tool will encounter lesser friction, as the front tool cleans the machined surface and helps in bringing out graphite on the surface. At the same time, due to the inhomogeneous nature of grey cast iron, inner layers are softer. The net effect is that on an average rear tool experience lesser force. Irrespective of the distances between the cutting tools, for a particular machining condition the feed force remains constant. It is influenced a lot by the flank wear. However, in the present work, the wear of the cutting tool has no influence on the cutting forces because the insert is replaced after

each pass of machining. From this, it is inferred that the forces are independent of the distances under the range of cutting conditions in which the experiments were carried out.

4.3.2 Effect of Depth of Cut and Cutting Speed on the Forces for 2 mm Distance Between the Cutting Tools

Tables 4.1 shows the average cutting forces and feed forces at four depths of cut at a cutting speed of 75 m/min. The distance between the cutting edges of front and rear cutting tool was 2 mm. Equal depth of cut was assigned for both the tools.

Table 4.1. Effect of depth of cut on cutting and feed force in double tool turning of grey cast iron (75 m/min cutting speed, 0.08 mm/rev feed and 2 mm distance between cutting tools)

Depth of cut (mm)	Cutting force (N)		Feed force (N)	
	Front tool	Rear tool	Front tool	Rear tool
0.25	69	53	42	27
0.50	112	99	95	60
0.75	163	154	152	143
1.0	232	193	178	144

It was observed that repeatability of force measurement is about ± 10%. The reason for keeping a lesser distance between the cutting tools was to derive some benefit from the preheating effect of front cutting tool in reducing the forces of rear cutting tool. The reduction in cutting and feed forces was obtained for the cutting speed of 75 m/min. For cutting speeds of 120 m/min and 185 m/min, 1 mm depth of cut and 2 mm tool separation distance reduction in rear cutting tool feed forces was observed. This is revealed in the Figure 4.7. The error bars in the figure indicate ±10% variation in forces.

Reduction in the equivalent coefficient of friction seems to be the main factor for reducing the forces, not the temperature. Astakhov (2011) argued that

conventional metal cutting is a cold working process and maximum temperature in the deformation zone normally does not exceed 200 °C, although the chip temperature may be much higher. As per the ideal mechanistic model (Kapoor *et al*., 1998) the cutting force components should vary linearly with the depth of cut as the uncut chip area increased in that proportion. In practice due to size effect, presence of cracks and several kinds of non-homogeneities, the exact linear proportionality is not maintained.

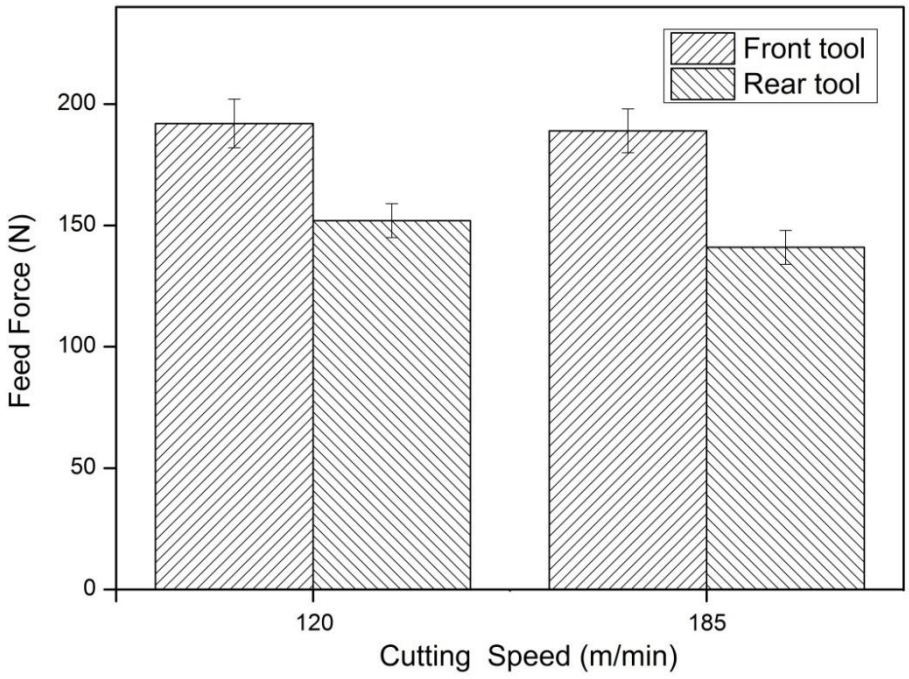

Figure 4.7. Variation of feed force in double tool turning of grey cast iron (0.08 mm/rev feed, 1 mm depth of cut and 2 mm distance between the two cutting tools)

Following relation was fitted between force component and depth of cut.

$$F = ad^{b}, \tag{4.1}$$

where F is the force component, d is the depth of cut, a is the proportionality constant and b is the exponential constant. For the main cutting force at the cutting speed of 75 m/min, the values of b are 0.86 and 0.95 for front and rear tools, respectively. The corresponding values for feed force component are 1.1 and 1.3, respectively. This indicates that as a first approximation, the linear relation between force components and depth of cut is justified. This is more so in the case of cutting force, as the feed force is influenced a lot by friction forces, which distorts linearity.

4.3.3 Effect of Distance Between the Front and Rear Cutting Tools on the Cutting Temperature

In the double tool turning, the effect of cutting speed and depth of cut on the cutting and feed forces are similar to the conventional turning process. By utilising two cutting tools, the rate of material removal and hence productivity can be doubled. The relative position of one cutting tool with respect to the other cutting tool is an additional parameter in addition to the conventional turning parameters. Hence, an attempt has been made to understand the effect of distance between front and the rear cutting tool on cutting temperature. Figure 4.8 shows the effect of distance between two cutting tool and cutting speed on the workpiece temperature. With the increase in cutting speed, workpiece exhibited an increase in temperature; however no effect of distance between two cutting tools was observed.

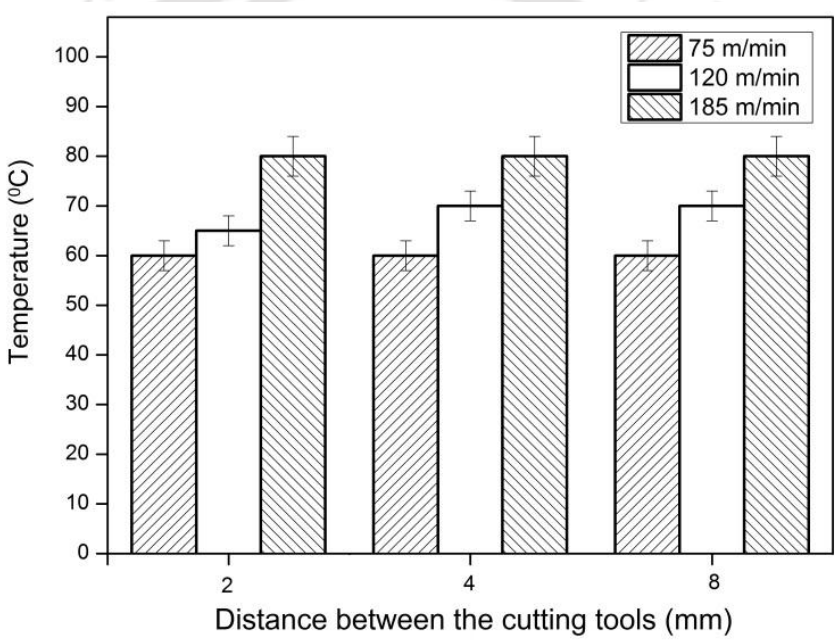

Figure 4.8. Effect of cutting speed and distance between the front and rear cutting tools on work material surface temperature

Figure 4.8 reveals that the workpiece temperature increased from 60 °C to 80 °C when the cutting speed was increased from 75 to 185 m/min. The high metal removal rate caused high rate of plastic deformation contributing to more heat generation. Figure 4.9 shows the thermographic view of two cutting tools at cutting speed of 75 m/min, feed of 0.08 mm/rev, depth of cut of 1 mm for both the front and rear cutting tools and 2 mm distance between the cutting tools. Figure 4.10 represents the temperature rise of the workpiece. The region A corresponds to the initial

temperature of the workpiece at a particular location. The region B represents the temperature rise caused by the first cutting tool at that location. The region C is the dwell period between passing of the front tool and the arrival of the rear tool. The region D represents the temperature rise caused due to the second cutting tool. The instantaneous field of view keeps changing as the cutting zone moves during the turning process. This may result in operating the IR camera operating out of its spatial resolution capabilities. This results in low temperature of the thermographic image. Moreover, due to the presence of chips and tool flank at the cutting zone, the IR camera can capture only the workpiece temperature in the vicinity of cutting zone. Thus, these temperatures should be treated as workpiece temperature. A small portion of heat generated during cutting goes into the workpiece. This gets diffused into the workpiece quickly due to high thermal diffusivity. Hence, only a small portion of heat developed due to cutting by one tool is available at the other cutting zone. Thus, no appreciable effect of separation distance of the tools is observed on the temperatures in the vicinity of two cutting zones.

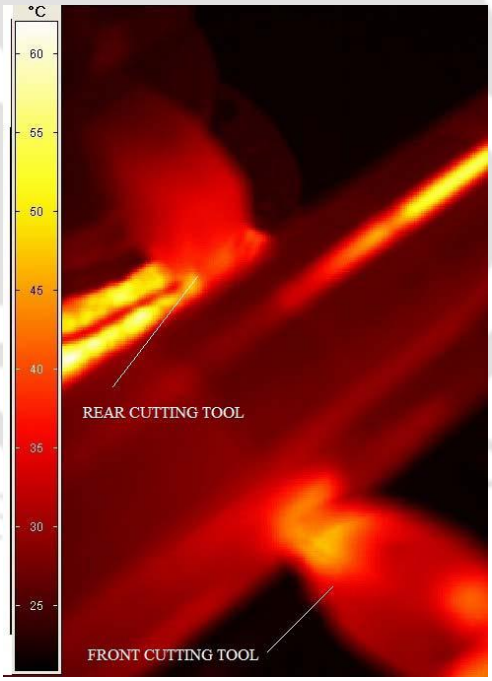

Figure 4.9. Thermographic image while machining grey cast iron with coated carbide front and rear cutting tool (75 m/min cutting speed, 0.08 mm/rev feed, 1 mm depth of cut and 2 mm distance between cutting tools)

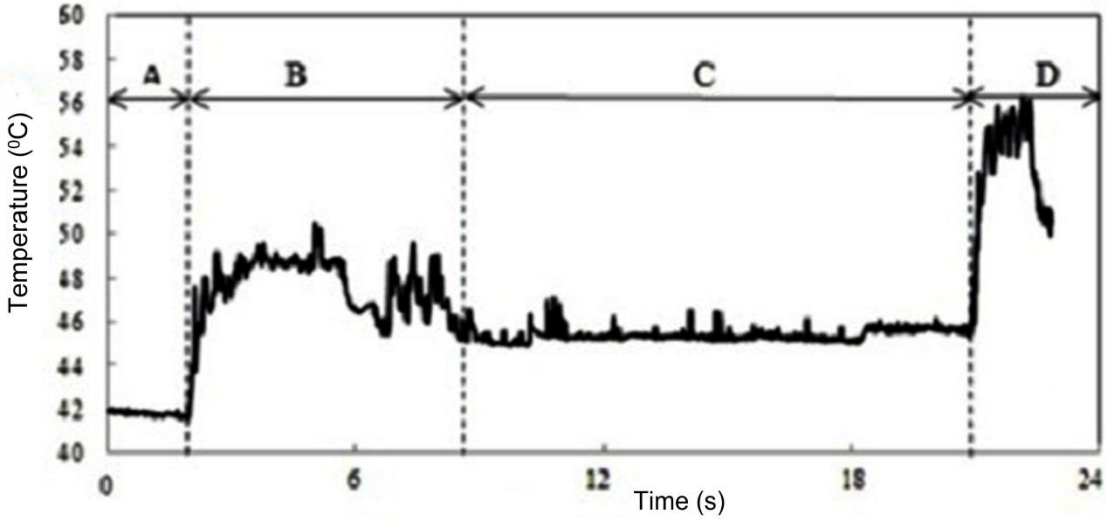

Figure 4.10. Surface temperature of work material at various periods of machining

4.4 Estimation of Cutting Forces and Cutting Temperature in Single Tool Turning with a Simplified Model

Estimating the cutting forces helps in determining the power consumption during the process. Atkins (2003) published a paper on the modelling of metal cutting using modern ductile fracture mechanics. According to this theory, the work required for machining comprises the following three components: (1) work required for plastic deformation along the shear plane, (2) work due to friction at tool-chip interface and (3) work due to the formation of new cut surface. Equating the total work to the work supplied by the cutting tool, the expression for cutting force F_c is obtained as

$$F_c = wt_0 Y_s \frac{\cos(\beta-\alpha)}{\sin\phi\cos(\phi+\beta-\alpha)}\left(1+\frac{R\cos(\alpha-\phi)\sin\phi}{t_0 Y_s\cos\alpha}\right), \tag{4.2}$$

where w is the width of cut, t_0 is the uncut chip thickness, Y_s is the shear yield strength, β is the friction angle given by $\tan\beta = \mu$, where μ is the equivalent coefficient of friction, α is the rake angle, ϕ is the shear angle and R is the specific work of surface formation (fracture toughness). The shear yield strength Y_s can be obtained from the Johnson-Cook's model (Dixit and Dixit, 2015). The expression for the Johnson-Cook's model is given as

$$Y_s = \frac{1}{\sqrt{3}}\left(A + B\varepsilon^n\right)\left(1 + C\ln\frac{\dot{\varepsilon}}{\dot{\varepsilon}_0}\right)\left\{1 - \left(\frac{T - T_a}{T_m - T_a}\right)^m\right\}, \tag{4.3}$$

where *A*, *B*, *C*, *n* and *m* are material parameters usually obtained from curve-fitting. The process temperature, ambient temperature and the melting temperatures are denoted by T, T_a and T_m, respectively. In the metal cutting, the process temperature refers to the cutting temperature. The equivalent strain, equivalent strain-rate and reference strain-rate are denoted by ε, $\dot{\varepsilon}$, and $\dot{\varepsilon}_0$. In the present work, the reference strain-rate is taken as 1 s^{-1}. In Equation (4.2), Y_s should be taken as the average shear yield strength. As a first approximation, the cutting temperature and strain-rate are assumed constant during the process, but the strain changes from 0 to the maximum value. The maximum shear strain is given by

$$\gamma = \frac{\cos\alpha}{\cos(\phi - \alpha)\sin\phi}. \tag{4.4}$$

Assuming von Mises criterion, the maximum equivalent strain is calculated as

$$\varepsilon_{\max} = \frac{\gamma}{\sqrt{3}}. \tag{4.5}$$

The average shear yield stress is obtained as

$$Y_s = \frac{\int_0^{\varepsilon_{\max}} Y_s(\varepsilon)\mathrm{d}\varepsilon}{\varepsilon_{\max}}, \tag{4.6}$$

where Y_s on the left side denotes the average shear yield stress and Y_s (ε) denotes the shear yield stress as a function of equivalent strain as the temperature and strain-rate are kept constant for one iteration in Equation (4.3). The Equation (4.6) can be evaluated numerically by two-point Gauss quadrature that provides exact integration for a cubic function. Many a times, in modelling, even linear strain-hardening is assumed. Hence, cubic approximation for Y_s (ε) is expected to provide almost zero error. Application of two-Gauss point formula provides the following expression for the average shear yield stress:

$$Y_s = \frac{Y_s(\varepsilon_1) + Y_s(\varepsilon_2)}{2}, \tag{4.7}$$

$$\varepsilon_1 = \frac{\varepsilon_{\max}}{2}\left(1+\frac{1}{\sqrt{3}}\right), \quad \varepsilon_2 = \frac{\varepsilon_{\max}}{2}\left(1-\frac{1}{\sqrt{3}}\right). \tag{4.8}$$

It can be observed from Equation (4.7) that average flow stress is simply the arithmetic average of two sampling points which are far away from the minimum and the maximum strain. As Johnson-Cook's model is obtained by fitting the data, its accuracy is expected to be poor near the extreme strain values. The use of two-point Gauss quadrature is better as the Gauss-points fall well within the range and accuracy of fitting at these points is expected to be better.

The average strain rate is the ratio of the maximum strain to cutting time. The cutting time may be considered to be the order of chip thickness divided by cutting velocity. The chip thickness can be considered as a characteristic length. This is an approximation, but it seems reasonable. Astakhov (2011) argued that strain-rate in metal cutting is expected to be less than 10 s^{-1}, unlike the estimate of 10^3–10^6 s^{-1} by several researchers (Chao and Bisacre, 1951; Shaw, 1954; Kronenberg, 1966; von Turkovich, 1970; Oxley, 1989; Stephenson and Agapiou, 1996; Trent and Wright 2000). As will be shown later the strain rate used in this work are about 10^3 s^{-1}, a value showing some bias towards the observation of Astakhov (2011). The following expression for the strain-rate is used.

$$\dot{\varepsilon} = \frac{\gamma}{\sqrt{3}}\frac{V}{t_c}, \tag{4.9}$$

where V is the cutting speed and t_c is the chip thickness.

The cutting temperature at the primary shear zone is estimated which is as follows (Ghosh and Mallik, 2010).

The force due to friction on the rake face is calculated as

$$F_f = F_c \sin\alpha + F_c \tan(\beta-\alpha)\cos\alpha. \tag{4.10}$$

The power during the plastic deformation process taking place in the primary deformation zone is calculated as

$$P_p = F_c V - F_f r V, \tag{4.11}$$

where F_c and F_f are the main cutting force and the frictional force, respectively, V is the cutting speed and r is the cutting ratio given by

$$r = \frac{\sin\phi}{\cos(\phi - \alpha)}. \tag{4.12}$$

The proportion of heat conducted to the workpiece is determined by

$$p_{wp} = 0.15 \ln \frac{27.5}{(T_N \tan\phi)}, \tag{4.13}$$

where T_N refers to the Thermal Number (Chattopadhyay, 2011) which is calculated as follows

$$T_N = \frac{\rho c V t_0}{k}, \tag{4.14}$$

where ρ is the density of the workpiece, c is the specific heat capacity, t_0 is the uncut chip thickness and k is the thermal conductivity.

Finally, the temperature rise in the cutting zone is obtained by

$$\theta_p = \frac{(1 - p_{wp}) P_p}{\rho c V t_0 w}, \tag{4.15}$$

where w is the width of cut.

The Equation (4.2) shows that the cutting force is dependent on the shear angle ϕ. Following the minimum energy principle, the optimum value of shear angle can be obtained using interval-halving method (Deb, 1995). The entire procedure is explained in the form of a flow chart as given in Figure 4.11. Considering that cylindrical turning is a three-dimensional machining, the rake angle α corresponding to orthogonal machining is replaced by the effective rake angle α_e given by Stabler (1951).

$$\sin\alpha_e = \sin^2 i + \cos^2 i \sin\alpha_n. \tag{4.16}$$

The inclination angle i is given by Bhattacharya (1984)

$$\tan i = \cos\psi \tan\alpha_b - \sin\psi \tan\alpha_s, \tag{4.17}$$

where α_b the back rake angle, α_s is the side rake angle and ψ is the side cutting edge angle all in ASA system. The normal rake angle α_n is given by

$$\alpha_n = \tan^{-1}\left\{\left(\tan\alpha_b \sin\psi + \tan\alpha_s \cos\psi\right)\cos i\right\}. \tag{4.18}$$

The uncut chip thickness and width are $f\cos\psi$ and $d/\cos\psi$ respectively, where f is the feed and d is the depth of cut.

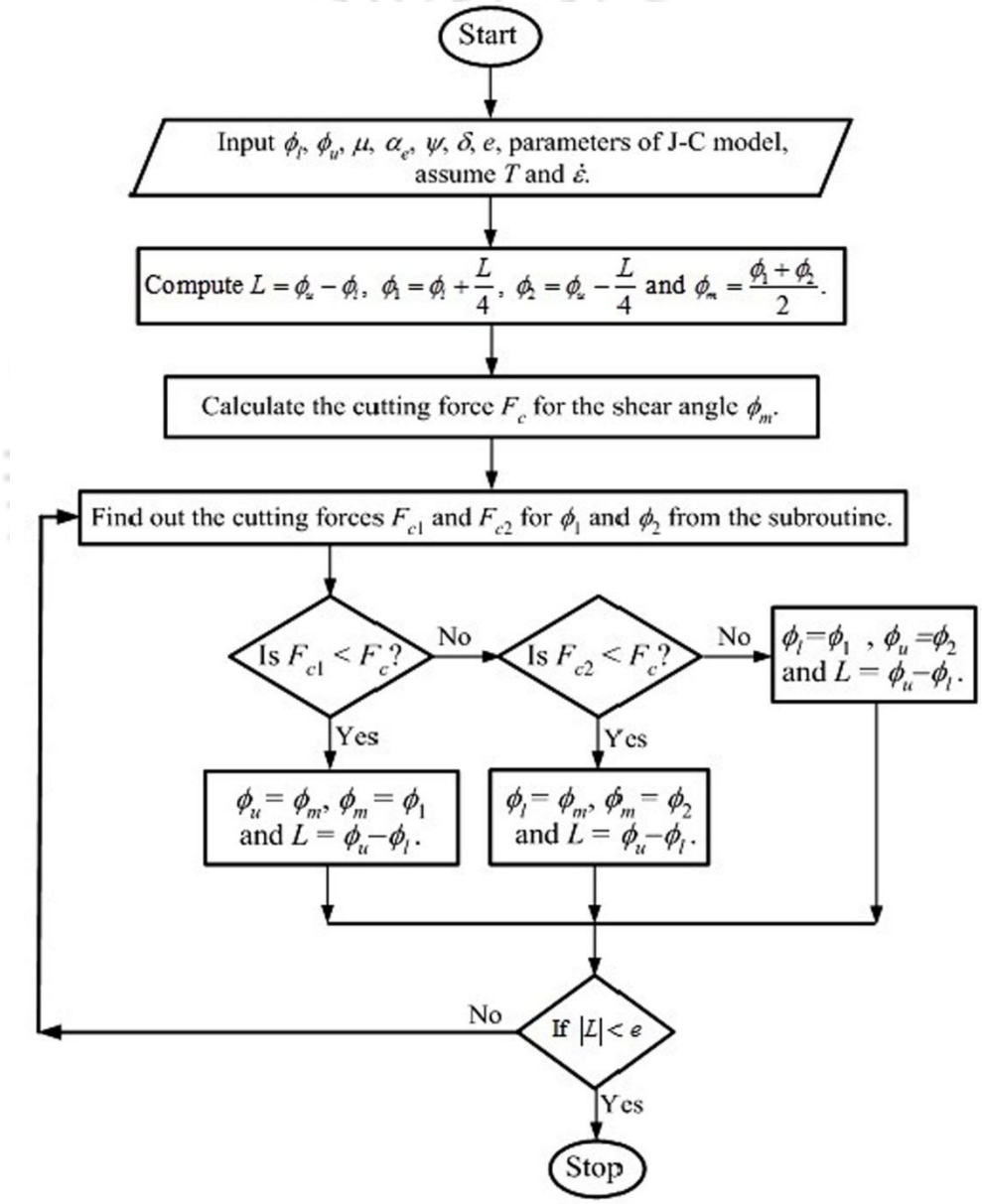

Figure 4.11. The flow chart of the main program for obtaining the cutting force by minimizing shear angle using interval-halving method

For each particular value of shear angle, the force F_c is calculated by Equation (4.2), which needs the value of Y_s as a function of strain, strain-rate and temperature. Equation (4.5) and Equation (4.9) provide strain and strain-rate respectively. The temperature is estimated by the procedure described earlier. The estimated value of temperature is used to modify the value of Y_s and F_c is calculated again. This procedure is repeated till the convergence is obtained. Figure 4.12 shows the flow chart of the subroutine for estimating the cutting force for a particular shear angle. This subroutine is called in the main program as described in Figure 4.11.

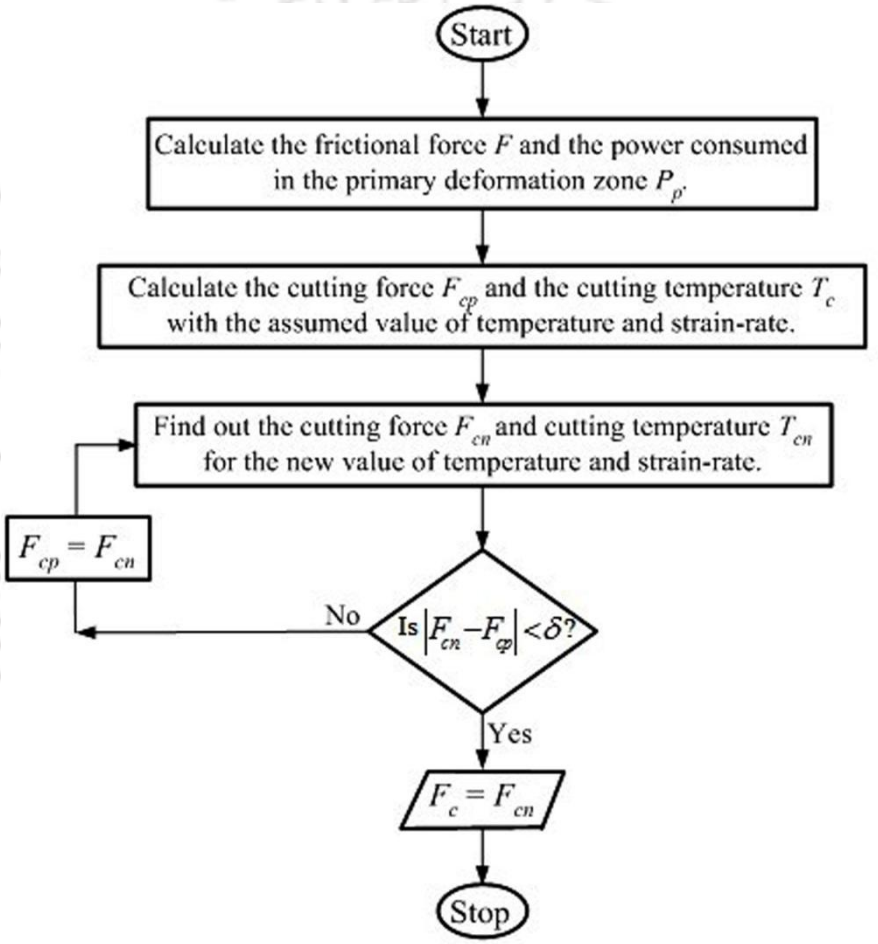

Figure 4.12. The flow chart of the subroutine for estimating the cutting force

The code was run by assuming various assumed values of equivalent coefficient of friction. For mild steel (AISI 1010) workpiece, following parameters of Johnson-Cook model were used from Brar *et al.* (2007): A=367 MPa, B=700 MPa, n=0.935, C=0.045, m=0.643. For μ=0.9, the cutting force was obtained as 187 N and feed force as 133 N.

Table 4.2. Cutting forces and workpiece surface temperature while double tool turning of typical mild steel with TiN coated tungsten carbide tools (75 m/min cutting speed, 0.08 mm/rev feed and 1 mm depth of cut)

Distance between the cutting tools (mm)	Average force component (N)				Average workpiece surface temperature between cutting edges (°C)
	Front tool		Rear tool		
	Cutting force	Feed force	Cutting force	Feed force	
2	215	117	230	89	50
5	216	120	227	90	50
10	217	120	226	92	55
20	207	114	216	87	55
30	206	119	218	87	55
40	200	114	214	85	55
50	220	121	214	88	55

Note: Theoretical cutting force is 193 N and feed force is 105 N. Theoretical model does not consider the effect of separation.

A comparison of these values with Table 4.2 reveals that error in the estimation of cutting force varies from 6.5% to 15% and that in the estimation of feed force varies from 9% to 15.8%. The errors of this magnitude should not be considered high considering the uncertainty in the estimation of flow stress and friction in metal cutting. Schey (1983) observed that in a real metal, flow stress cannot be reproduced to better than ±5% accuracy. In metal cutting the accuracy of ±10% in flow stress should be considered as a good accuracy. Chisholm (1951) felt that in orthogonal machining the coefficient of friction lies between 0.5 and 1. Considering dry turning, a value of 0.9 for the coefficient of frictions seems reasonable. For the proper estimate of the rear cutting tool force values, strain hardening and residual stresses must be taken into account. It is not easy to find these effects analytically. However, the overall effect may be visualized by assuming some pre-strain while using Johnson-

Cook's model. Here, a pre-strain of 0.25 is assumed with reduced friction coefficient of 0.7. This provided the cutting force of 193 N and feed force of 105 N. The error in the estimation of cutting force varies between 9.8% and 16.1%. The error in the estimation of feed force varies between 4.4% and 12.9%. The values of pre-strain and coefficient of friction were manually adjusted. It is possible to find them using an inverse approach based on an efficient optimization algorithm. The present analytical method also provided the estimate of temperature at tool-work interface. It came out to be 282 °C for the front tool and 325 °C for the rear tool. These values are below the recrystallization temperature of mild steel. This agrees with the viewpoint of Astakhov (2011) that metal cutting is mostly a cold working process. Table 4.2 shows average cutting forces and temperature of mild steel workpiece for different distances between front and rear cutting tools. In all the cases, the cutting speed was 75 m/min, 0.08 mm/rev feed and depth of cut 1 mm for each tool. Except for the tool separation of 50 mm, in all the cases, main cutting force of rear tool is more than the main cutting force of front tool. This may be due to strain hardening of the surface machined by front cutting tool and possibly the residual stresses. On the other hand, the feed forces for the rear tool are lesser. This indicates that the equivalent Coulomb's coefficient of friction encountered by the rear cutting tool is lesser than that encountered by front cutting tool. The front cutting tool provided a good surface finish and enhanced hardness that contributed to reduced friction. At a separation distance of 50 mm, the vibrations get increased, which increased the main cutting force on both the cutting tools. The average workpiece surface temperature between the cutting edges is 50–55 °C. When the distance is lesser (2–5 mm), the temperature is about 50 °C.

Figures 4.13–4.15 show the thermograms for different cutting conditions. It shows the temperature variation starting from the vicinity of cutting tools up to revolving centre of the tailstock. It does not provide much idea about the temperature at tool-work interface, but one can estimate it by using the technique of inverse heat transfer. Figure 4.13 shows that for cutting speed of 75 m/min, feed of 0.08 mm/rev and depth of cut of 0.5 mm, the maximum temperature on the visible surface of the workpiece is about 60 °C. When the depth of cut was doubled, the maximum visible surface temperature increased to about 85 °C as shown in Figure 4.14. With a further

increase of the feed to 0.24 mm/rev, the maximum temperature on the visible surface increased to 220 °C, as shown in Figure 4.15. A quick analysis can reveal that increase of temperature is dependent on the uncut chip cross-sectional area.

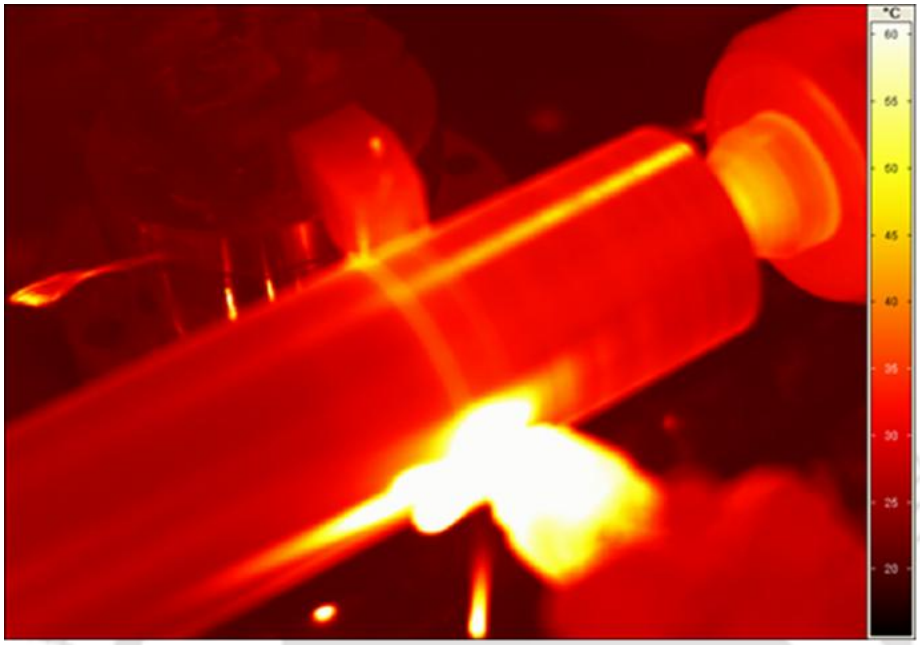

Figure 4.13. Thermogram of mild steel workpiece during cutting (75 m/min cutting speed, 0.08 mm/rev feed, 0.5 mm depth of cut and 10 mm distance between cutting tools)

Figure 4.14. Thermogram of mild steel workpiece during cutting (75 m/min cutting speed, 0.08 mm/rev feed, 1 mm depth of cut and 10 mm distance between cutting tools)

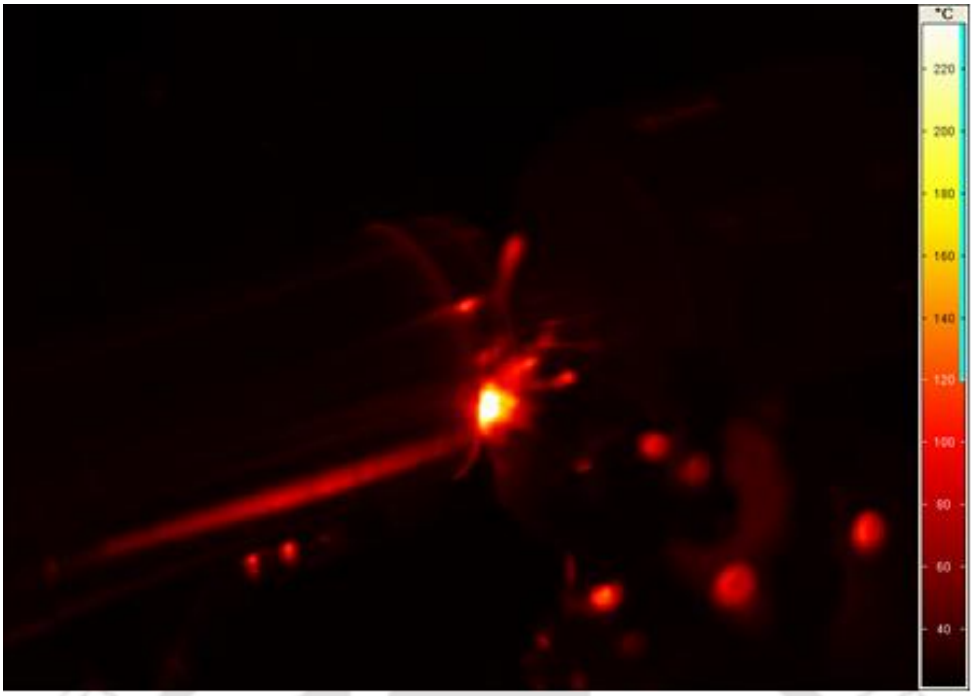

Figure 4.15. Thermogram of mild steel workpiece during cutting (120 m/min cutting speed, 0.24 mm/rev feed, 1 mm depth of cut and 10 mm distance between cutting tools)

The analytical model for single tool was developed to predict the cutting forces and cutting temperature, which helps in determining the power consumption. Theoretically, the power consumed for double tool turning is twice as that of single tool turning for the same cutting conditions. The analytical model provided theoretical explanation for the experimentally obtained values. This model is not taking the interaction effect (like separation distance) of the tools. A detailed analytical model considering all the aspects is left for future work. The present model could explain some observations successfully in a qualitative manner.

4.5 The Influence of Machining Parameters on Cutting Tool Vibration in Double Tool Turning Process

Considerable amount of investigations on vibration has been carried out in the conventional machining process (Mehta *et al.*, 1983; Zeng and Forssberg, 1994; El-Wardany *et al*., 1996; Risbood *et al.*, 2003; Abu-Mahfouz, 2003; Salgado and Alonso, 2006; Orhan *et al*., 2007; Alonso and Salgado, 2008). However there was no attempt made to understand the dynamics of double tool machining. The present research

work deals about the influence of cutting speed and tool separation distance on cutting tool vibration in double tool turning process of grey cast iron work material.

Generally cutting tool vibrations are dependent on machining parameter such as cutting speed, feed and depth of cut in the conventional turning process. In the case of double tool turning process, the introduction of second tool and distance between both front and rear cutting tool are also expected to affect cutting tool vibration. In order to study the effect of cutting speed on tool vibration, the feed of 0.08 mm/rev and the depth of cut of 1 mm are maintained constant and the cutting speed is varied for the different tool separation distances. Figure 4.16 and Figure 4.17 shows the amplitude of vibrational signal of the front and rear cutting tool, for various tool separation distances. It can be observed from the figures that, with the increase in cutting speed 75 to 185 m/min, cutting tool vibration decreases. This behaviour is due to that fact that shear zone temperature increases with increase in cutting speed. Rise in shear zone temperature plasticize the work material and hence reduces cutting forces and provides more damping. Subsequently cutting tool vibration reduces. This is confirmed with the measured cutting force. When the cutting speed increases from 75 to 120 m/min and further to 185 m/min, cutting force measured at front cutting tool are 232, 216 and 200 N and at the rear 245, 233 and 206 N respectively. Ghani *et al*. (2002) machined nodular cast iron with a ceramic tool. With the increase in cutting speed from 364 to 685 m/min cutting tool vibrations reduced. Dimla and Lister (2000) machined EN 24 steel with coated carbide tool and found that the power spectral peak of the vibration signals decreases with the increase in the cutting speed. Fang *et al*. (2010) reported dynamically stable cutting tool with increase in cutting speed.

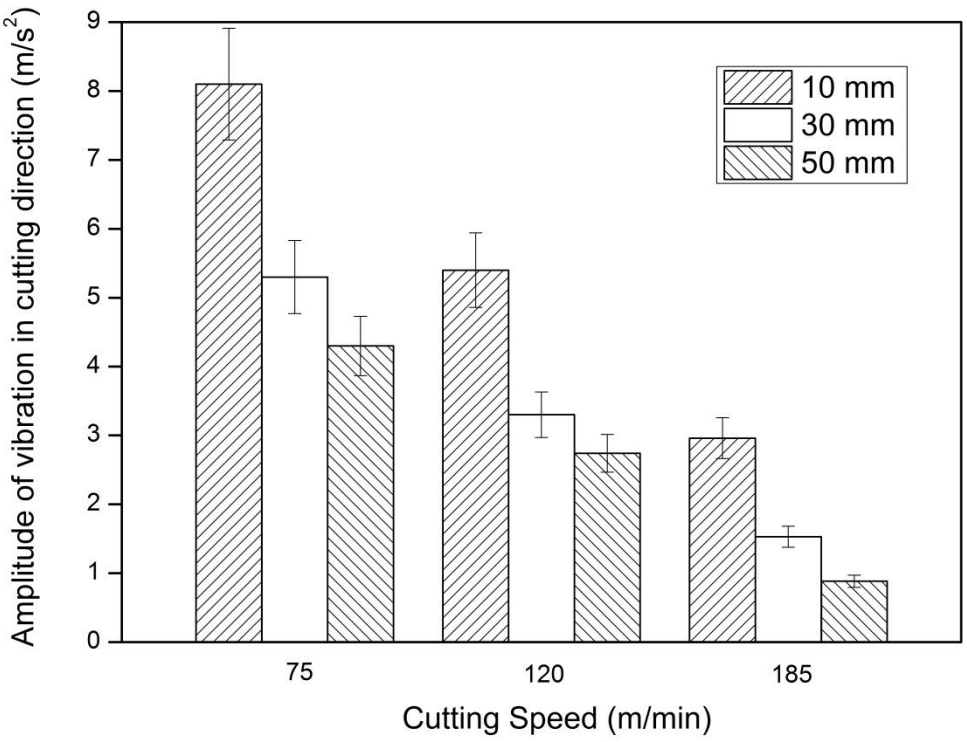

Figure 4.16. Front cutting tool vibration amplitude in cutting direction (0.08 mm/rev feed and 1 mm depth of cut)

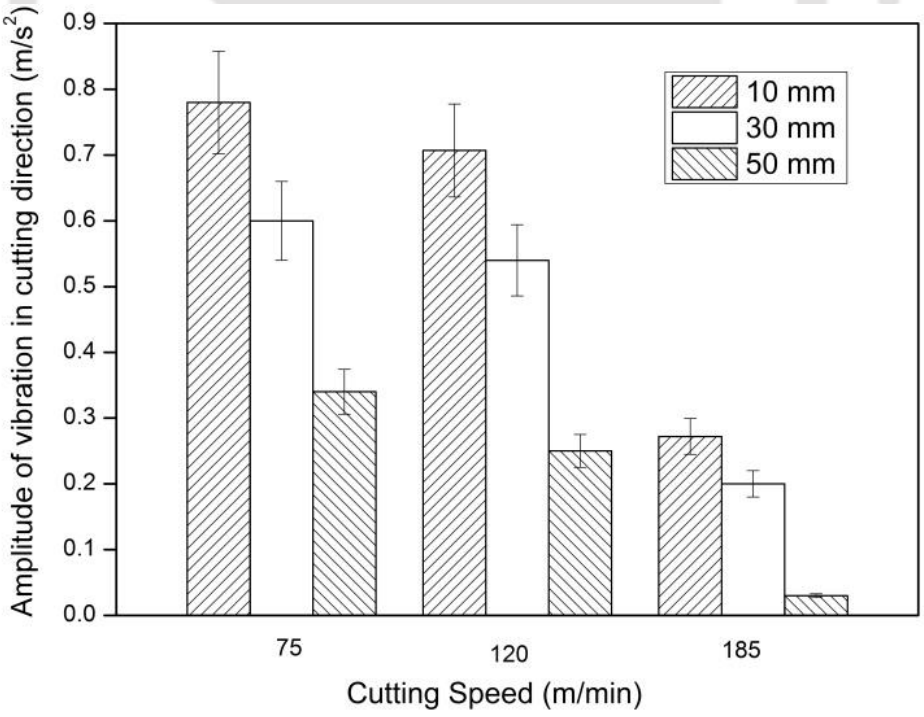

Figure 4.17. Rear cutting tool vibration amplitude in cutting direction (0.08 mm/rev feed and 1 mm depth of cut)

With the increase in distance between front and rear cutting tool, cutting tool vibration decreases. When the distance between front and rear cutting tool increases, cutting tool moves towards chuck and hence workpiece rigidity improves during the machining. Improved rigidity of workpiece contributes to the reduction in the cutting tool vibration. The front cutting tool is held in a tool holder. It is rigidly fixed at one end and at the other end (cutting edge) the cutting forces act. Hence the support and loading condition resemble a cantilever beam subjected to point load at one end. Whereas the rear tool is attached to a tool holder which is fixed to cross-slide. The cross-slide is mounted over a base plate which is of overhanging in nature. In addition rear tool holder base plate is made of cast iron which also contributes to improve the damping performance Thus due to the superior damping property of the material and rigidity of rear tool holder, vibration of rear cutting tool is found to be far less than that of front cutting tool. In fact, it would have been better to make both front and rear fixture by cast iron to get good damping property. Thus the present experimental investigation reveals the influence of cutting speed on the tool vibration of front and rear cutting tool. Increase in cutting speed reduces the tool vibration for both the front and rear cutting tool. Vibration of front cutting tool is higher than that of rear cutting tool for the chosen cutting conditions.

4.6 Conclusion

A conventional centre lathe was slightly modified to mount the second cutting tool at the rear side. Turning was performed at various cutting speeds, depths of cut and various distances between the two cutting tools. Cutting and feed forces of both front and rear cutting tools were measured along with temperatures. The following are the salient observations.

- For grey cast iron work material, the cutting force and feed force components are not affected significantly by the distance between the front and rear cutting tool. There is a positive correlation between cutting force components and depth of cut. However, it is not a linear correlation. The deviation from linearity is more in the case of feed forces than in the case of cutting forces. It was observed that at a cutting speed of 75 m/min, the rear tool encountered lesser force compared to front tool for 2 mm distance between the cutting tools. This is attributed to reduced friction due to cleansing effect of the front

tool. Due to reduced friction, the ratio of feed force to cutting force also got reduced.

- The distances between the front and rear cutting tools (2, 4, and 8 mm) exhibited no significant effect on cutting temperature. The increase in cutting speed from 75 m/min to 185 m/min causes a rise in temperature of grey cast iron workpiece from 60 °C to 80 °C. At this much rise in temperature, material properties are not affected significantly.
- With the aid of an analytical model, theoretical explanation was provided for the experimentally obtained cutting forces and temperature for single tool turning process of mild steel work material. Comparison between the experimental and analytical model revealed an error varying between 9.8% and 16.1% for cutting force and for feed force it is between 4.4% and 12.9%.
- The cutting tool vibration of front and rear cutting tool decreased with the increase in cutting speed. Moreover the front cutting tool vibration was higher than the rear cutting tool for the selected cutting conditions while double tool turning of grey cast iron.

Chapter 5

Diametral Error, Cutting Tool Wear and Chip Morphology in Double Tool Turning Process

5.1 Introduction

Cylindrical parts with length to diameter ratio of more than six are used as transmission shafts, broaching tools, lead screws and feed rods of machine tools. The dimensional deviation becomes prominent while machining these slender workpieces. In a turning operation, the dimensional deviation mainly refers to the diametral error. It is the deviation between the desired and actual diameter of the workpiece. The deviation of the workpiece diameter from the desired diameter is shown in Figure 5.1 schematically. It is caused due to the deflection of the workpiece, cutting tool, tool holder and other machine components; the effective depth of cut is smaller than the set depth of cut. Steady rest and follower rest are often used to reduce the diametral deviation, while turning the slender jobs in a lathe. In double tool turning process, the rear cutting tool not only removes the work material but also provides support to the workpiece. Hence, the diametral error is expected to decrease in double tool turning process.

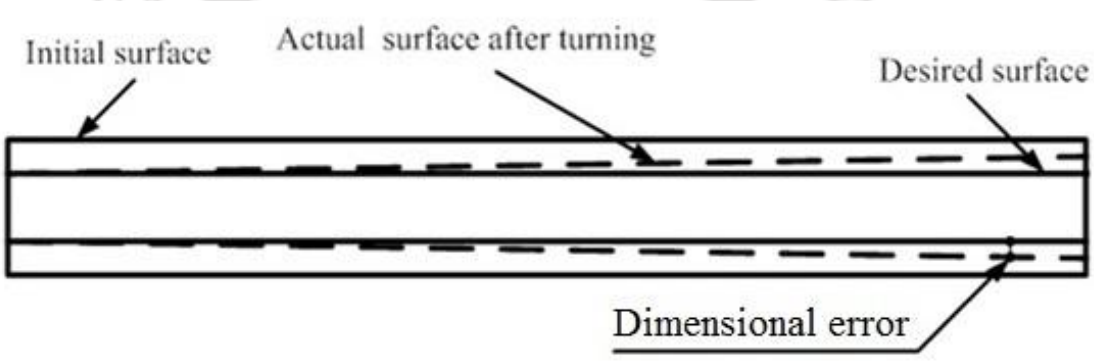

Figure 5.1. A schematic of dimensional deviation of a slender workpiece

Another major factor influencing the machining performance is tool wear. It indicates the amount of material lost from the cutting tool during machining. Flank

wear and crater wear are the two types of tool wear; former occurs due to the rubbing action of the cutting tool on the machined surface and the latter occurs due to the sliding action of the chip on the rake face of the cutting tool. The time period during which the tool gives a satisfactory performance is called the tool life and it is expressed in minutes. Mechanics of chip formation and chip characteristics are essential to understand the mechanics of metal cutting. Chip morphology and its characteristics are revealed by scanning electron microscope.

From prior research works it was observed that the effects of the workpiece slenderness ratio, cutting forces and follower rest on diametral errors are well understood for conventional turning process. However, there has been no attempt made to understand these effects for the double tool turning process. This work attempts the same by turning a cylindrical workpiece with two cutting tools mounted on the same carriage. It is well understood that considerable work on tool wear and chip morphology has been carried out in turning operation to understand the mechanism of cutting. However, no work has been carried out to understand the cutting mechanism in the double tool turning process pertaining to tool wear and chip morphology. The present research work fills up that gap.

5.2 Experimental Procedure

The procedure for measuring the diametral deviation was described in Chapter 3, here further details are described. In the present work, machining was performed at cutting speed of 116 m/min, feed of 0.24 mm/rev at various depths of cut (1, 1.5 and 2 mm). Figure 5.2 shows force signals of the front and rear cutting tools during turning for a specific cutting condition. The cutting forces of the front as well as the rear cutting tool are measured while turning. The measured cutting forces are used to predict workpiece deflection with the aid of an approximate analytical model. To measure the diametral deviation, a precision dial gauge (Make: Mitutoyo, Accuracy: 1 μm) was used and moved along the length of the workpiece from the tailstock to the chuck end without removing the workpiece after machining. Figure 5.3 shows the close up view of the experimental setup with a dial gauge used to measure the diametral error (refer Fig. 3.7 for other photograph). Grey cast iron and titanium nitride coated carbide was taken as work and cutting tool material, respectively. The machining length and

diameter of the workpiece is 220 mm and 52 mm respectively. For measurement purpose the workpiece was divided into 11 divisions each of 20 mm length. For every division, the workpiece was rotated by 60° and the deviation was measured on six equidistant points on the circumference and the average value was recorded. The machining experiments were repeated three times and a good repeatability within ±10% was observed. The details of the experiments for measuring cutting forces and temperature are given in Chapter 3.

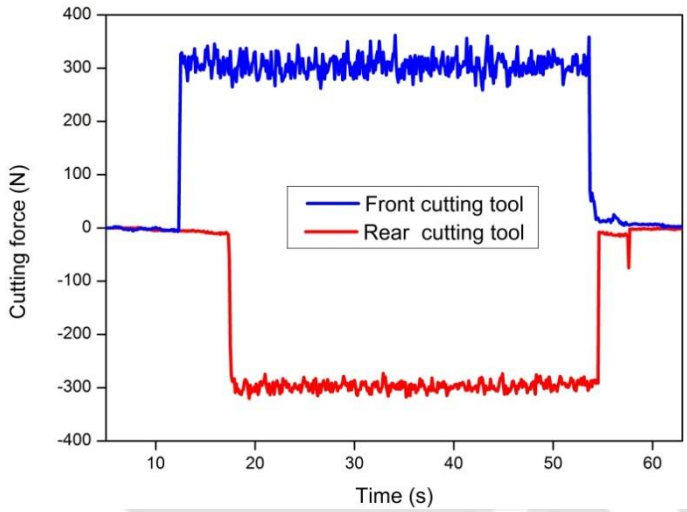

Figure 5.2. Measured cutting forces of the front and rear cutting tools in double tool turning of grey cast iron (116 m/min cutting speed, 0.24 mm/rev feed, 1 mm depth of cut and 10 mm separation distance between the cutting tools)

Figure 5.3. Measurement of the diametral error

5.3 Results and Discussion

Figure 5.4 shows the measured diametral deviation of grey cast iron machined surface from the chuck to the tailstock end when machined at 1 mm depth of cut. Based on three replicates, the maximum error in the measurement was less than ±5%. Hence, in the figure, the error bars have been drawn considering uniform deviation of ±5% in all the cases. The diametral deviation from the set diameter increased towards the tailstock end. This behaviour is due to the increased workpiece deflection at the tailstock end as compared to the chuck end. The maximum deviation at the tailstock end was 108 μm. The cutting forces generated while turning with a single (front) cutting tool, deflect the workpiece. When the second cutting tool (rear) was engaged, the rear cutting tool restricted the deflection of the workpiece due to the front cutting tool. Hence the maximum workpiece deflection got reduced to 22 μm. This contributed to the improvement of workpiece diametral accuracy by 80%. The front and rear cutting tools acted as a follower rest for each other.

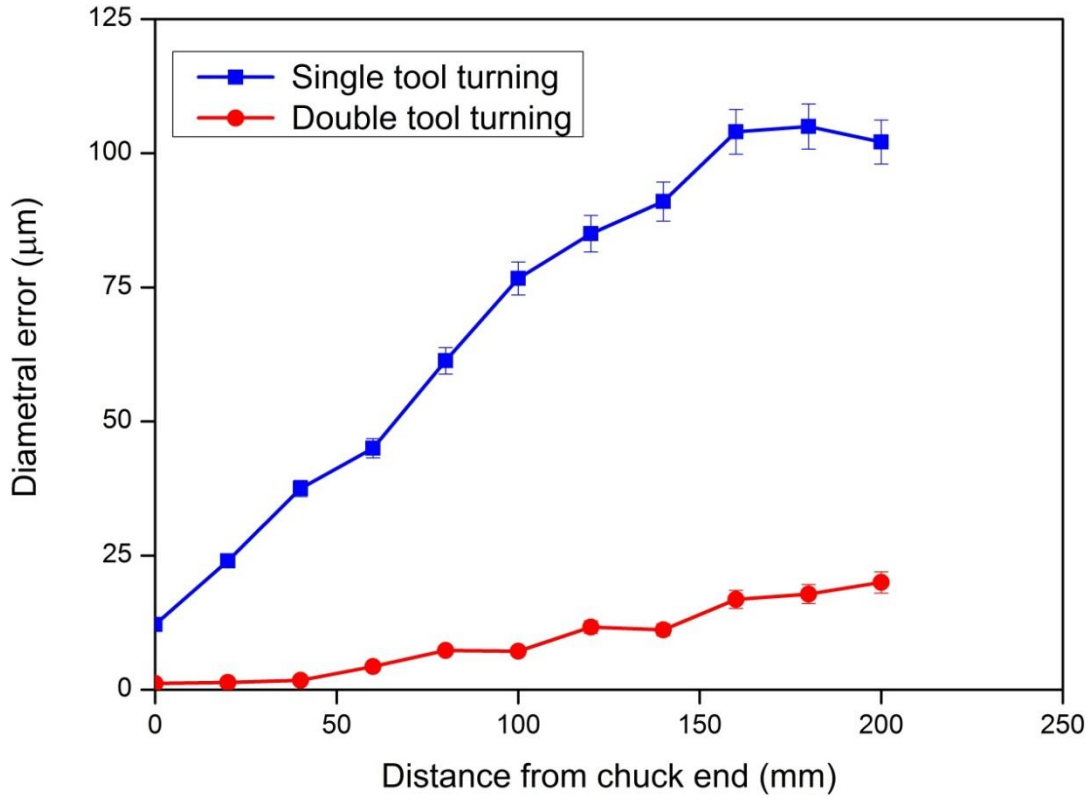

Figure 5.4. Diametral error of the machined surface of grey cast iron at 1 mm depth of cut (116 m/min cutting speed and 0.24 mm/rev feed)

Due to the flexible tailstock end compared to rigid support at the chuck end, the workpiece deflects more at the tailstock end. This deflection generates vibration, causing slight increase in the cutting force. Figure 5.5 shows the measured main cutting force from the tailstock end to chuck end. The mean cutting force increased from 300 N to 350 N. Killic *et al*. (2007) also observed a similar increase in cutting force behaviour while machining a long aluminium workpiece. They observed an increase of 500 N (from 1500 N to 2000 N) while machining a length of 170 mm at a cutting speed of 87.8 m/min, feed of 1 mm/rev and depth of cut of 1 mm. This was due to reduced diametral deviation as the tool moves from tailstock end to chuck end.

When the rear cutting tool was engaged, workpiece experienced support from the rear for the complete length since the rear cutting tool moves along the entire machining length. Figure 5.6 shows the measured cutting force of the front cutting tool when both the tools are engaged. Unlike the previous case, the mean cutting force varied between 300 N and 325 N. Thus, the range of force reduced by 25 N. The dynamic stiffness of the machining system is influenced by the compliance of headstock, tailstock and carriage. Apart from this, the workpiece length, cutting tool, tool post and work holding device such as chuck also affect the dynamic stiffness. The accuracy of holding the workpiece during machining and position of cutting tool play a major role in dimensional and shape accuracy.

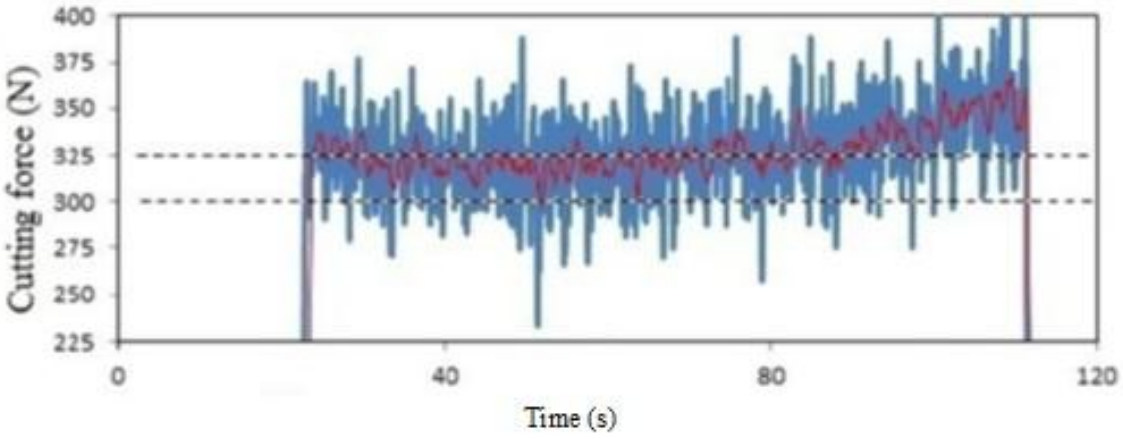

Figure 5.5. Variation of cutting force while turning from tailstock to chuck with single cutting tool for grey cast iron work material (116 m/min cutting speed, 0.24 mm/rev feed and 1 mm depth of cut)

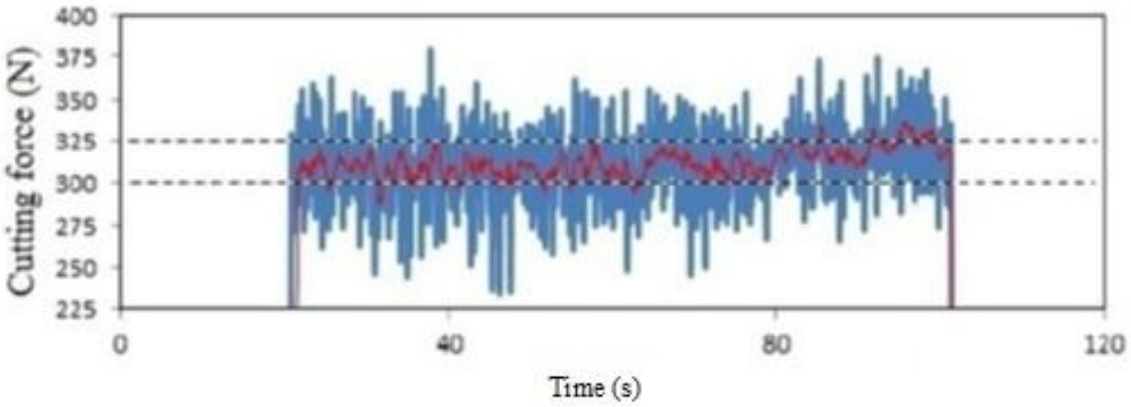

Figure 5.6. Variation of cutting force while turning from tailstock to chuck with two cutting tools for grey cast iron work material (116 m/min cutting speed, 0.24 mm/rev feed and 1 mm depth of cut)

5.3.1 The Effect of Depth of Cut

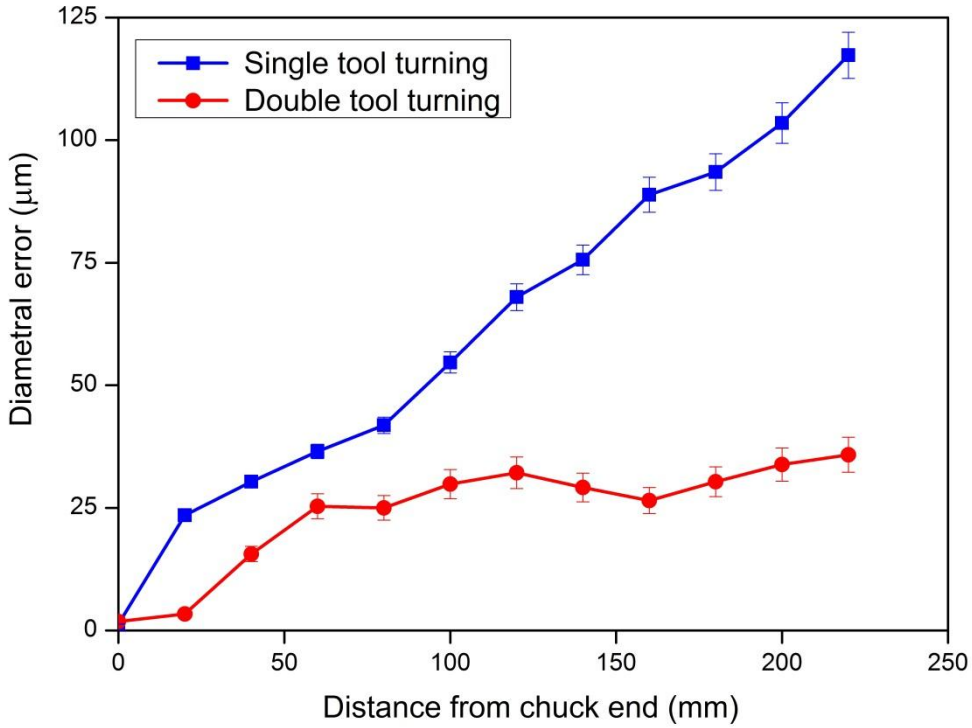

Figure 5.7. Diametral error at 1.5 mm depth of cut for grey cast iron work material (116 m/min cutting speed and 0.24 mm/rev feed)

Figures 5.7 and 5.8 show the measured diametral error from chuck to tailstock end for the depths of cut of 1.5 mm and 2 mm, respectively. It confirms that actual depth of cut is achieved near the chuck end, whereas the diametral error increases while measuring towards the tailstock end and it is higher for 2 mm depth of cut. The measured average deviation at the tailstock end was 120 µm and 155 µm for the

depths of cut of 1.5 mm and 2 mm, respectively. When the depth of cut increased from 1 mm to 1.5 mm and further to 2 mm the diametral error increased by 11% and 43%, respectively. Thus, it can be said that higher depth of cut of the front cutting tool leads to higher diametral error. This behaviour is due to the increased cutting force at higher depth of cut.

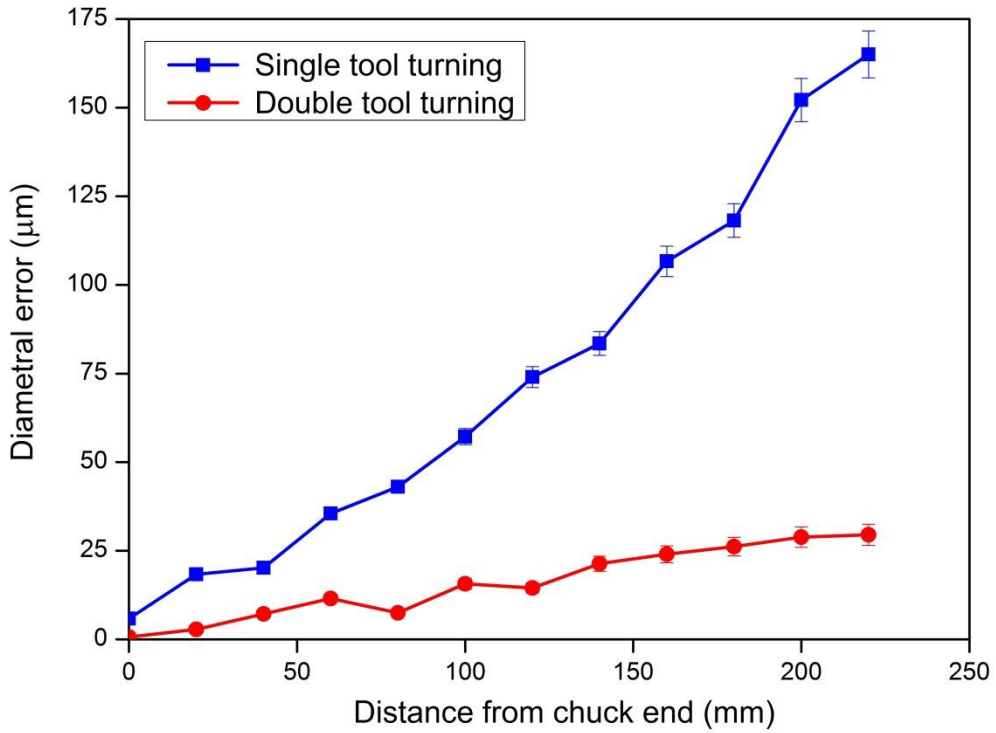

Figure 5.8. Diametral error at 2 mm depth of cut for grey cast iron work material (116 m/min cutting speed and 0.24 mm/rev feed)

The diametral error was proportional to the cutting force of the front cutting tool when machining was carried out without the rear cutting tool. Higher cutting force of front cutting tool led to higher diametral error. The cutting force is influenced by many parameters, such as cutting speed, feed, depth of cut, work and tool material and rigidity of machine tool. Among these parameters, depth of cut is an important parameter. In the present investigation depths of cut of 1 mm, 1.5 mm and 2 mm were used. In order to confirm the effect of depth of cut on diametral error and cutting forces, the metal cutting experiments were performed at other cutting conditions. The cutting force values of front and rear cutting tool are given in Table 5.1. From the table, it is observed that when the depth of cut increased from 1 mm to 1.5 mm, the cutting force of rear cutting tool increased by 1.2 times. Similarly, when the depth of

cut increased from 1.5 mm to 2 mm the rear cutting tool force increased by 1.4 times. Similar increase was observed for the front cutting tool.

Table 5.1. Variation of cutting forces for various depths of cut

Depth of cut (mm)	Front cutting tool force (N)	Rear cutting tool force (N)
1	214	239
1.5	280	295
2	392	408

5.3.2 Physical Explanation for the Improvement of the Accuracy through the Double Tool Turning

A simple strength of material approach was used to compute the workpiece deflection due to the cutting forces. The workpiece was assumed as a cantilever beam due to the rigid support at chuck as compared to the tailstock. The measured main cutting force (tangential component) of the front and rear cutting tools were considered as a point load. Although the radial component of the force is the most influencing component for dimensional deviation, a qualitative idea can be obtained by considering the deflection due to tangential force. In practice, all the components influence dimensional deviation (Mayer *et al.* 2000).

The Young's modulus of the workpiece material (Grey cast iron) is taken as 140 GPa and the weight of the workpiece is assumed as the uniformly distributed load. Here a multiplying factor was used to convert the main cutting force to the equivalent force that causes the radial deflection of the job. The multiplying factor was obtained by the least square method minimizing the error between the theoretical and experimental diametral error. For single tool turning the multiplying factor came out to be 0.9 and for double tool turning it was 0.92. Comparisons of theoretical and experimental radial deflection of workpiece for single tool turning and double tool turning are shown in Figure 5.9 and Figure 5.10.

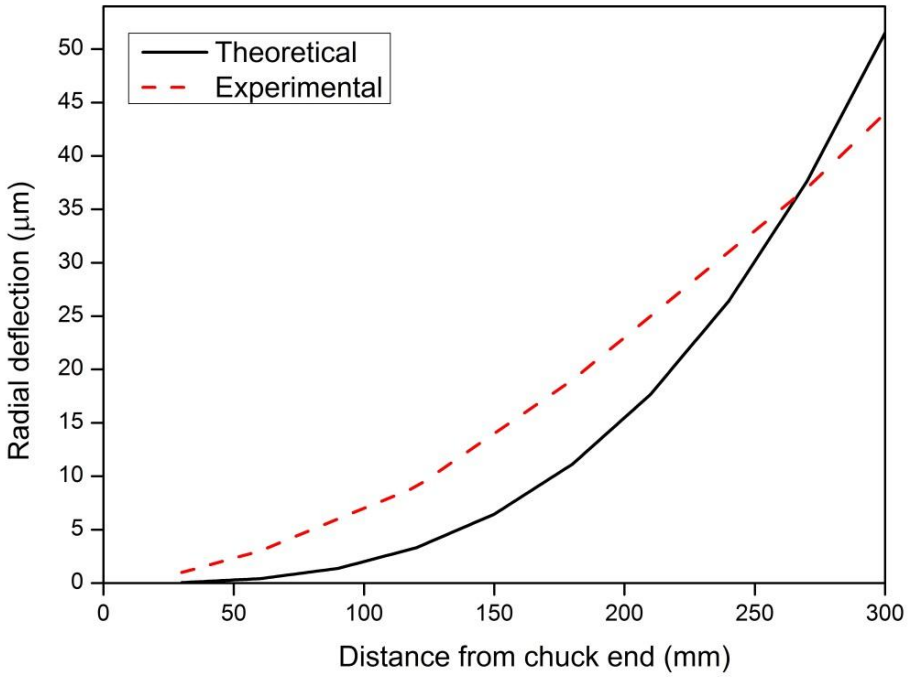

Figure 5.9. Theoretical and experimental workpiece deflection for single tool turning process (116 m/min cutting speed, 0.24 mm/rev feed and 1 mm depth of cut)

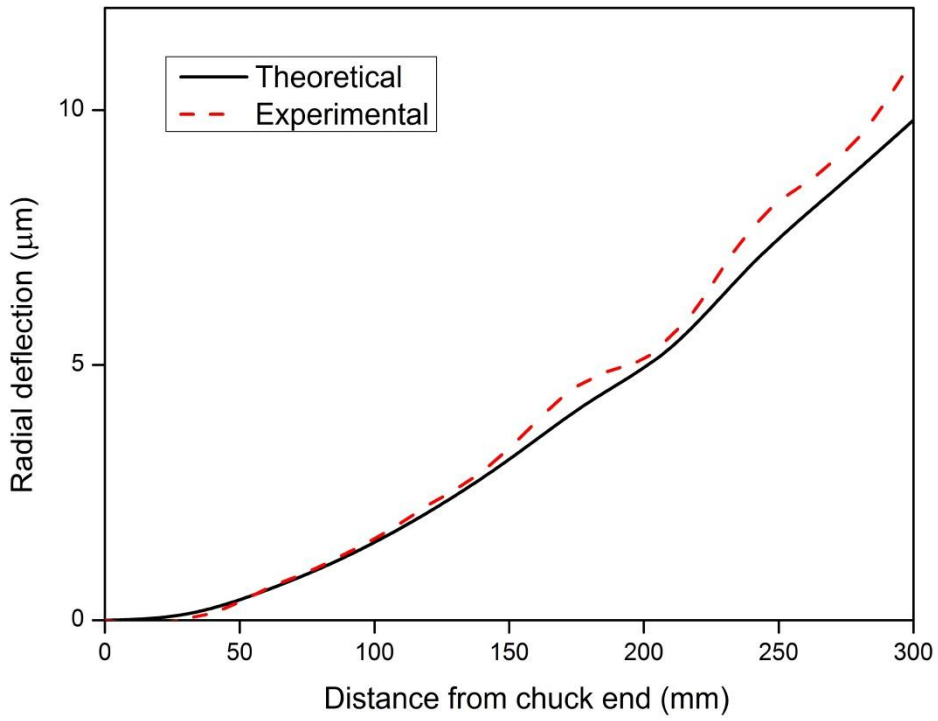

Figure 5.10. Theoretical and experimental workpiece deflection for double tool turning process (116 m/min cutting speed, 0.24 mm/rev feed, 1 mm depth of cut and 10 mm separation distance between the cutting tools)

In turning, workpiece deflects in radial direction with the maximum deflection at the tailstock end. Due to this deflection, in spite of setting uniform depth of cut, the actual depth of cut varies along the length. The desired and actual diameters are almost equal at the chuck end. The diametral error increases along the length of workpiece due to workpiece deflection and reaches the maximum at the tailstock end. This is because the compliance of tailstock is higher than the compliance of headstock. It can be observed from the work of Murthy (1970) that the form errors, such as diametral error caused due to the machine tool compliance and because of workpiece compliance act opposite to each other. In the double tool turning, cutting forces due to the front and the rear cutting tool act opposite to each other and the net deflection of workpiece due to the net cutting force is reduced. Due to the reduction in workpiece deflection, the diametral error of the machined workpiece in double tool turning is reduced.

5.3.3 Temperature during Double Tool Turning

An infrared camera was used to measure the net average surface temperature of the workpiece during double tool turning. Two different regions were considered, one region is the front cutting tool work interface (T_f) another is the rear cutting tool work interface (T_r). The temperatures of these two regions were measured with respect to time. It is to be noted that this temperature is not an actual temperature of the tool-work interface. It is only the average temperature of the workpiece near tool-work interface. This temperature can provide an idea about the relative amount of heat generated by front and the rear cutting tools. The mean cutting temperature gradually increased in the beginning and reached saturation for both the front and the rear cutting tools. It is to be noted that the cutting speed and feed of both front and rear cutting tools are same, since both are mounted on the same carriage. Figure 5.11 shows the average temperature at the interface of workpiece near the front and the rear cutting tools. The region near the rear cutting tool exhibited higher temperature as compared to the region near the front cutting tool. This is due to prior heating of the workpiece by the front cutting tool.

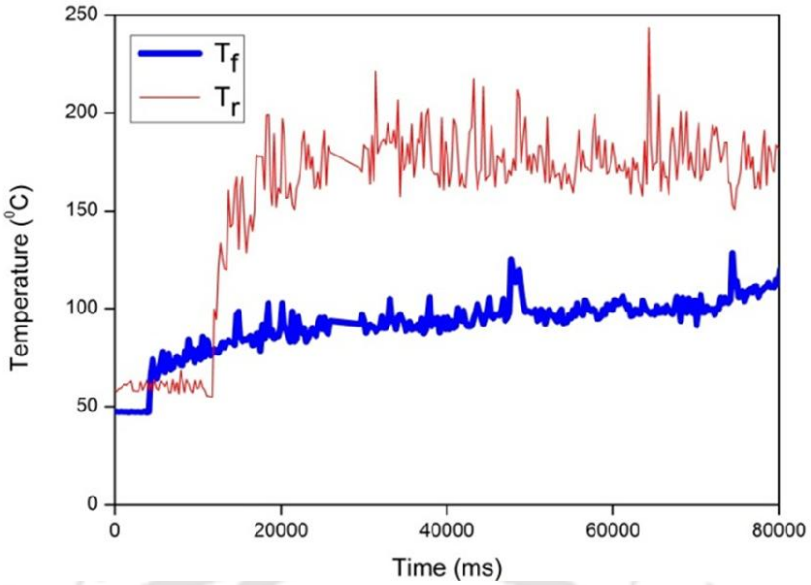

Figure 5.11. Tool-work interface temperatures while turning with two tools (116 m/min cutting speed, 0.24 mm/rev feed and 1 mm depth of cut)

5.3.4 Cutting Tool Wear

The double tool turning of grey cast iron was carried out for 320 s (cutting speed 150–200 m/min, 0.24 mm/rev feed and 1 mm depth of cut) to understand the flank wear of the front and rear cutting tools. The cutting speed kept on reducing due to reduction in the diameter of the workpiece. The starting speed was 200 m/min that reduced up to 150 m/min. During the machining time of 320 s, flank wear was measured at regular intervals with the aid of tool maker's microscope. Figure 5.12 shows the flank wear of both front and the rear cutting tools. It was observed that flank wear of the rear cutting tool was less due to the heat generated by the front cutting tool and reduced coefficient of friction. The presence of elements such as manganese (Mn) and sulphur (S) forms manganese sulphide (MnS) in the work material. It is well known that MnS is a good lubricant. At higher temperature the effectiveness of the lubricant increases. Whereas the rear cutting tool experiences a lesser abrasive flank wear as it is subjected to higher temperatures than the front cutting tool. Heck *et al*. (2008) reported the self-lubricating behaviour of MnS inclusion while machining cast iron. These MnS inclusions are accumulated on the cutting tool tip and provide an effective lubrication at tool-chip interface.

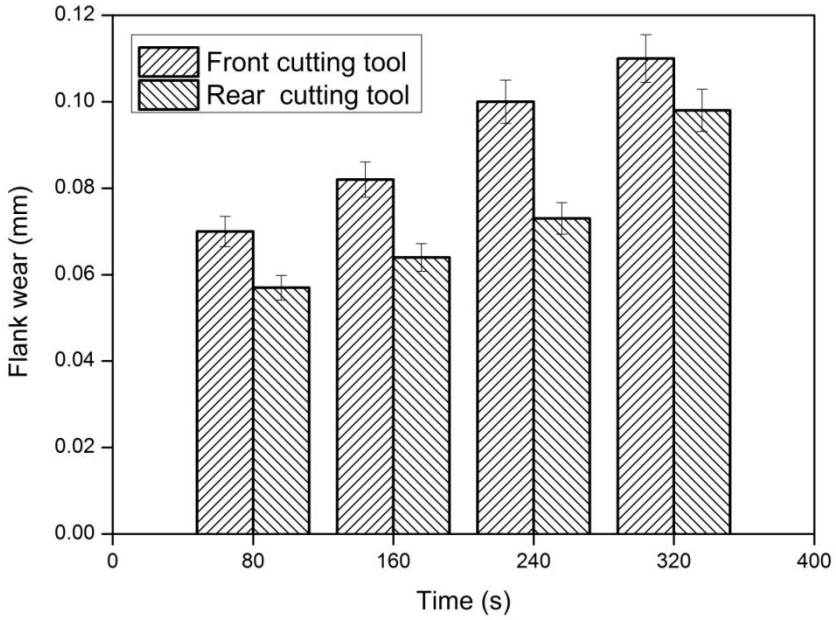

Figure 5.12. Measured flank wear of front and rear cutting tools (0.24 mm/rev feed, 1 mm depth of cut and cutting speed 150–200 m/min)

Additionally the MnS inclusions also act as diffusion barrier in reducing the tool wear. It was investigated in this work that the equivalent coefficient of friction for the rear cutting tool and front cutting tool was 0.6 and 0.8, respectively (see Section 4.3.1). Pereira *et al*. (2006) revealed that the presence of MnS inclusion in grey cast iron reduced the coefficient of friction at the tool chip interface by 5 times. The presence of graphite flakes in grey cast iron also reduces the friction coefficient. The rear cutting tool experienced a lesser flank wear due to reduced equivalent coefficient of friction. To understand further, the cutting tool insert was observed under the scanning electron microscope after 320 s of machining. Figure 5.13 (a) and (b) shows the flank wear of the front cutting tool. Abrasive wear was identified as the dominant mode. Abrasive marks in the direction of workpiece rotation were observed with no traces of adhesive or diffusion wear. The manganese additions apart from forming manganese sulphide (MnS) if present in excess will result in the formation of hard brittle intermetallic second phase iron carbide. Moreover, cast iron also contains silicon and other hard elements. Generally, the outer surface of casting is hard. During lower cutting speed the temperature generation in the cutting zone is less and there is no much softening. All this contributes to abrasion wear of the front tool. Figure 5.13 (c) and (d) shows the flank wear of the rear cutting tool, where the adhesive and diffusion marks were distinctly observed. Machining by the leading front cutting tool

raises the workpiece temperature. This temperature rise promotes diffusion wear while reducing abrasion wear.

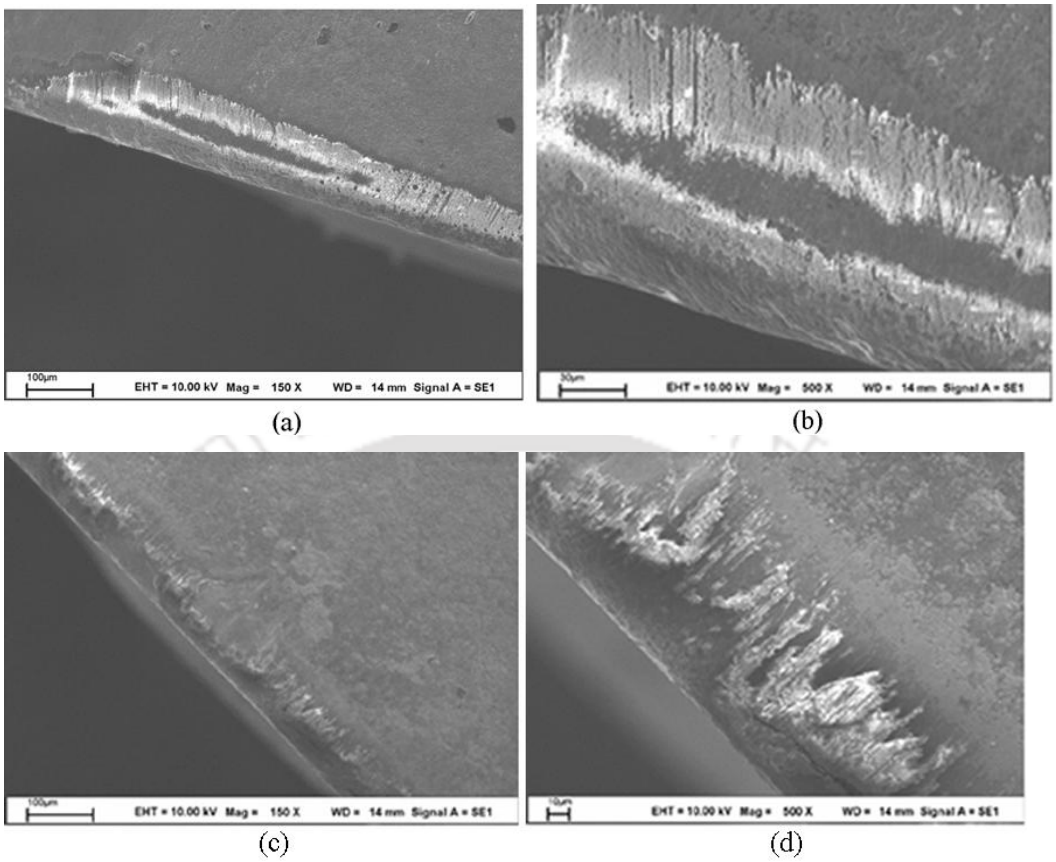

Figure 5.13. Flank wear (a) Of front cutting tool at 150X magnification (0.24 mm/rev feed and 1 mm depth of cut) (b) Of front cutting tool at 500X magnification (0.24 mm/rev feed and 1 mm depth of cut) (c) Of rear cutting tool at 150X magnification (0.24 mm/rev feed and 1 mm depth of cut) and (d) Of rear cutting tool at 500X magnification (0.24 mm/rev feed and 1 mm depth of cut)

5.3.5 Chip Morphology

In the present investigation, due to the distance between the two cutting tools the chips produced by the individual tools do not interfere with each other. The chips were carefully collected from the machining experiments and observed under scanning electron microscope to understand the mechanism of material removal in double tool turning. Figure 5.14 (a) and (b) shows the back surface of the chips generated from the front and rear cutting tool. Back surface experiences higher contact pressure and frictional force due to the motion of the chip along the rake face of the tool. Due to this phenomenon apart from cracks, streaks were also formed. It was observed for the chips generated from both front and rear cutting tools.

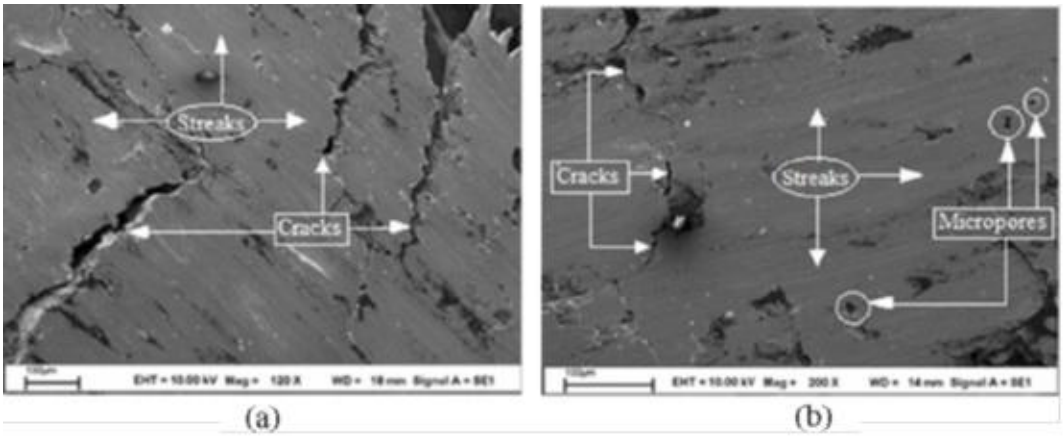

Figure 5.14. Back surface of the generated chip (a) From the front cutting tool (0.24 mm/rev feed and 1 mm depth of cut) and (b) From the rear cutting tool (0.24 mm/rev feed and 1 mm depth of cut)

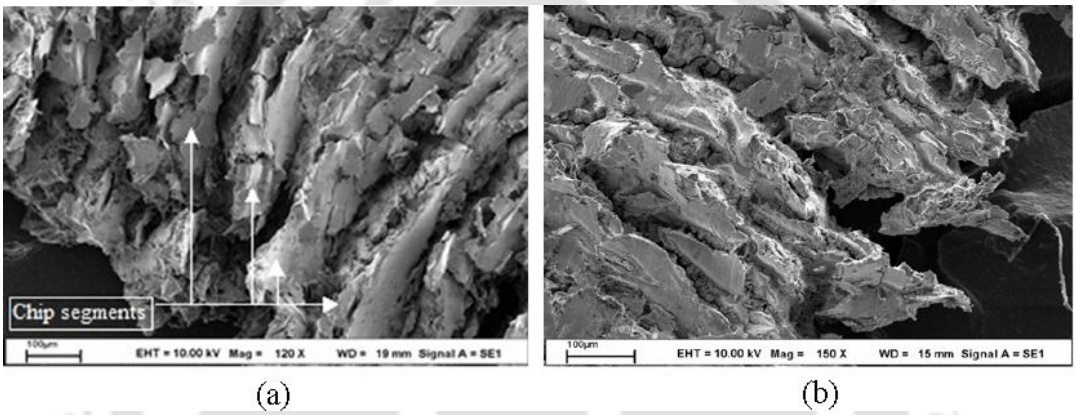

Figure 5.15. Free surface of the generated chip (a) From the front cutting tool (0.24 mm/rev feed and 1 mm depth of cut) and (b) From the rear cutting tool (0.24 mm/rev feed and 1 mm depth of cut)

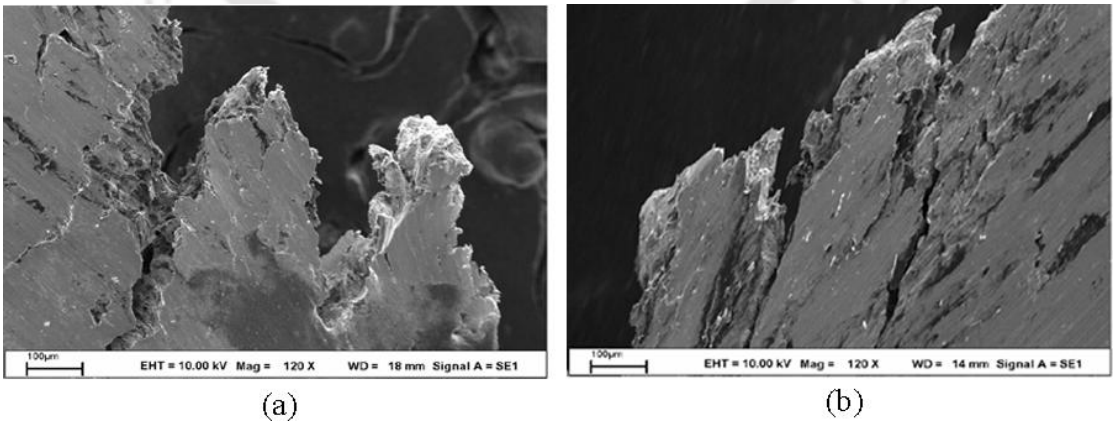

Figure 5.16. Chip segmentation formation generated (a) From the front cutting tool (0.24 mm/rev feed and 1 mm depth of cut) and (b) From the rear cutting tool (0.24 mm/rev feed and 1 mm depth of cut)

In addition to cracks and streaks, micro pores were also seen on the back surface of chips generated from the rear cutting tool due to the prior heat of the workpiece. Higher cutting speed caused higher sliding velocity that contributed to the softening and partial melting of material and resulted in the formation of micro pores. Katuku *et al*. (2009) and Farhat (2003) also observed micro pores along with streaks at higher cutting speed and only streaks at lower cutting speed. Nodular, lamella and loose structure of chip segments were observed on the free surface of the chips generated from both the front and rear cutting tools (Figure 5.15 (a) and (b)). These lamellas, are normal to the direction of chip flow and extend across the width of the chips. Presence of lamella structure on the free surface of the chips is an evidence of shear localisation. It is evident that machining of brittle materials like grey cast iron produces discontinuous chips in the form of small segments as marked in Figure 5.15 (a).The free surface of the chips were further investigated; chips generated from the front cutting tool exhibited only fracture (Figure 5.16 (a)) where no traces of the thermal effect was observed. However, chips generated from the rear cutting tool (Figure 5.16 (b)) exhibited fracture as well as curling of the segmented chip. In spite of lower cutting speed, the feed (0.24 mm/rev) used in this investigation resulted in the segmental chip formation. It is also likely that machining by rear tool also caused some thermal softening.

The thermal softening happens due to recovery and recrystallization of the material in the shear zone. The chips produced due to the rear cutting tool experienced higher temperature compared with that of front cutting tool. It can be noted from the work of Dearnley (1985) that thermal softening at the secondary shear zone took place while machining spheroidal cast iron with coated tool at a cutting speed of 200 m/min. During machining, work material deforms at the higher strain rate which causes work hardening. At elevated temperature, strain rate sensitivity of the work material decreases that causes a reduction in the part of the fracture in segment formation. Shashikant *et al*. (2013) also observed that at room temperature fracture was visible in the form of a crack and propagated over the entire chip thickness. At 100 °C, chip segments were formed by the combination of thermal softening and fracture. At 260 °C and 350 °C, segments were formed only by thermal softening.

5.4 Conclusion

This chapter presents the investigation of the diametral error of cylindrical work piece, cutting tool wear and chip morphology when two single point cutting tools simultaneously turned the workpiece. Following are the major conclusions:

- The diametral error of a machined workpiece was the maximum at the tailstock end and the minimum at the chuck end. This is due to the higher workpiece deflection caused by the cutting forces at the tailstock end.
- The additional cutting tool at the rear side not only removed more material but also acted as a follower rest. The rear cutting tool followed the front cutting tool at a distance of 10 mm and reduced the workpiece deflection by 80% due to the resistance offered by rear tool cutting forces.
- A simple strength of material approach was employed to support the trend of experimentally obtained diametral error of the workpiece. It was found that higher depth of cut leads to higher diametral error.
- Wear of front cutting tool exhibited predominant abrasive marks and very less adhesive and diffusion wear. However, rear cutting tool in the double tool turning exhibited predominant adhesive and diffusion wear.
- Chips generated from the front cutting tool did not show any thermal effect; however, chips produced from the rear cutting tool exhibited curling of chip segments which may be due to thermal softening and fracture.

Chapter 6

The Influence of Machining Parameters on Surface Roughness in Double Tool Turning Process

6.1 Introduction

Surface roughness is an important factor that determines the quality of a machined surface. It depends on many parameters such as cutting condition, machine tool vibration, cutting tool and work holding devices. The cutting speed, feed and depth of cut has a major influence on the surface roughness of the finished component. A lot of research work has been directed towards improving the surface quality of the machined component. The researchers used soft computing approaches comprising neural network, fuzzy logic and genetic algorithms either individually or in combination. The corresponding studies on double tool turning are not available. From the literature survey, it was recognized that no work has been performed to understand about the effect of machining parameters on surface roughness in double tool turning process, although a lot of work has been carried out on conventional turning process. Present research work attempts to shed light on the influence of cutting speed, feed, depth of cut and tool separation distance on the surface roughness during double tool turning process. It also compares the average surface roughness generated by double tool turning process with conventional turning process.

6.2 Experimental Procedure

The cutting conditions employed in metal cutting experiments are specified. Cutting speed, feed and depth of cut are the common machining parameters in a conventional turning process. Besides this, tool separation distance also forms an additional cutting parameter in double tool turning process. In the present research work, the surface roughness was evaluated for grey cast iron and AISI 1050 steel work materials while turning with TiN coated carbide tool. The details of experiments are given in Chapter 3. The cutting conditions are listed in Table 6.1. The upper limit values of the cutting

parameters are chosen based on the compliance of the machine tool and the rigidity of rear tool fixture.

Table 6.1. Values of cutting parameters

Cutting speed (m/min)	75, 100, 125,150, 175, 200, 225 and 250
Feed (mm/rev)	0.04, 0.08, 0.12, 0.16, 0.20 and 0.24
Depth of cut (mm)	0.25, 0.5, 0.75 and 1.0
Tool separation distance (mm)	0, 2, 4, 6, 8 and 10

The surface roughness was measured by Pocket Surf (Make: Mahr GMBH). The evaluation length was taken as 2.4 mm with cut off length as 0.8 mm. The surface roughness was measured at three different locations and the average was taken. Additionally 3D profilometer (Make: Taylor Hobson) was also used for surface roughness measurement. The scanned area for 3D surface roughness measurement is 0.8 mm X 0.8 mm. The cutting temperature was measured using an infrared camera (Make: Infratec varioCAM hr head).

6.3 Results and Discussion

In machining, the quality of the machined surface is mainly determined by its surface roughness. Double tool turning of AISI 1050 steel and grey cast iron was investigated. In this study, the effect of cutting speed, feed, depth of cut and tool separation distances on surface roughness was studied.

6.3.1 Effect of Cutting Speed on Surface Roughness

The effect of cutting speed on surface roughness was carried out on AISI 1050 steel and grey cast iron work materials. Figure 6.1 reveals the variation of average surface roughness with the increase in cutting speed for various feeds of AISI 1050 steel work material. The cutting speed is increased from 75 m/min to 250 m/min in the increments of 25 m/min. The feed is varied from 0.04 mm/rev to 0.24 mm/rev in the increments of 0.04 mm/rev. A depth of cut of 1 mm for each cutting tool and a tool separation distance of 2 mm was maintained for all the cutting conditions. The surface roughness decreased with the increase in cutting speed. When the cutting speed is

increased from 75 m/min to 250 m/min the surface roughness decreased in the range of 33% to 51% for the various feeds ranging between 0.04 mm/rev and 0.24 mm/rev. Sahin and Motorcu (2005) asserted 20% reduction in the average surface roughness, when the cutting speed was increased from 181 m/min to 240 m/min while turning AISI 1040 steel with a coated carbide tool. At lower cutting speed the built up edge is formed and the material fails due to tensile rupture.

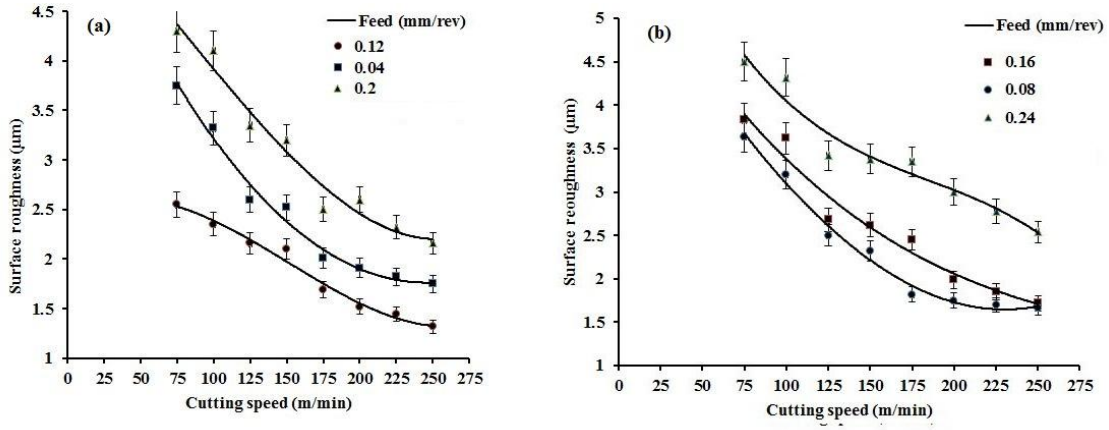

Figure 6.1. Variation of surface roughness with cutting speed for AISI 1050 steel for 1 mm depth of cut and 2 mm tool separation distance (a) For feeds of 0.04, 0.12 and 0.20 mm/rev (b) For feeds of 0.08, 0.16 and 0.24 mm/rev

Previous research works of Philip (1971) and Selvam and Radhakrishnan (1974) unveiled the existence of the built up edge while machining plain carbon steel using a carbide tool and high speed steel tool at cutting speeds of 70 m/min and 40 m/min respectively. The built up edge causes the side flow of the work material over the machined surface. The side flow and the built up edge increased the surface roughness along the cutting direction and feed direction respectively. The increase in the size of built up edge results in the increase of side flow. It gives rise to a triangular uncut region of work material adhering to the machined surface; this is called as spanzipfel. Selvam and Radhakrishnan (1973) observed spanzipfel, while machining a plain carbon steel with a high speed steel tool in the cutting speed domain of 6 m/min to 50 m/min. Spanzipfel, side flow and built up edge contributes to higher surface roughness. It is seen that a higher average surface roughness of 4.5 µm is obtained at a lower cutting speed of 75 m/min with a feed of 0.24 mm/rev. When the cutting speed is increased the built up edge formation retards, and at higher cutting speed it ceases to exist. A surface roughness of 2.54 µm was obtained at a higher cutting speed

of 250 m/min with 0.24 mm/rev feed. Thus the average surface roughness was less at higher cutting speed and more at lower cutting speed. Thomas *et al*. (1996) observed a 13% reduction in surface roughness when the cutting speed was increased from 160 m/min to 265 m/min while dry turning mild carbon steel with a carbide cutting tool. Lalwani *et al*. (2008) noted that when the cutting speed was increased from 55 m/min to 93 m/min the surface roughness was lowered by 11%, while turning maraging steel with a coated ceramic insert.

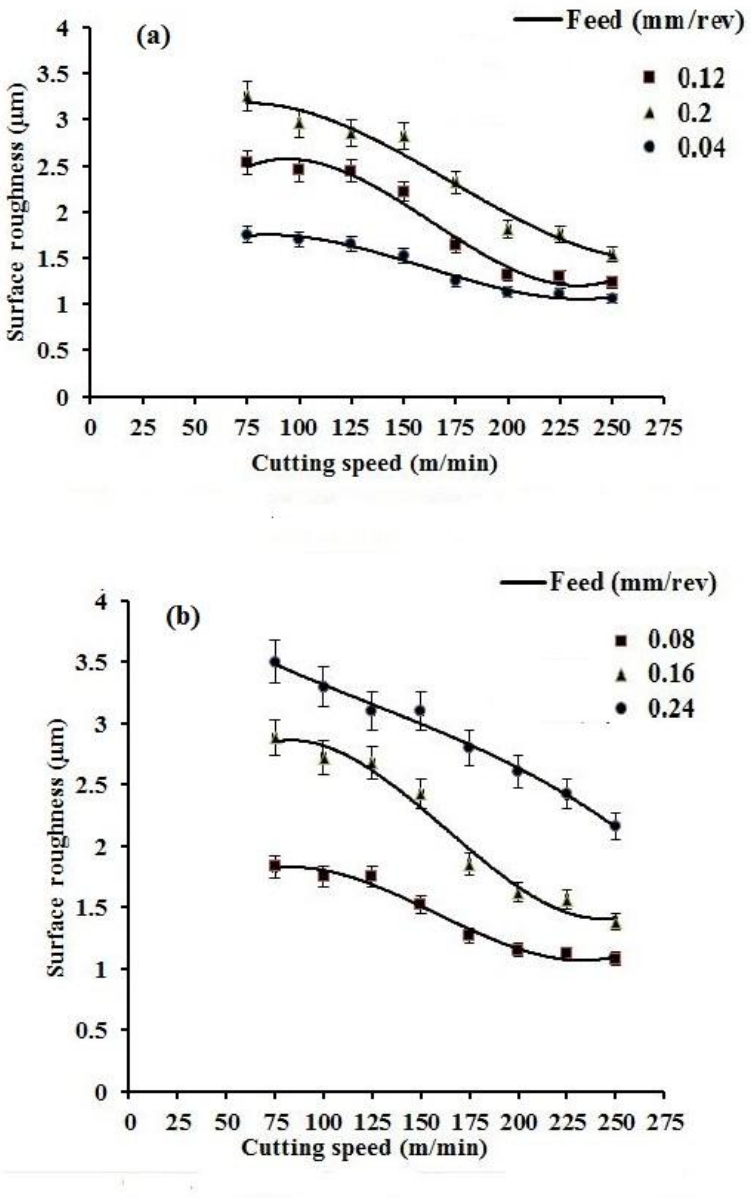

Figure 6.2. Variation of surface roughness with cutting speed for grey cast iron for 1 mm depth of cut and 2 mm tool separation distance (a) For feeds of 0.04, 0.12 and 0.20 mm/rev (b) For feeds of 0.08, 0.16 and 0.24 mm/rev

Figure 6.2 represents the variation of average surface roughness with the change in cutting speed for various feeds of grey cast iron work material. A depth of cut of 1 mm was given individually to the front cutting tool and rear cutting tool. The tool separation distance was kept as 2 mm. With the increase in cutting speed the average surface roughness decreased. It decreased in the range of 25% to 47% when the cutting speed increased from 75 m/min to 250 m/min for the various feeds ranging between 0.04 and 0.24 mm/rev. Yigit (2008) revealed 19% reduction in average surface roughness, when the cutting speed was increased from 150 m/min to 200 m/min while turning nodular cast iron with a coated carbide tool. In this investigation an average surface roughness of 1.75 µm was achieved for grey cast iron when compared to an average surface roughness of 3.75 µm for AISI 1050 steel. This is for 75 m/min cutting speed, 0.04 mm/rev feed, 1 mm depth of cut for each cutting tool and 2 mm tool separation distance. The average surface roughness stabilizes for the cutting speeds ranging between 200 m/min to 250 m/min for all the feeds, except for 0.24 mm/rev feed. A reduction of 14% to 17% in average surface roughness was obtained when the cutting speed is increased from 200 m/min to 250 m/min, for the feed ranges of 0.16 mm/rev to 0.24 mm/rev. Whereas for the lower feeds ranging from 0.04 mm/rev to 0.12 mm/rev a reduction not more than 7% in average surface roughness was attained. Due to the rigidity constrain of the rear tool holding fixture, further increase in cutting speed beyond 250 m/min is insurmountable. Nevertheless, surface finish of grey cast iron workpiece is found to be superior to AISI 1050 steel, especially at higher cutting speeds. This might be due to the brittle discontinuous chip formation and good vibration damping capacity of grey cast iron.

Additionally higher cutting speeds results in higher cutting temperature which in turn favours lower surface roughness. The shear yield strength of the work material is lowered at elevated temperatures, which in turn reduces the cutting forces. It was already mentioned in Section 4.3.1 of Chapter 4 that reduced cutting forces are obtained when the cutting speed is increased from 75 m/min to 185 m/min while turning grey cast iron with coated carbide tool. Figure 6.3 and Figure 6.4 shows the thermographic image demonstrating the temperature distribution in AISI 1050 steel and grey cast iron work materials under similar machining conditions. It is noticed, that the cutting zone temperature of the grey cast iron workpiece is lesser by 20 °C on

comparison with the cutting zone temperatures of AISI 1050 workpiece. This difference may be due to the presence of free graphite in grey cast iron which provides both lubrication and cooling.

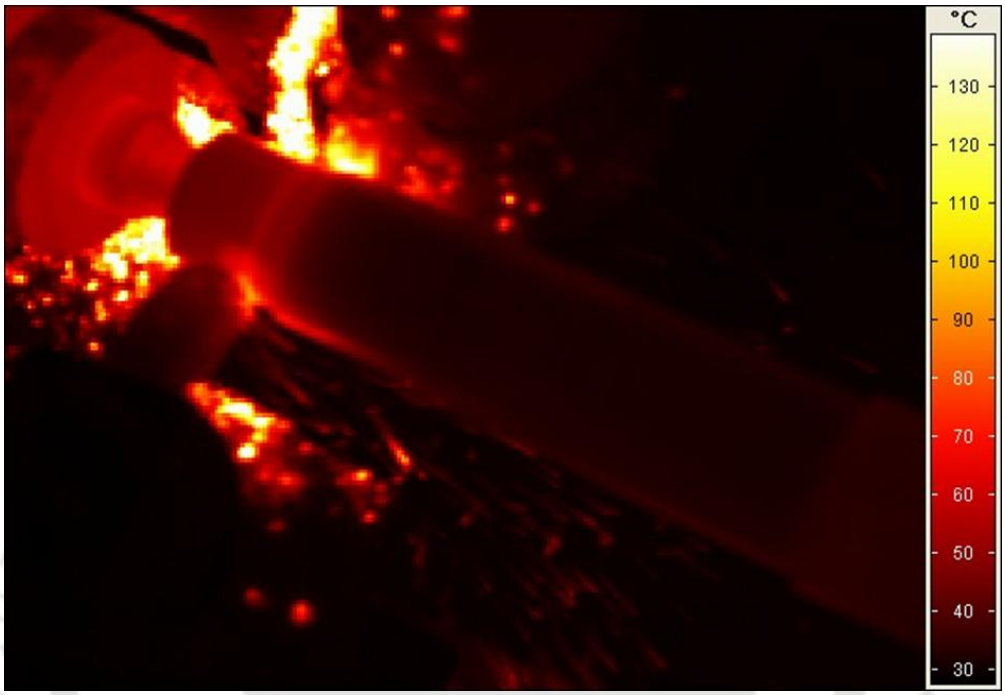

Figure 6.3. Thermogram of AISI 1050 steel (75 m/min cutting speed, 0.04 mm/rev feed, 1 mm depth of cut and 2 mm tool separation distance)

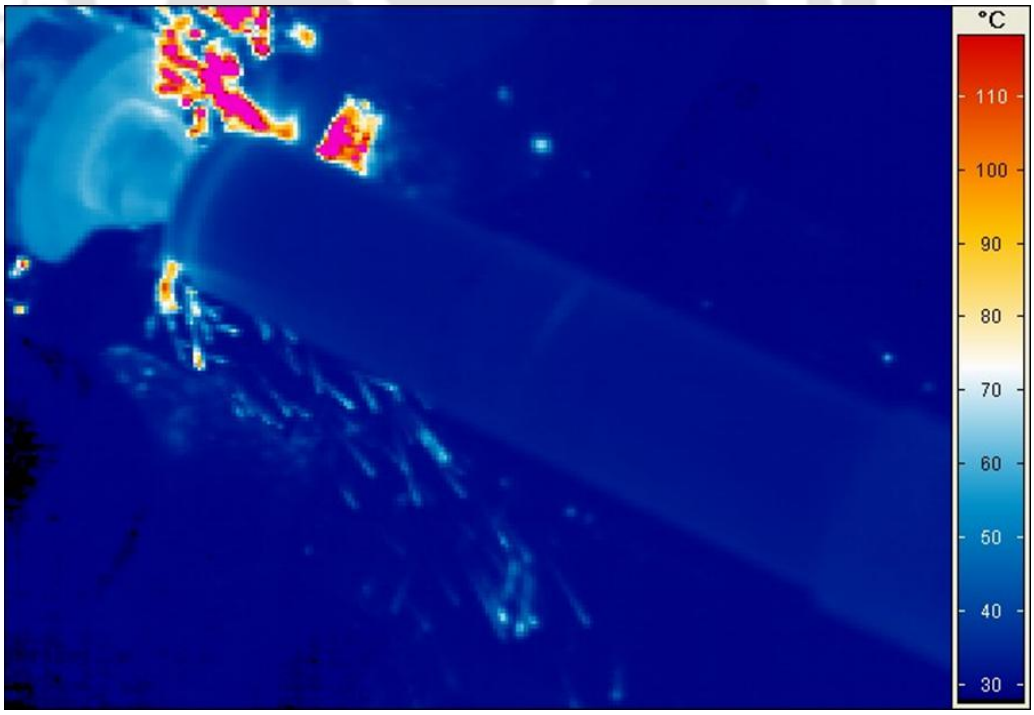

Figure 6.4. Thermogram of grey cast iron (75 m/min cutting speed, 0.04 mm/rev feed, 1 mm depth of cut and 2 mm tool separation distance)

The thermogram (Figure 6.4) displays the brittle chips flowing away from the cutting zone causing lesser heat generation in the secondary deformation zone. The details of brittle chip morphology of grey cast iron are mentioned in Section 5.3.5 of Chapter 5. The chips exhibited fracture and no thermal effect was observed. On the other hand for AISI 1050 steel workpiece material, the continuous chips are produced which in turn generate more heat due to sliding of chips over the rake face of the cutting tool. Unlike the front cutting tool as the rear cutting tool is inverted, its cutting zone is only partially visible. Apart from this, the cutting tool vibration also plays a significant role in determining the average surface roughness of the machined work piece. Increase in cutting speed results in decreased tool vibration. It was already reported in Section 4.5 of Chapter 4 that when the cutting speed is increased from 75 m/min to 185 m/min the amplitude of tool vibration along the cutting direction is reduced. This in turn reduces the surface roughness, thereby improving the surface finish and stability of the double tool turning process. Dimla (2004) also observed a reduction in amplitude of cutting tool vibration when the cutting speed was increased from 100 m/min to 300 m/min while machining steel with a carbide tool. Thus it can be summarised that the double tool turning process resembles conventional turning process where the surface roughness decreased with the increase in cutting speed and increased with the decrease in cutting speed.

6.3.2 Effect of Feed on Surface Roughness

The variation of surface roughness with the change in feed for various cutting speeds for AISI 1050 steel is expressed in the Figure 6.5. The depth of cut and tool separation distance has already been mentioned in Section 6.3.1. The average surface roughness initially decreased when the feed is increased from 0.04 mm/rev to 0.12 mm/rev. Then it increased on further increase of feed from 0.12 mm/rev to 0.24 mm/rev. This phenomenon is prominently noticed at lower cutting speeds of 75 m/min and 100 m/min. For these low cutting speeds the average surface roughness decreased by 32% and 29% when the feed was increased from 0.04 mm/rev to 0.12 mm/rev. Further increase of feed from 0.12 mm/rev to 0.24 mm/rev increased the average surface roughness by 76% and 84% respectively. Initially at lesser feed, the material removal takes place by ploughing action leading to higher average surface roughness in case of

ductile materials like steel. On increasing the feed from 0.04 mm/rev to 0.12 mm/rev material is removed by shearing action, thereby reducing the average surface roughness. The burnishing action of the cutting tool over the workpiece might also lead to decreased average surface roughness. Thereafter an increased average surface roughness is obtained up to 0.24 mm/rev feed.

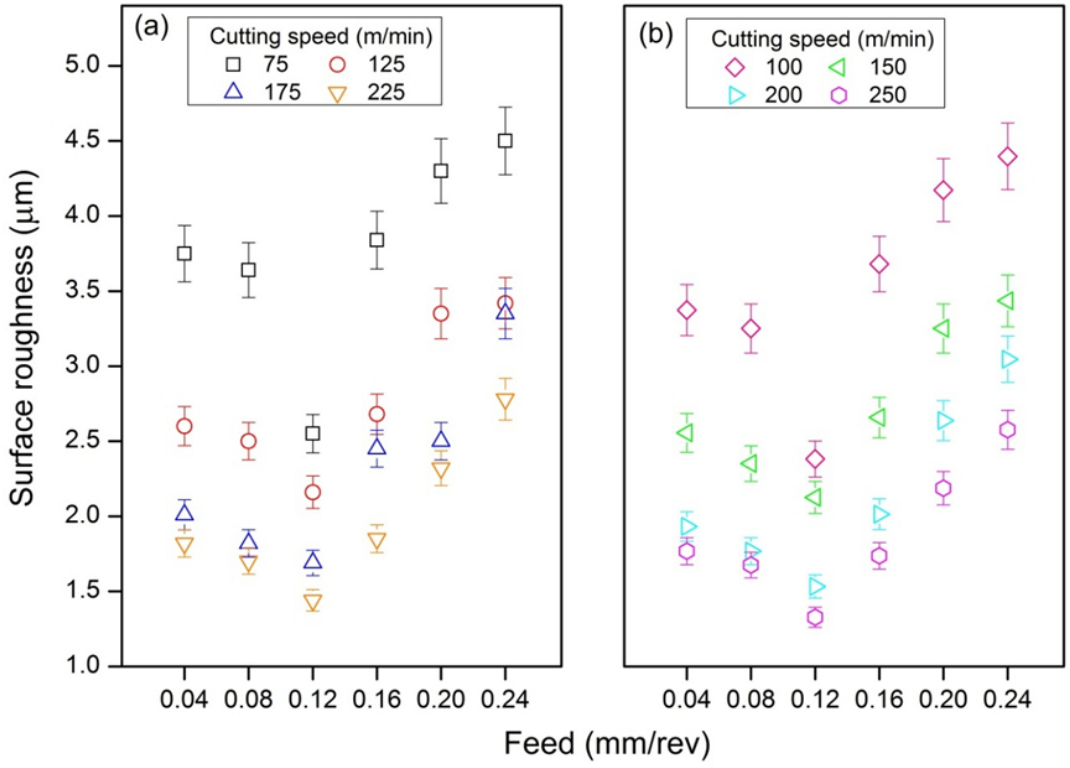

Figure 6.5. Variation of surface roughness with feed for AISI 1050 steel for 1 mm depth of cut and 2 mm tool separation distance (a) For the cutting speeds ranging from 75 to 225 m/min (b) For the cutting speeds ranging from 100 to 250 m/min

Risbood *et al*. (2003) observed a similar trend for mild steel; the average surface roughness got minimised by 68% when the feed was increased from 0.05 mm/rev to 0.14 mm/rev and on further increase of feed to 0.36 mm/rev the average surface roughness increased. Gokkaya and Nalbant (2007) observed an increase of surface roughness from 1.616 µm to 6.833 µm when the feed was increased from 0.15 mm/rev to 0.35 mm/rev while turning AISI 1030 steel with coated carbide tool. Higher rate of deformation of the work material and cutting edge feed marks are the reasons behind higher surface roughness at higher feed. It is noteworthy to mention here that cutting edge feed marks depends on the nose radius of the cutting tool also, which is 0.8 mm in the present investigation. The feed marks for three different feeds

of AISI 1050 steel are unfolded in Figure 6.6, Figure 6.7 and Figure 6.8. It can be seen that the average surface roughness is lower at a feed of 0.12 mm/rev when compared to 0.04 mm/rev and 0.24 mm/rev. The three dimensional topographies reveal the peak to valley height of the scanned areas for various feed. This gives an apprehension of the maximum surface roughness of the machined surface. The Table 6.2 provides the peak to valley height and average surface roughness at different feeds of AISI 1050 steel work material. The machining parameters are 75 m/min cutting speed, 1 mm depth of cut for both front cutting tool and rear cutting tool and 2 mm tool separation distance.

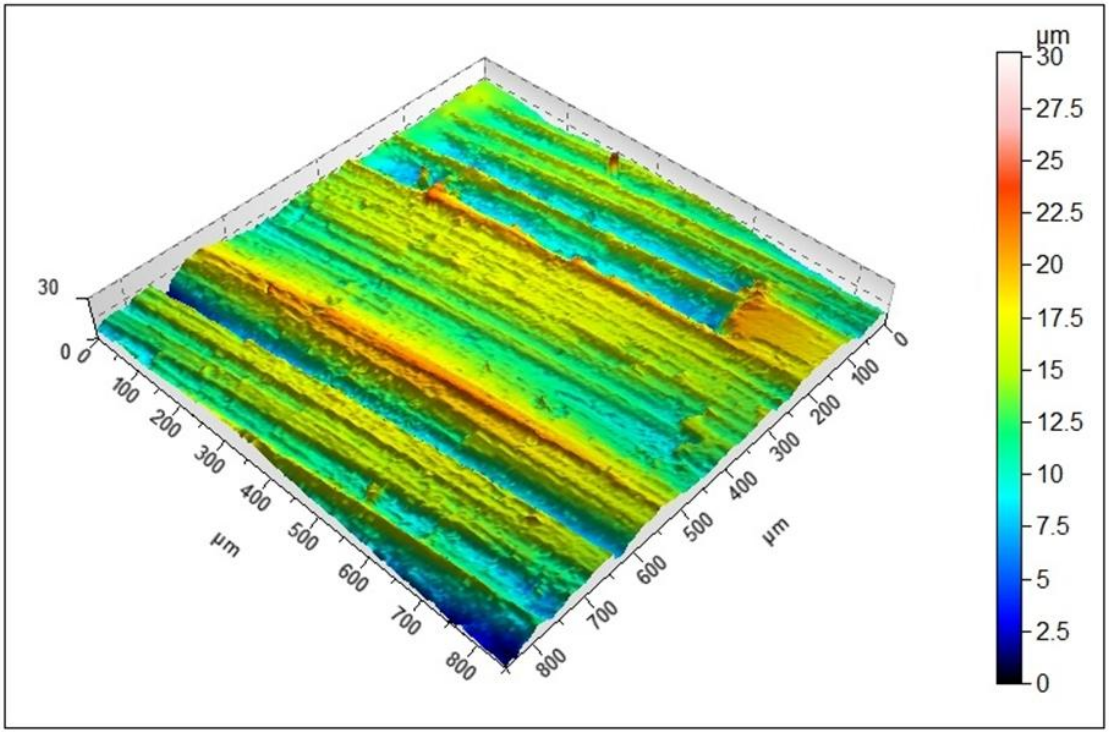

Figure 6.6. Three dimensional topography of AISI 1050 steel at 0.04 mm/rev feed (75 m/min cutting speed, 1 mm depth of cut 2 mm tool separation distance)

It was identified that the peak to valley height decreased by 37% when the feed increased from 0.04 mm/rev to 0.12 mm/rev. For further increase of feed to 0.24 mm/rev, it increased by 89%. It can be envisaged that for the same cutting conditions the average surface roughness decreased by 32% and then increased by 76%. The three dimensional surface roughness profile of Figure 6.6 has a predominance of green colour. This shows that the existing grooves are of uniform depth. It can also be noted that the waviness of the surface is minimal.

Table 6.2. Variation of peak to valley height and average surface roughness with feed for AISI 1050 steel

Feed (mm/rev)	Peak to valley height R_{max} (µm)	Average surface roughness R_a (µm)
0.04	19.8	3.75
0.12	12.5	2.55
0.24	23.6	4.5

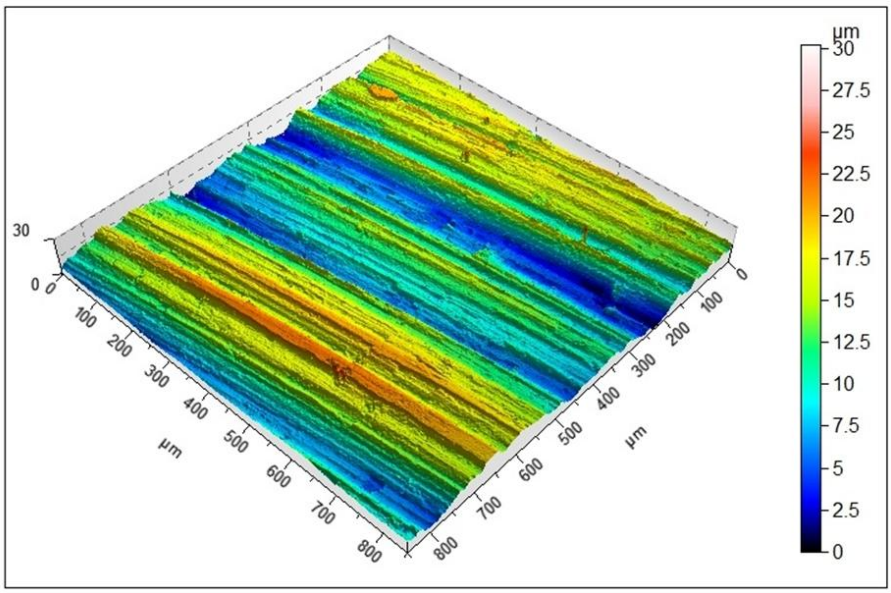

Figure 6.7. Three dimensional topography of AISI 1050 steel at 0.12 mm/rev feed (75 m/min cutting speed, 1 mm depth of cut 2 mm tool separation distance)

In Figure 6.7, substantial amount of blue region is present along with slight red and green regions. The blue region represents a minimum height of peak to valley, hence the surface roughness is lesser at this feed. In the Figure 6.8 apart from the grooves along the cutting direction, some micro grooves are also observed along the direction perpendicular to it. It is due to the ploughing action of the cutting tool. This deteriorates the surface finish resulting in higher surface roughness. Apart from this, pertinent red region showing the maximum peak to valley height also exists. Hence the average surface roughness is maximum at higher feed. It is to be noted that the lowest and highest average surface roughness value of 1.32 µm and 4.5 µm for AISI

1050 steel is obtained at cutting speed of 250 m/min and 75 m/min for the feeds of 0.12 mm/rev and 0.24 mm/rev respectively.

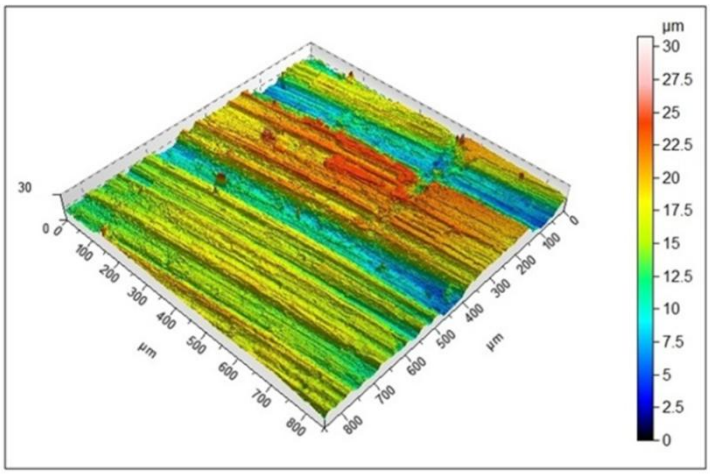

Figure 6.8. Three dimensional topography of AISI 1050 steel at 0.24 mm/rev feed (75 m/min cutting speed, 1 mm depth of cut 2 mm tool separation distance)

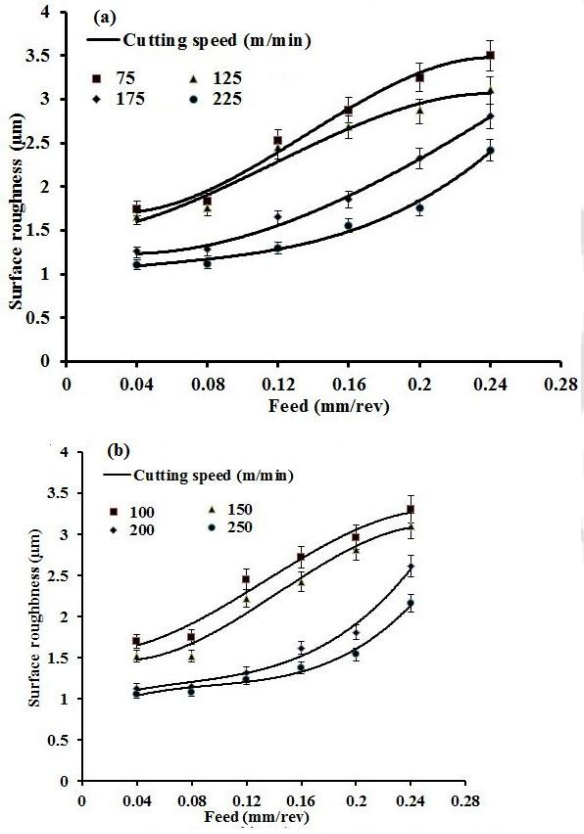

Figure 6.9. Variation of surface roughness with feed for grey cast iron for 1 mm depth of cut and 2 mm tool separation distance (a) For cutting speed ranging from 75 m/min to 225 m/min (b) For cutting speed ranging from 100 to 250 m/min

Figure 6.9 (a) and (b) exhibits the variation of surface roughness of grey cast iron with the change in feed for various cutting speeds. Previous researchers had suggested an increase of surface roughness with the increase in feed (Ramesh *et al*., 2012; Upadhyay *et al*., 2013). It is seen that the average surface roughness increased from 1.40 µm to 2.87 µm with the increase in feed from 0.04 mm/rev to 0.24 mm/rev for the investigated cutting speeds. This coincides with the results of Gunay and Yucel (2013), it was observed that the surface roughness increased by 42% when the feed was increased from 0.05 mm/rev to 0.1 mm/rev while turning white cast iron with a ceramic tool. In the current investigation the lowest and highest surface roughness value of 1.06 µm and 3.5 µm was obtained for a feed of 0.04 mm/rev and 0.24 mm/rev at a cutting speed of 250 m/min and 75 m/min respectively. At this juncture it can be well emphasized that combination of low feed with high cutting speed will produce lower surface roughness for grey cast iron and vice versa. On similar lines the work of Xavior and Adhithan (2009) revealed that the surface roughness increased from 1.91 µm to 2.68 µm when the feed was increased from 0.2 mm/rev to 0.28 mm/rev, while turning austenitic steel with carbide tool using different cutting fluids. It is to be noted that in the present work, feed of both the front and rear cutting tools are equal as both are mounted on the same carriage. Thus the investigation reveals that for grey cast iron the average surface roughness increases with the increase in feed. However AISI 1050 steel the average surface roughness decreases when the feed was increased from 0.04 mm/rev to 0.12 mm/rev and on further increase of feed from 0.12 mm/rev to 0.24 mm/rev the average surface roughness increased.

6.3.3 Effect of Depth of Cut and Tool Separation Distance on Surface Roughness

Figure 6.10 depicts the influence of depths of cut on surface roughness for AISI 1050 steel when the depth of cut is increased from 0.25 mm to 1.5 mm in the increments of 0.25 mm. A cutting speed of 125 m/min and a tool separation distance of 2 mm is maintained constant for all the cutting conditions. The feed is changed from 0.04 mm/rev to 0.24 mm/rev in the increments of 0.04 mm/rev. It is seen that the average surface roughness increased with the increase in depths of cut. It can be observed that when the depth of cut is increased from 0.25 mm to 1.5 mm the average surface

roughness increased in the range of 20% to 50% for the different feeds ranging from 0.04 mm/rev to 0.24 mm/rev.

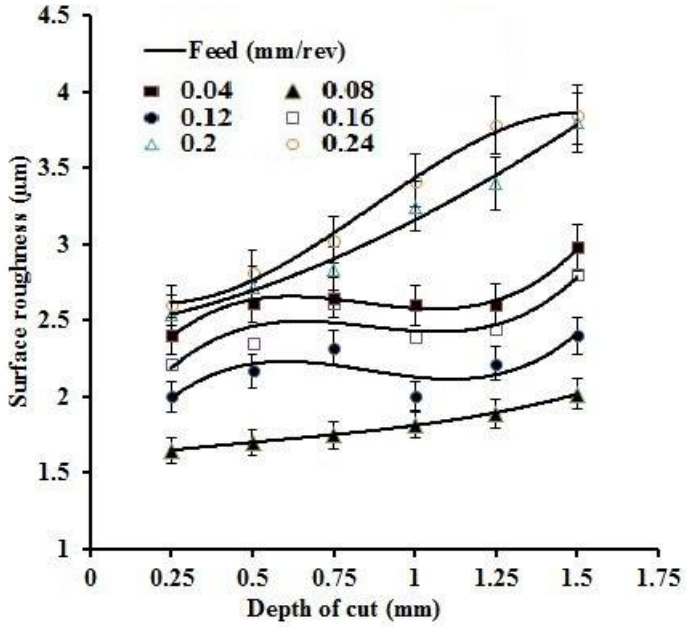

Figure 6.10. Variation of surface roughness with depth of cut for AISI 1050 steel (125 m/min cutting speed and 2 mm tool separation distance)

Due to the increase in depths of cut the cutting forces and amplitude of cutting tool vibration increases, which in turn increase the average surface roughness. Davim *et al*. (2008) found while turning free machining steel with cemented carbide tool that the average surface roughness increased from 1.17 µm to 1.23 µm when the depth of cut is increased from 0.5 mm to 1 mm. Similarly Chelladurai *et al*. (2008) reported an increase in amplitude of cutting tool vibration when the depth of cut was increased from 3 mm to 5 mm while turning steel with a carbide tool.

Figure 6.11 demonstrates the effects of depths of cut on surface roughness for grey cast iron. The values of cutting speed and tool separation distance is taken as 125 m/min and 2 mm respectively. With the increase in depth of cut the average surface roughness increased for higher feeds from 0.12 mm/rev to 0.24 mm/rev, but in case of lower feeds of 0.04 mm/rev and 0.08 mm/rev it remains almost constant. It can seen that when the depth of cut is increased from 0.25 mm to 1.5 mm the average surface roughness increased in the range of 31% to 39% for the feed ranging from 0.12 mm/rev to 0.24 mm/rev.

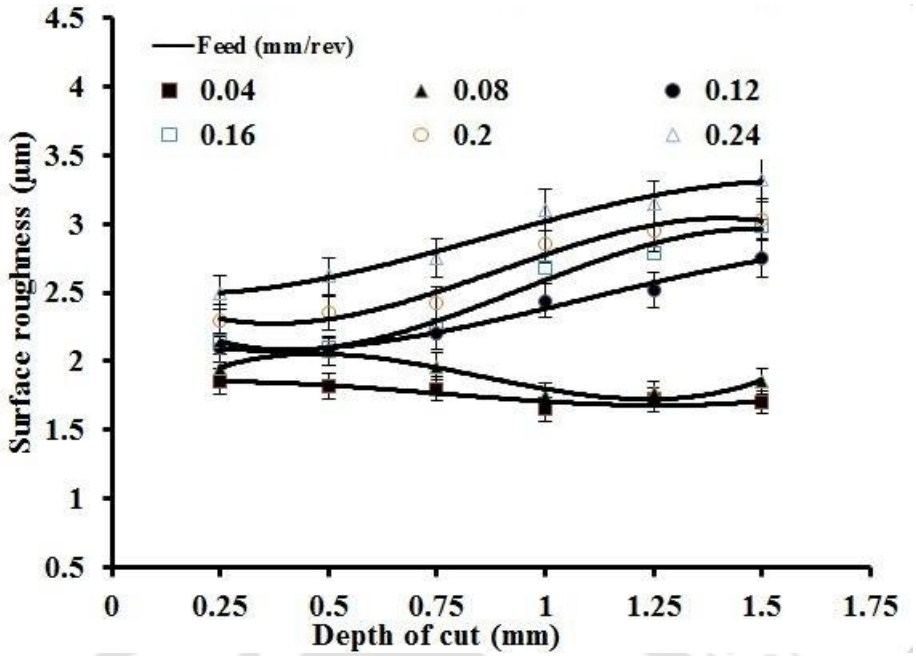

Figure 6.11. Variation of surface roughness with depth of cut for grey cast iron (125 m/min cutting speed and 2 mm tool separation distance)

From the work of Akdemir *et al*. (2012), it was ascertained that 33% increase in average surface roughness was obtained when the depth of cut was increased from 1 mm to 2 mm while turning austempered ductile iron with a carbide insert. The increased cutting forces due to the increase in depths of cut will increase the average surface roughness. It has been previously reported in Section 5.3.1 of Chapter 5 that the cutting forces of the front and rear cutting tools increased by 30% and 23% respectively, when the depth of cut was increased from 1 mm to 1.5 mm while turning grey cast iron with coated carbide tool. When the tool separation distance was varied from 0 mm to 10 mm in the increments of 2 mm the surface roughness remains almost constant for both the work materials as shown in Figure 6.12. The effect of process parameters in double tool turning process shows a similar trend like conventional turning process. The average value of surface roughness is 2.22 µm for AISI 1050 steel for 125 m/min cutting speed, 0.12 mm/rev feed, 1 mm depth of cut and with a tool separation distance of 2 mm. For the same cutting conditions for grey cast iron the average surface roughness value is 2.4 µm. The deviation of minimum and maximum values for the average surface roughness values for AISI 1050 steel is 10% and 6%. In case of grey cast iron it is 8% and 5%. For all the investigated cutting

conditions the tool separation distance does not have much influence on the average surface roughness of both AISI 1050 and grey cast iron work materials.

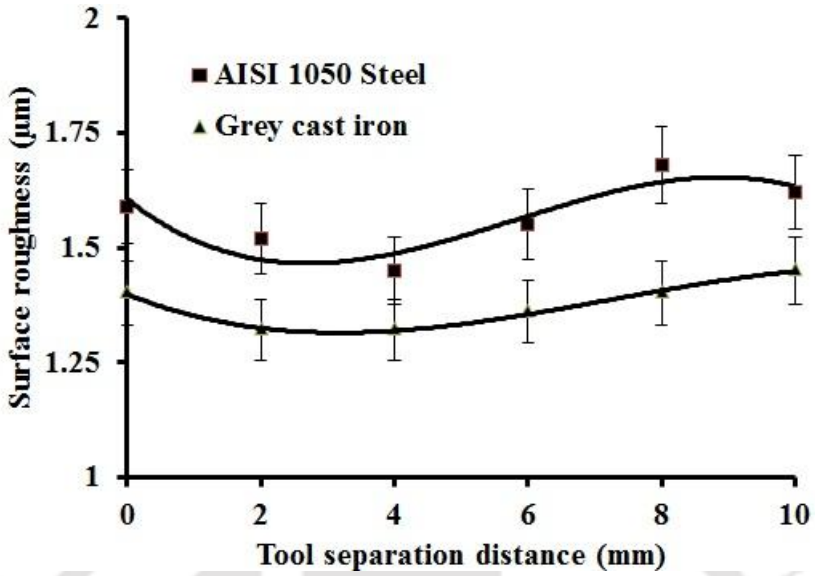

Figure 6.12. Variation of surface roughness with tool separation distance for AISI 1050 steel and grey cast iron (200 m/min cutting speed, 0.12 mm/rev feed and 1 mm depth of cut)

6.3.4 Comparison of Surface Roughness Between Double Tool Turning Process and Conventional Turning Process

The average surface roughness produced during double tool turning and conventional turning processes for different cutting conditions for AISI 1050 steel and grey cast iron work materials are shown in Table 6.3 and Table 6.4, respectively. The tool separation distance was kept as 2 mm in double tool turning. The depths of cut of 1 mm and 2 mm were given for conventional turning process while 1 mm depth of cut was given to each tool in double tool turning process. The average surface roughness was measured in these cutting conditions and compared. From the Table 6.3 it is noted that for AISI 1050 steel, the surface roughness reduced in double tool turning process in the range of 13% to 20% for 2 mm depth of cut. In case of double tool turning process, the depth of cut of 2 mm is shared equally between the front cutting tool and rear cutting tool. Therefore, the individual depth of cut of front cutting tool and rear cutting tool are 1 mm. Double tool turning with 1 mm depth of cut for each tool was compared with conventional turning with 1 mm depth of cut. In this case also the surface roughness reduced from 4% to 14% for double tool

turning on comparison with conventional turning process. From the Table 6.4 it is observed that for grey cast iron the surface roughness reduced in double tool turning process in the ranges of 13%–18% and 6%–14% as compared to conventional turning for 2 mm and 1 mm depths of cut, respectively. Overall, the average surface roughness was lower in double tool turning process compared to conventional turning process for both the AISI 1050 steel and grey cast iron.

Table 6.3. Average surface roughness of double tool turning and conventional turning process for AISI 1050 steel

Cutting parameters		Average surface roughness (µm)		
		Double tool turning	Conventional turning	
Cutting speed (m/min)	Feed (mm/rev)	2 mm depth of cut (1 mm for each tool)	1 mm depth of cut	2 mm depth of cut
100	0.12	2.35	2.54	2.75
100	0.24	4.32	4.52	4.98
150	0.12	2.10	2.28	2.52
150	0.24	3.38	3.70	3.90
200	0.12	1.52	1.74	1.84
200	0.24	3.00	3.16	3.54
250	0.12	1.32	1.44	1.65
250	0.24	2.54	2.96	3.12

Table 6.4. Average surface roughness of double tool turning and conventional turning process for grey cast iron

Cutting parameters		Average surface roughness (µm)		
		Double tool turning	Conventional turning	
Cutting speed (m/min)	Feed (mm/rev)	2 mm depth of cut (1 mm for each tool)	1 mm depth of cut	2 mm depth of cut
100	0.12	2.45	2.60	2.86
100	0.24	3.30	3.80	3.92
150	0.12	2.22	2.58	2.64
150	0.24	3.10	3.44	3.66
200	0.12	1.32	1.46	1.60
200	0.24	2.62	2.96	3.12
250	0.12	1.24	1.32	1.42
250	0.24	2.16	2.46	2.64

In double tool turning process the radial cutting force of the front and rear cutting tools get cancelled as they act in opposite direction to each other. The cutting tools also act as follower rest to one another. This increases the rigidity of the work piece. The depth of cut given to a single cutting tool in conventional turning is divided equally between two cutting tools in double tool turning. This results in decreased cutting forces causing lesser deflection of the workpiece. Thereby it improves both the surface finish and accuracy of the machined surface. It was mentioned in Section 5.3 of Chapter 5 that the workpiece deflection got lowered by 80% while double tool turning of grey cast iron with coated carbide cutting tool at 116 m/min cutting speed, 0.24 mm/rev feed and 1 mm depth of cut. Hence it can be concluded that the surface finish obtained in double tool turning process is superior when compared to conventional turning process.

6.4 Cost Comparison of Single and Double Tool Turning Process

Preceding discussion has ascertained that for same depth of cut for each tool and the same other process conditions, the surface roughness in double tool turning is lesser than that in single tool turning. It can be safely assumed that the tool life in both the process remains same; although it is expected to be lesser in double tool turning. This is because, double tool turning encounters lesser vibration and forces due to supporting action of the opposite tool. The operating cost per hour can be assumed same in both the process. Operating cost includes depreciation cost of the machine tool, labour cost, electricity cost and overheads. Compared to the cost the lathe, additional fixture cost in double tool turning is very small. Hence, the depreciation cost can be assumed same. Similarly, other costs can also be assumed same for both the processes.

Considering this,

$$C_p = C_0 T_p + C_t F_t, \tag{6.1}$$

where C_p is the production cost per piece, C_0 is the operating cost per unit time, T_p is the time of production per piece, C_t is the tool cost and F_t is the fraction of tool consumed in making one piece. As discussed earlier, C_0, C_t and F_t can be assumed equal in double tool turning and conventional single tool turning. It is the T_p that differentiates the production cost in the two cases. In single tool turning, the same depth of cut has to be achieved in two passes. Hence, T_p is twice of that in double tool turning. If the double tool turning takes x minutes to produce a piece, the single tool turning will require $2x$ minutes. Hence, saving in cost in double tool turning will be $C_0 x$. The percentage saving in cost is expressed as

$$\%\,\text{saving in cost} = \frac{C_0 x}{2C_0 x + C_t F_t} \times 100. \tag{6.2}$$

An example: For the typical lathe machine in a workshop, operating cost C_0 is \$12 per hour (\$0.2 per minute). Tool cost C_t is \$2. Taking the total time to produce a component, x, as 3 minutes, out of which 2 minute is the time of actual machining. Typical tool life is 30 minutes. Hence, a tool can produce 15 components in its life-time. Hence, F_t=1/15=0.067. Putting this values in Eq. (6.2), % saving in cost comes out to be 45%, which is a significant saving.

6.5 Conclusion

In this work, the effect of process parameters like cutting speed, feed, depth of cut and tool separation distance on surface roughness in double tool turning process were studied and the following conclusion are arrived:

- ❖ Double tool turning process produced a superior surface finish for both AISI 1050 steel and grey cast iron work materials for the range of investigated cutting conditions, apart from improving productivity of the process. On comparison with conventional turning process, a lowered average surface roughness for AISI 1050 steel and grey cast iron work materials was obtained in double tool turning process.
- ❖ The average surface roughness decreased with the increase in cutting speed for both AISI 1050 steel and grey cast iron work material for the range of explored cutting conditions. The average surface roughness was lower at higher cutting speed and higher at lower cutting speed. This behaviour was identical to conventional turning process.
- ❖ With the increase in feed the average surface roughness increased under all the studied cutting conditions for grey cast iron. In case of AISI 1050 steel the average surface roughness initially decreased from 0.04 mm/rev feed till 0.12 mm/rev feed. On further increasing the feed from 0.12 mm/rev the average surface roughness increased till 0.24 mm/rev feed.
- ❖ The average surface roughness increased with the increase in depth of cut for AISI 1050 steel for all the chosen cutting conditions. For grey cast iron the same phenomenon is observed for feeds above 0.08 mm/rev. At lower feeds of 0.04 mm/rev and 0.08 mm/rev the average surface roughness remained almost constant with the increase in depth of cut.
- ❖ For all the investigated cutting conditions the tool separation distance did not have much effect on the average surface roughness of both AISI 1050 steel and grey cast iron work materials.
- ❖ Double tool turning is advantages as it leads to reduction in machining cost. For a particular cutting condition, 45% savings in cost is obtained in double tool turning process compared to single tool turning process.

Chapter 7

Conclusions and Scope for Future Work

7.1 Conclusions

In this thesis, experimental investigation was carried out on the double tool turning process. The main cutting parameters in double tool turning process are cutting speed, feed, depth of cut and distances between the two cutting tools. The effect of these cutting parameters on cutting forces, cutting temperature, cutting tool vibration, diametral error, cutting tool wear and surface roughness were studied. An analytical model was developed to estimate the cutting forces and cutting temperature for single tool turning process. The experimental results were matched with the analytically predicted cutting force and cutting temperature for single tool turning process. The chip characteristics and cutting tool wear of both front cutting tool and rear cutting tools were investigated. The effect of cutting conditions on the surface roughness of the machined workpiece was studied. A comparison was drawn between the surface finish generated by single tool turning process and double tool turning process. The main conclusions from the thesis are presented in the following subsections.

7.1.1 Effect of Cutting Parameters on Cutting Forces, Cutting Temperature and Cutting Tool Vibration

- The cutting force and feed force was found to be lower for the rear cutting tool while machining grey cast iron, compared to front cutting tool for 75 m/min cutting speed, 0.08 mm/rev feed, 2 mm distance between the cutting tools and for depths of cut ranging from 0.25 mm to 1 mm. The coefficient of friction of the rear cutting tool is reduced due to the cleansing effect of the front cutting tool. This is attributed for the reduced cutting forces of the rear cutting tool.
- The distance between the cutting tools did not affect the cutting force and feed force significantly for both and front and rear cutting tools while machining grey cast iron. Similarly the cutting temperatures were not influenced

significantly when the distances between the front cutting tool and rear cutting tools was varied in the range of 2 mm to 8 mm. The workpiece temperature increased marginally from 60 °C to 80 °C when the cutting speed was increased from 75 m/min to 185 m/min. As the temperature rise is not high the work material properties did not vary.

- An analytical model was developed for single tool turning to predict the cutting forces and cutting temperature for mild steel work material. Experiments were also performed for single tool turning process. The analytical model provided theoretical explanation for the experimentally obtained cutting forces and cutting temperatures. An error ranging between 10% to 16% for cutting force and 4% to 13% for feed force was observed between experimental and the developed analytical model.
- The influence of cutting speed on cutting tool vibration was evaluated while double tool turning of grey cast iron workpiece. It was observed that the cutting tool vibration of both the front cutting tool and rear cutting decreased with the increase in cutting speed. The rear cutting tool vibration was found to be lesser than the front cutting tool vibration for the chosen cutting conditions. The rear cutting tool was mounted over the fixture made out of cast iron and the front cutting tool was mounted over the fixture made out of steel. The good vibration damping property of cast iron causes lesser rear tool vibration.

7.1.2 Influence of Cutting Parameters on Diametral Error, Tool Wear and Chip Morphology

- In double tool turning process, the rear cutting tool provided additional support to the workpiece and also removed the work material. It acted like a follower rest. Due to this the workpiece deflection got reduced by 80 %, which led to reduced diametral error and improved machining accuracy.
- The workpiece diametral error was found to be the maximum at the tailstock due to its lesser rigidity and the minimum at the headstock because of higher rigidity.
- The radial deflection of the workpiece was predicted by using a simple strength of material theory, for both single and double tool turning process. It

was observed that higher depth of cut generated higher cutting force which in turn led to higher diametral error.

- The rear cutting tool was found to have a lesser flank wear compared to front cutting tool for the considered cutting conditions. Abrasive wear was predominant for the front cutting tool whereas for the rear cutting tool adhesive and diffusion wear were predominant.
- During the double tool turning there was a noticeable difference between the chips generated by the front cutting tool and the rear cutting tools. More curling of chip segments were observed for the chips produced by rear cutting tool. It was due to thermal softening and fracture. However, the chips generated by the front cutting tool did not exhibit any thermal effect.

7.1.3 Effect of Cutting Parameters on Surface Roughness in Double Tool Turning Process

- The average surface roughness decreased with the increase in cutting speed for the selected cutting conditions. The surface roughness increased with the decrease in cutting speed. This was applicable to both grey cast iron and AISI 1050 work materials. This behaviour resembles the conventional turning process.
- It was observed for AISI 1050 steel work material that the average surface roughness decreased when the feed was increased from 0.04 mm/rev to 0.12 mm/rev and thereafter it increased; on further increase of feed from 0.12 mm/rev to 0.24 mm/rev. For grey cast iron the average surface roughness increased on increasing the feed under all the studied cutting conditions.
- The average surface roughness remained constant with the increase in depth of cut for the feeds of 0.04 mm/rev and 0.08 mm/rev for grey cast iron. For the feeds above 0.08 mm/rev the surface roughness increased with the increase in depth of cut. For AISI 1050 steel the surface roughness increased with the increase in depth of cut for all selected cutting conditions. Higher depth of cut led to higher cutting force which in turn causes more workpiece deflection. This increased the surface roughness.

- The distance between the cutting tools did not have any effect on the average surface roughness of both grey cast iron and AISI 1050 steel work materials for all the ranges of investigated cutting conditions.
- On comparison with single tool turning process, double tool turning process produced superior surface finish on the machined grey cast iron and AISI 1050 steel work surfaces. A lowered average surface roughness for AISI 1050 steel and grey cast iron work materials was obtained in double tool turning process, when compared with single tool turning process.
- Double tool turning leads to reduced machining cost compared to conventional turning process, hence it is advantageous. An approximate analysis showed a 45% reduction in machining cost for a typical case.

7.2 Scope for Future Work

- In the present work double tool turning process was explored. The work can be extended to other multi-tool machining process.
- A conventional lathe was modified to perform double tool turning process. The feeds of both the cutting tools were same. A separate mechanism can be developed such that the different feeds can be given to the two cutting tools. It may help in improving the surface finish.
- In this thesis experimental investigation on double tool turning process was carried out. Numerical study on double tool turning process can be carried out. It further increases the understanding of the process. This will save time and cost by avoiding time consuming and expensive metal cutting experiments.

References

- Abukhsim, N. A., Mativenga, P.T. and Sheik, M.A., (2004), An investigation of the tool-chip contact length and wear in high-speed turning of EN 19 steel, Proceedings of the Institution of Mechanical Engineers, Part B: Journal of Engineering Manufacture, 218, pp. 889–903.
- Abu-Mahfouz, I., (2003), Drill wear detection and classification using vibration signals and artificial neural network, International Journal of Machine Tools and Manufacture, 43, pp. 707–720.
- Akdemir, A., Yazman, Ş., Saglam, H. and Uyaner, M., (2012), The effects of cutting speed and depth of cut on machinability characteristics of austempered ductile iron, ASME Journal of Manufacturing Science and Engineering, 134(2), pp. 021013-1–021013-9.
- Alonso, F.J. and Salgado, D.R., (2008), Analysis of the structure of the vibration signals for tool wear detection, Mechanical Systems and Signal Processing, 22, pp. 735–748.
- Astakhov, V.P., (2011), Authentication of FEM in metal cutting, in Davim, J.P. (Ed.): Finite Element Method in Manufacturing Processes, pp.1–44, ISTE Ltd., London.
- Atkins, A.G., (2003), Modelling metal cutting using modern ductile fracture mechanics: quantitative explanations for some longstanding problems, International Journal of Mechanical Sciences, 45, pp. 373–396.
- Bhattacharyya, A., (1984), Metal Cutting: Theory and Practice, Central Book Publishers, Kolkata.
- Brar, N.S., Joshi, V.S. and Harris, B.W., (2007), Constitutive Model Constant for Low Carbon Steels from Tension and Torsion Data, AIP Conference Proceedings on Shock Compression of Condensed Matter, Waikoloa, Hawaii.
- Budak, E. and Ozturk, E., (2011), Dynamics and stability of parallel turning operations, CIRP Annals Manufacturing Technology, 60(1), pp. 383–386.
- Cakir, M. C., Ensarioglu, C. and Demirayak, I., (2009), Mathematical modeling of surface roughness for evaluating the effects of cutting parameters

and coating material, Journal of Materials Processing Technology, 209(1), pp. 102–109.

- Camusu, N., (2008), Effect of cutting speed on the performance of Al2O3 based ceramic tools in turning nodular cast iron, Materials and Design, 27, pp. 997–1006.
- Carrino, L., Giorleo, G., Polini, W. and Prisco, U., (2002a), Dimensional Errors in Longitudinal Turning Based on the Unified Generalized Mechanics of Cutting Approach: Part I: Three-Dimensional Theory, International Journal of Machine Tools and Manufacture, 42(14), pp. 1509–1515.
- Carrino, L., Giorleo, G., Polini, W. and Prisco, U., (2002b), Dimensional Errors in Longitudinal Turning Based on the Unified Generalized Mechanics of Cutting Approach: Part II: Machining Process Analysis and Dimensional Error Estimate, International Journal of Machine Tools and Manufacture, 42(14), pp. 1517–1525.
- Chao, B.T. and Bisacre, G.H., (1951), The effect of speed and feed on the mechanics of metal cutting, Proceedings of the Institution of Mechanical Engineers, 165, pp. 1–13.
- Chattopadhayay, A.B. (2011), Machining and Machine Tools, Wiley India, New Delhi.
- Chelladurai, H., Jain, V. K. and Vyas, N. S., (2008), Development of a cutting tool condition monitoring system for high speed turning operation by vibration and strain analysis, The International Journal of Advanced Manufacturing Technology, 37(5–6), 471–485.
- Chisholm, A.J., (1951), Communications on paper 'The fundamental geometry of cutting tools' by Stabler. G.V., Proceedings on Mechanical Engineers, 165(1), pp.14–21.
- Choudhury, I. A. and El-Baradie, M. A., (1997), Surface roughness prediction in the turning of high-strength steel by factorial design of experiments, Journal of Materials Processing Technology, 67(1), pp. 55–61.
- Correia, A. E. and Davim, J. P., (2011), Surface roughness measurement in turning carbon steel AISI 1045 using wiper inserts, Measurement, 44(5), pp. 1000−1005.

- Davim, J. P., Gaitonde, V. N. and Karnik, S. R., (2008), Investigations into the effect of cutting conditions on surface roughness in turning of free machining steel by ANN models, Journal of Materials Processing Technology, 205(1), pp. 16–23.
- Dearnley, P.A., (1985), A Metallurgical evaluation of tool wear and chip formation when machining pearlitic grey cast irons with dissimilar graphite morphologies, Wear, 101, pp. 33–68.
- Deb, K. (1995), Optimization for Engineering Design Algorithms and Examples, Prentice Hall of India, New Delhi.
- Dewes, R.C., Ng, E., Chua, K.S., Newton, P.G. and Aspinwall, D.K., (1999), Temperature measurement when high speed machining hardened mould/die steel, Journal of Materials Processing Technology, 92–93, pp. 293–301.
- Dimla, D. E., (2004), The impact of cutting conditions on cutting forces and vibration signals in turning with plane face geometry inserts, Journal of Materials Processing Technology, 155, pp. 1708–1715.
- Dimla Sr, D.E. and Lister, P.M., (2000), On-line metal cutting tool condition monitoring I: Force and vibration analyses, International Journal of Machine Tools and Manufacture, 40, pp. 739–768.
- Dixit, P.M. and Dixit, U.S., (2015), Plasticity: Fundamentals and Applications, CRC Press, Boca Raton.
- Dixit, U.S., Hazarika, M. and Davim, J.P., (2017), A brief History of Mechanical Engineering, Springer, Switzterland.
- El-Hossainy, T. M., (2010), Enhancement of surface quality using a newly developed technique in turning operations, Proceedings of the Institution of Mechanical Engineers, Part B: Journal of Engineering Manufacture, 224(9) pp. 1389–1397.
- El-Wardany, T.I., Gao, D. and Elbestawi, M.A., (1996), Tool condition monitoring in drilling using vibration signature analysis, International Journal of Machine Tools and Manufacture, 36, pp. 687–711.
- Fang, N., Srinivasa Pai, P. and Mosquea, S., (2010), The effect of built-up edge on the cutting vibrations in machining 2024-T351 aluminum alloy, International Journal of Advanced Manufacturing Technology, 49, pp. 63–71.

- Farhat, Z. N., (2003), Wear Mechanism of CBN Cutting Tool during High-speed Machining of Mold Steel, Material Science Engineering A, 361(1), pp. 100–110.
- Gatto, A. and Luliano, L., (1994), Chip formation analysis in high speed machining of a nickel base super alloy with silicon carbide whisker-reinforced alumina, International Journal of Machine Tools and Manufacture, 34, pp. 1147–1161.
- Ghani, A.K., Choudhury, I.A. and Husni, (2002), Study of tool life, surface roughness and vibration in machining nodular cast iron with ceramic tool, Journal of Materials Processing Technology, 127, pp. 17–22.
- Ghosh, A. and Mallik, A.K., (2010), Manufacturing Science, East West Press, New Delhi.
- Gökkaya, H. and Nalbant, M., (2007), The effects of cutting tool geometry and processing parameters on the surface roughness of AISI 1030 steel, Materials and Design, 28(2), pp. 717–721.
- Günay, M. and Yücel, E., (2013), Application of Taguchi method for determining optimum surface roughness in turning of high-alloy white cast iron, Measurement, 46(2), pp. 913–919.
- Heck, M., Ortner, H.M., Flege, S., Reuter, U. and Ensinger,W., (2008), Analytical investigations concerning the wear behavior of cutting tools used for the machining of compacted graphite iron and grey cast iron, International Journal of Refractory Metals & Hard Materials, 26(3), pp. 197–206.
- Huang, J., Olson, W., Sutherland, J. and Aifentis, E., (1996), On the Shear Instability in Chip Formation in Orthogonal Machining, Journal of Mechanical Behaviour of Materials. 7(4), pp. 279–292.
- Iqbal, S.A., Mativenga, P.T. and Sheikh, M.A., (2009), A comparative study of tool-chip contact length in turning of two engineering alloys for a wide range of cutting speeds, International Journal of Advanced Manufacturing Technology, 42, pp. 30–40.
- Jesuthanam, C. P., Kumanan, S. and Asokan, P., (2007), Surface roughness prediction using hybrid neural networks, Machining Science and Technology, 11(2), pp. 271–286.

- Jianliang, G. and Rongdi, H., (2006), A United Model of Diametral Error in Slender Bar Turning With a Follower Rest, International Journal of Machine Tools and Manufacture, 46(9), pp. 1002–1012.
- Jiao, Y., Lei, S., Pei, Z. J. and Lee, E. S., (2004), Fuzzy adaptive networks in machining process modeling: surface roughness prediction for turning operations, International Journal of Machine Tools and Manufacture, 44(15), pp. 1643–1651.
- Kang, M.C., Kim, J.S. and Kim, J.H., (2001), A monitoring Technique using a multi-sensor in high speed machining, Journal of Materials Processing Technology, 113, pp. 331–336.
- Kapoor, S.G., DeVore, R.E., Zhu, R., Gajjela, R., Parakkal, G. and Smithey, D., (1998), Development of mechanistic models for the prediction of machining performance: model building methodology, Machining Science and Technology, 2(2), pp. 213–238.
- Karpat, Y. and Ozel, T., (2008), Analytical and Thermal Modeling of High-Speed Machining With Chamfered Tools, ASME Journal of Manufacturing Science and Engineering, 130, pp. 011001-1–011001-15.
- Katuku, K., Koursaris, A. and Sigalas, I., (2009), Wear, Cutting Forces and Chip Characteristics when Dry Turning ASTM Grade 2 Austempered Ductile Iron with PcBN Cutting Tools under Finishing Conditions, Journal of Materials Processing Technology, 209(5), pp. 2412–2420.
- Killic, B., Cruz, J.A.A. and Raman, S., (2007), Inspection of the Cylindrical Surface Feature After Turning Using Coordinate Metrology, International Journal of Machine Tools and Manufacture, 47(12–13), pp.1893–1903.
- Kops, L., Gould, M. and Mizrach, M., (1993), Improved Analysis of the Workpiece Accuracy in Turning. Based on the Emerging Diameter, ASME Journal of Engineering for Industry, 115(3), pp. 253–257.
- Krammer, B.M., (1987), On Tool Materials for High Speed Machining, ASME Journal of Engineering for Industry, 109, pp. 87–91.
- Kronenberg, M., (1966), Machining Science and Application Theory and Practice for Operation and Development of Machining Processes, Pergamon Press, New York.

- Lalwani, D. I., Mehta, N.K. and Jain. P.K., (2008), Experimental investigations of cutting parameters influence on cutting forces and surface roughness in finish hard turning of MDN250 steel, Journal of Materials Processing Technology, 206(1), pp. 167–179.
- Levin, J. B. and Dutta, D., (1996), PMPS: A prototype CAPP system for parallel machining, ASME Journal of Manufacturing Science and Engineering, 118(3), pp. 406−414.
- Lin, Y.J., Agrawal, A. and Fang, Y., (2008), Wear progressions and tool life enhancement with AlCrN coated inserts in high-speed dry and wet steel lathing, Wear, 264, pp. 226–234.
- List, G., Sutter, G. and Bi, X.F., (2009), Investigation of tool wear in High Speed Machining by using a ballistic set-up, Wear, 267, pp. 1673–1679.
- Lu, C., (2008), Study on prediction of surface quality in machining process, Journal of Materials Processing Technology, 205(1), pp. 439–450.
- Mayer, J.R.R., Phan, A.V. and Cloutier, G., (2000), Prediction of Diameter Errors in Bar Turning: A Computationally Effective Model, Applied Mathematical Modelling, 24(12), pp. 943–956.
- McCollogh, E.M., (1963), Economics of Multitool Lathe Operations, ASME Journal of Engineering for Industry, pp. 402–404.
- Mehta, N.K., Pandey, P.C. and Chakravarti, G., (1983), An investigation of tool wear and the vibration spectrum in milling, Wear, 91, pp. 219–234.
- Mian, J., Driver, N. and Mativenga, P.T., (2011), Chip Formation in Microscale Milling and Correlation with Acoustic Emission Signal, International Journal of Advanced Manufacturing Technology, 56, pp. 63–78.
- Muller, B., Renz, U., Hoppe, S. and Klocke, F., (2004), Radiation Thermometry at a High-Speed Turning Process, ASME Journal of Manufacturing Science and Engineering, 126, pp. 488–495.
- Murthy, R.L., (1970), Interaction of Machine Tool and Workpiece Rigidities, International Journal of Machine Tool Design and Research, 10(2), pp.317–325.
- Nalbant, M., Gökkaya, H., Toktaş, İ. and Sur, G., (2009), The experimental investigation of the effects of uncoated, PVD-and CVD-coated cemented

carbide inserts and cutting parameters on surface roughness in CNC turning and its prediction using artificial neural networks, Robotics and Computer-Integrated Manufacturing, 25(1), pp. 211–223.

- Nouari, M. and Molinari, A., (2005), Experimental verification of a diffusion tool wear model using a 42CrMo4 steel with an uncoated cemented tungsten carbide at various cutting speeds, Wear, 259, pp. 1151–1159.
- Orhan, S., Er, A.O., Camusu, N. and Aslan, E., (2007), Tool wear evaluation by vibration analysis during end milling of AISI D3 cold work tool steel with 35 HRC hardness, NDT and E International., 40,121–126.
- Oxley, P.L.B., (1989), Mechanics of Machining: An Analytical Approach to Assessing Machability, John Wiley & Sons, New York.
- Ozturk, E., Comak, A. and Budak, E., (2016), Tuning of tool dynamics for increased stability of parallel (simultaneous) turning processes, Journal of Sound and Vibration, 360, pp. 17–30.
- Pereira, A. A., Boehs, L. and Guesser, W.L., (2006), The influence of sulfur on the machinability of gray cast iron FC25, Journal of Materials Processing Technology, 179(1), pp. 165–171.
- Phan, A.V., Baron. L., Mayer, J.R.R. and Cloutier, G. (2002), Finite Element and Experimental Studies of Diametral Errors in Cantilever Bar Turning, Applied Mathematical Modelling, 27(3), pp. 221–232.
- Philip, P. K., (1971), Built-up edge phenomenon in machining steel with carbide, International Journal of Machine Tool Design and Research, 11(2), pp. 121–132.
- Polini, W. and Prisco, U., (2003), The estimation of the diameter error in bar turning: a comparison among three cutting force models, The International Journal of Advanced Manufacturing Technology, 22, pp. 465–474.
- Ramanuj,V., (2013), Multi-tool turning: Dynamics Characteristics, M.Tech. Thesis, Department of Mechanical Engineering, Indian Institute of Technology Guwahati, India.
- Ramesh, S., Karunamoorthy, L. and Palanikumar, K., (2012), Measurement and analysis of surface roughness in turning of aerospace titanium alloy (gr5), Measurement, 45(5), pp. 1266–1276.

- Ravignani, G.L., Zompi, A. and Levi, R., (1979), Multi-Tool Machining Analysis Part 2 Economic Evaluation in view of Tool Life Scatter, ASME Journal of Engineering for Industry, 101, pp. 237–240.
- Recht, R.F., (1985), A Dynamic Analysis of High-Speed Machining, ASME Journal of Engineering for Industry, 107, pp. 309–315.
- Reddy, N. S. K. and Rao, P. V., (2006), Selection of an optimal parametric combination for achieving a better surface finish in dry milling using genetic algorithms, The International Journal of Advanced Manufacturing Technology, 28(5–6), pp. 463–473.
- Ren, H. and Altintas.Y., (2000), Mechanics of Machining With Chamfered Tools, ASME Journal of Manufacturing Science and Engineering, 122, pp. 650– 659.
- Risbood, K. A., Dixit, U. S. and Sahasrabudhe, A. D., (2003), Prediction of surface roughness and dimensional deviation by measuring cutting forces and vibrations in turning process, Journal of Materials Processing Technology, 132(1), pp. 203–214.
- Sahin, Y. and Motorcu, R.A., (2005), Surface roughness model for machining mild steel with coated carbide tool, Materials and Design 26(4), pp. 321–326.
- Salgado, D.R. and Alonso, F.J., (2006), Tool wear detection in turning operations using singular spectrum analysis, Journal of Materials Processing Technology, 171, pp. 451–458.
- Sandeep. K., (2015), Modeling of Multi-Tool Turning, M.Tech. Thesis, Department of Mechanical Engineering, Indian Institute of Technology Guwahati, India.
- Sarma, D. K. and Dixit, U. S., (2007), A comparison of dry and air-cooled turning of grey cast iron with mixed oxide ceramic tool, Journal of Materials Processing Technology, 190(1), pp. 160–172.
- Schey, J. A., (1983), Tribology in Metal Working (Friction, Lubrication and Wear). American Society for Metals, Metals Park, OH.
- Segonds, S., Cohen, G., Landon, Y., Monies, F. and Lagarrigue, P., (2006), Characterising the behaviour of workpieces under the effect of tangential cutting force during NC turning: Application to machining of slender

workpieces. Journal of Materials Processing Technology, 171(3), pp. 471–479.

- Selvam, M. S. and Radhakrishnan, V., (1973), Influence of side-flow and built-up edge on the roughness and hardness of the surface machined with a single point tool, Wear, 26(3), pp. 393–403.
- Selvam, M. S. and Radhakrishnan, V., (1974), Groove wear, built-up edge and surface roughness in turning, Wear, 30(2), pp. 179–188.
- Shashikant, J., Asim, T. and Suhas, J. (2013), Influence of Preheating on Chip Segmentation and Microstructure in Orthogonal Machining of Ti6Al4V, ASME Journal of Manufacturing Science and Engineering, 135(6), pp. 061017-1–061017-11.
- Shaw, M.C., (1954), Metal Cutting Principles, Massachusetts Institute of Technology Publication, Cambridge.
- Sheikh, A.K., Kendall, L.A. and Pandit, S.M., (1980), Probabilistic Optimization of Multitool Machining Operations, ASME Journal of Engineering for Industry, 102, pp. 239–246.
- Stabler, G.V., (1951), The Fundamental Geometry of Cutting Tools, Proceedings of the Institution of Mechanical Engineers, 165, pp. 14–26.
- Stephenson, D.A. and Agapiou, J.S., (1996), Metal Cutting Theory and Practice, Marcel Dekker, New York.
- Sudhakara, R. and Landers, R. G., (2003), Output feedback force control for a parallel turning operation, In IEEE Proceedings of the American Control Conference, 3, pp. 2596–2601.
- Sutter, G., Molinari, A., Faure, L., Klepaczko, J.R. and Dudzinski, D. (1998), An Experimental Study of High Speed Orthogonal Cutting, Trans. ASME Journal of Manufacturing Science and Engineering, 127, pp. 169–172.
- Sutter, G., Faure, L., Molinari, A., Ranc, N. and Pina, V. (2003), An experimental technique for the measurement of temperature fields for the orthogonal cutting in high speed machining, International Journal of Machine Tools and Manufacture, 43, pp. 673–678.

- Sutter, G. and Molinari. A., (2005), Analysis of Cutting Force Components and Friction in High Speed Machining, ASME Journal of Manufacturing Science and Engineering, 127, pp. 245–250.
- Tang, L., Landers R.G. and Balakrishnan, S.N., (2008), Parallel Turning Process Parameter Optimization Based on a Novel Heuristic Approach, ASME Journal of Manufacturing Science and Engineering, 130, pp. 031002-1–031002-12.
- Thomas, M., Beauchamp, Y., Youssef, A. Y. and Masounave, J., (1996), Effect of tool vibrations on surface roughness during lathe dry turning process, Computers & Industrial Engineering, 31(3), pp. 637–644.
- Trent, E.M. and Wright, P.K., (2000), Metal Cutting, Butterworth Heinemann, Woburn.
- Upadhyay, Vikas., Jain, P.K. and Mehta. N.K., (2013), In-process prediction of surface roughness in turning of Ti–6Al–4V alloy using cutting parameters and vibration signals, Measurement, 46(1), pp. 154–160.
- Vaibhav. J., (2014), Multi-Tool Turning: Investigation, M.Tech. Thesis, Department of Mechanical Engineering, Indian Institute of Technology Guwahati, India.
- von Turkovich, B. F., (1970), Shear stress in metal cutting, ASME Journal of Engineering for Industry, 92, pp. 151–157.
- Xavior, M. A., and Adithan. M., (2009), Determining the influence of cutting fluids on tool wear and surface roughness during turning of AISI 304 austenitic stainless steel, Journal of Materials Processing Technology, 209(2), pp. 900–909.
- Yadav, R. N., (2017), A hybrid approach of Taguchi-Response Surface Methodology for modelling and optimization of Duplex Turning process, Measurement, 100(1), 131−138.
- Yatin. M., (2013), Multi Tool Turning: Condition Monitoring, M.Tech. Thesis, Department of Mechanical Engineering, Indian Institute of Technology Guwahati, India.

- Yellowley, I. and Lai, C.T., (1993), The use of force ratio in the tracking of tool wear in turning, ASME Journal of Engineering for Industry, 115(3), pp.370–372.
- Yigit, R., Celik, E., Findik, F. and Koksal, S., (2008), Effect of cutting speed on the performance of coated and uncoated cutting tools in turning nodular cast iron, Journal of Materials Processing Technology, 204, pp. 80–88.
- Zeng,Y. and Forssberg, (1994), Monitoring of grinding parameters by vibration signal measurement A primary application, Minerals Engineering, 7, pp. 495–501.
- Zompi, A., Levi, R. and Ravignani, G.L., (1979), Multi-Tool Machining Analysis Part 1 Tool Failure Patterns and Implications, ASME Journal of Engineering for Industry, 101, pp. 230–236.

Publications from the Present Thesis

International Journals

[1] Kalidasan. R, Ramanuj. V, Sarma, D.K and Senthilvelan. S, (2014) Influence of Cutting speed and Offset Distance Over Cutting Tool Vibration in Multi-Tool Turning Process, Advanced Materials Research, Vols. 984-985, pp. 100-105.

[2] Kalidasan. R, Yatin. M, Sarma D.K. and Senthilvelan. S, (2014) Effect of Offset Distance on Cutting forces and Heat generation in Multi-Tool Turning Process. Applied Mechanics and Materials, Vols. 592-594, pp. 211-215.

[3] Kalidasan. R, Senthilvelan. S, Dixit. U.S. and Vaibhav. J, (2016) Double tool turning process machining accuracy, cutting tool wear and chip-morphology, International Journal of Precision Technology, Vol 6, No 2, pp. 142-157.

[4] Kalidasan. R, Yatin. M, Sarma. D.K, Senthilvelan. S and Dixit. U.S, (2016) An experimental study of cutting forces and temperature in multi-tool turning of grey cast iron, International Journal of Machining and Machinability of Materials, Vol 18, No 5/6, pp. 540-551.

[5] Kalidasan. R, Senthilvelan. S. and Dixit. U.S, (2017) An Experimental Study of Surface roughness in double tool turning process, International Journal of Additive and Subtractive Materials Manufacturing, (communicated).

Book Chapter

[1] Kalidasan. R, Senthilvelan. S. and Dixit. U.S, (2016) Double tool turning, in Paulo Davim. J, Metal cutting technologies progress and current trends, De Gruyter Oldenburg

International Conferences

[1] Kalidasan. R, Ramanuj. V, Sarma, D.K. and Senthilvelan. S, (2014) Influence of Cutting speed and Offset Distance Over Cutting Tool Vibration in Multi-Tool Turning Process, International Conference on Recent Advances in Mechanical Engineering and Interdisciplinary Developments, Tamil Nadu, India. [This paper has also been published as International Journal paper number #1]

[2] Kalidasan. R, Yatin. M, Sarma D.K. and Senthilvelan. S, (2014) Effect of Offset Distance on Cutting forces and Heat generation in Multi-Tool Turning Process, International Mechanical Engineering Congress, National Institute of Technology, Tiruchirapalli, Tamil Nadu, India. [This paper has also been published as International Journal paper number #2]

[3] Kalidasan. R, Yatin. M, Senthilvelan. S. and D.K.Sarma, (2014) Preliminary experimental investigation on Multi-Tool Turning Process, 5th International & 26th All India Manufacturing Technology, Design and Research Conference December 12^{th}–14^{th}, Indian Institute of Technology Guwahati, Assam, India. [Enhanced version of this paper has been published as International Journal paper number #4]

[4] Kalidasan. R, Senthilvelan. S. and Dixit. U.S, (2016) The influence of machining parameters on surface roughness in double tool turning process, IV^{th} International Conference on Production and Industrial Engineering, December 19^{th} – 21^{st}, National Institute of Technology, Jalandhar, Punjab, India. [Enhanced version of this paper has been communicated as International Journal paper number #5]